The role of histone H3K36me3 in mammalian cell cycle regulation and genome stability

Lee Dominic Armfield

A thesis presented for the degree of Doctor of Philosophy



CRUK MRC Institute for Radiation Oncology

Department of Oncology, University of Oxford

Wolfson College

Trinity 2019

The role of histone H3K36me3 in mammalian cell cycle regulation and genome stability

Lee Dominic Armfield Doctor of Philosophy

Wolfson College Trinity 2019

Although the molecular genetics regulating DNA replication onset have been studied in great detail, the epigenetic contribution to this step is poorly understood. H3K36me3 has been identified as a key factor regulating the catalytic ribonucleotide reductase subunit RRM2, suggesting an important role in DNA replication. To investigate this potential role, RNA-sequencing was carried out on SETD2 parental and CRISPR U2OS cell lines to identify genes differentially expressed in the absence of SETD2. Loss of SETD2 was found to lead to significantly reduced expression of a subset of E2F target genes critical for DNA replication and the G1/S transition. Consistent with this reduced expression, SETD2 deficient cells were found to have prolonged G1 delay, reduced replication fork progression and replication stress-associated 53BP1 bodies and γH2AX foci. Additionally, DNA under-replication was found to result in FANCD2-associated ultrafine anaphase bridges, micronuclei formation, and to G1 53BP1 bodies. A role was also identified for checkpoint-induced H3K36me3 in facilitating E2F transcription in response to replication stress. Together these findings support a dual role for H3K36me3 in the regulation of transcription of E2F target genes in the unperturbed G1/S transition, and as part of the replication stress response.

Further work focussed on investigating additional synthetic lethalities with WEE1 inhibition. The synthetic lethality between WEE1 inhibition and loss of p53 was found to be mechanistically similar to the SETD2/WEE1 synthetic lethality, contrary to previously published work. Novel synthetic lethalities were also investigated, and loss of three tumour suppressors (MGA, KMT2D and KDM5C) was found to sensitise cells to WEE1 inhibition, potentially expanding the subset of tumours that can be targeted by WEE1 inhibition.

Acknowledgements

Firstly, I would like to thank my supervisor Dr Tim Humphrey for his guidance over the last four years. I would also like to express my gratitude to Wolfson College and the Oxford-Wolfson-Marriott scholarship for funding me during this project.

I would also like to thank all the members of the Humphrey laboratory past and present for their support, and for making the lab such an enjoyable place to work. In particular I would like to thank Sovan, Kirsten, and Chen Chun for all the help and advice they have given me.

This project would not have been possible without our collaborators. I would particularly like to thank Dr Chris Chan for his help with the ultra-fine bridges, Dr Daniel Ebner for his help with the DDR and cell cycle siRNA screens, Dr Ross Chapman for the p53 CRISPR cell lines, Dr Rob De Bruin for the T98G cell line, and Dr Andy Ryan for the H1299 cell line. I would also like to thank Sovan and Sophia for the SETD2 CRISPR U2OS cell line.

Finally, I would like to thank my family and friends for all their support, advise, and inspiration.

Table of Contents

Acknowledgements **2**

Declaration **10**

List of Figures **11**

List of Tables **14**

Abbreviations **16**

Chapter 1 ..... **17**

Introduction **17**

1.1 Cancer 17

1.1.1 The cell cycle in cancer 17

1.2 Cell cycle regulation 18

1.2.2 G1 and the E2F transcriptional network 18

1.2.3 Replication origin licensing and initiation 20

1.2.4 Regulation of the G1/S transition 21

1.2.5 The intra-S checkpoint 25

1.3 DNA replication stress 27

1.3.1 Replication factor shortage 28

1.3.2 Replication-transcription conflicts 29

1.4 Post-translational histone modifications 29

1.4.2 Histone modifications in cell cycle regulation 33
1.4.2.1 Histone acetylation 33
1.4.2.2 Histone methylation 34
1.4.3 Histone H3K36 Trimethylation 36
1.4.3.1 H3K36me3 in cancer 36
1.4.3.2 H3K36 methylation in DNA repair 38
1.4.3.3 H3K36 methylation in DNA replication 39
1.5 Synthetic lethality with WEE1 inhibition 40
1.5.1 SETD2 and WEE1 40
1.5.2 The WEE1 kinase 41
1.6 Thesis aims 44
1.6.1 Understanding the how SETD2 regulates RRM2 44
1.6.2 Investigating a role for SETD2 in the replication stress response 44
1.6.3 Exploring synthetic lethal interactions with WEE1 inhibition 45
Chapter 2 45
Methods 46
2.1 Resuscitation of frozen cell lines 46
2.2 Maintenance of cell lines 46
2.3 Cryopreservation of cell lines 46
2.4 Cell lines 47
2.5 Cell Cycle Synchronisation 48
2.6 Bacterial transformation 48

2.7 Plasmid purification 48

2.8 siRNA transfection 49

2.9 Western blots 50

2.10 Inhibitors 51

2.11 Resazurin assay for cell viability 51

2.12 Cell cycle analysis by BrdU incorporation 52

2.13 RNA extraction 52

2.14 RNA-Seq Library preparation and Illumina sequencing 53

2.15 qRT-PCR (Quantitative reverse transcription polymerase chain reaction) 54

2.16 Immunofluorescence 57

2.17 Anaphase bridges 58

2.18 High-resolution deconvolution microscopy 58

2.19 Chromatin Immunoprecipitation (ChIP) 59

2.20 DNA Fibre Assay 61

2.21 Statistical Analysis 62

Chapter 3 64

RNA sequencing of SETD2 parental and CRISPR cell lines 64

3.1 Introduction 64

3.2 Results 65

3.2.1 Global effects of loss of H3K36me3 on transcription 65

3.2.2 Pathways of differentially expressed genes in SETD2 CRISPR U2OS compared to SETD2 parental 68

3.2.2.1 Upregulated GO terms 68
3.2.2.2 Upregulated KEGG pathways 71
3.2.2.3 Downregulated GO terms 74
3.2.2.4 Downregulated KEGG pathways 78
3.2.2.5 Global distribution of differentially expressed genes after SETD2 loss 80
3.2.3 Global effects of WEE1 inhibition of transcription 82
3.2.4 Pathways of genes differentially expressed in both U2OS parental and SETD2 CRISPR after WEE1 inhibition 85
3.2.4.1 Upregulated GO Terms 85
3.2.4.2 Upregulated KEGG pathways 87
3.2.4.3 Downregulated GO terms 89
3.2.4.4 Downregulated KEGG pathways 91
3.2.5 Pathways of genes differentially expressed in only SETD2 CRISPR after WEE1 inhibition 93
3.2.5.1 Upregulated GO Terms 95
3.2.5.2 Upregulated KEGG pathways 97
3.2.5.3 Downregulated GO Terms 99
3.2.5.4 Downregulated KEGG pathways 101
3.3 Discussion 103
3.3.1 Summary of chapter 3 103
3.3.2 Discussion of chapter 3 103

Chapter 4 106

Histone H3K36me3 facilitates efficient DNA replication through regulation of E2F transcription 106

4.1 Introduction 106

4.2 Results 107

4.2.1 qRT-PCR analysis of E2F target genes in SETD2 deficient cells 107

4.2.2 Complementation of SETD2 CRISPR U2OS 108

4.2.3 Readers of H3K36me3 111

4.2.4 Cell cycle analysis of SETD2 deficient cells 116

4.2.5 SETD2 deficient cells have increased endogenous damage 118

4.2.6 Replication stress induced DNA damage in SETD2 deficient cells 121

4.2.7 Loss of SETD2 leads to increased G1 53BP1 bodies 126

4.2.8 Under-replicated DNA leads to mitotic damage in SETD2 deficient cells 129

4.2.9 Increased micronuclei frequency in SETD2 deficient cells 133

4.2.10 Impaired replication stress response in SETD2-deficient cells 135

4.2.11 Replication stress induces SETD2 dependent upregulation of E2F target genes 136

4.2.12 KDM4A demethylation of H3K36me3 is not induced by replication stress 139

4.2.13 Replication stress induced H3K36me3 is checkpoint dependent 142

4.2.14 SETD2 has independent roles in DNA damage and replication stress responses 142

4.3 Discussion 147

4.3.1 Summary of chapter 4 147

4.3.2 Discussion of chapter 4..... 147

Chapter 5..... 150

Investigating synthetic lethalities with WEE1 inhibition..... 150

5.1 Introduction 150

5.2 Results..... 151

5.2.1 Synthetic lethality between loss of p53 and WEE1 151

5.2.1.1 Combined loss of SETD2 and p53 does not further sensitise to WEE1 inhibition 151

5.2.1.2 WEE1 inhibition induces S phase arrest in p53 negative cells 153

5.2.1.3 RRM2-T33A expression partially rescues p53/WEE1 synthetic lethality 155

5.2.1.4 MCF7 p53 CRISPR cells arrest in S phase after WEE1 inhibition... 157

5.2.1.5 WEE1 inhibition in p53 missense mutant cancers..... 159

5.2.1.6 WEE1 inhibition induces DNA damage in p53 deficient cells 160

5.2.1.7 Deletion of p53 does not sensitise non-cancerous cells to WEE1 inhibition 163

5.2.2 Identification of novel synthetic lethalities with AZD1775..... 166

5.2.2.1 A screen of cell cycle and DNA repair genes for synthetic lethality with AZD1775 166

5.2.2.2 Screen identified 37 genes potentially synthetic lethal with WEE1 inhibition 167

5.2.2.3 Novel synthetic lethalities between tumour suppressors and AZD1775 171

5.2.2.4 Initial screen results identified 9 tumour suppressors sensitive to WEE1 inhibition 173

5.2.2.5 Depletion of KMT2D, KDM5C or MGA sensitises cells to WEE1 inhibition 173

5.3 Discussion 178

5.3.1 Summary of chapter 5 178

5.3.2 Discussion of chapter 5 178

Chapter 6 181

General Discussion 181

6.1 The role of H3K36me3 in regulation of E2F transcription 182

6.2 H3K36 trimethylation in response to replication stress 182

6.3 The synthetic lethality between loss p53 and WEE1 inhibition 184

6.4 Novel tumour suppressor synthetic lethalities with WEE1 inhibition 184

6.5 Future work 185

Bibliography 186

Appendix 203

Declaration

I declare:

The work presented in this thesis is my own unless otherwise indicated.

No portion of this work has been previously submitted for another qualification at this, or any other university.

Signed ……..

Lee Dominic Armfield

List of Figures

Figure 1.1: Regulation of the E2F family of transcription factors by pRB and the pocket proteins 19

Figure 1.2: Model of replication origin initiation and firing in Saccharomyces cerevisiae 24

Figure 1.3: A model of canonical cell cycle checkpoints..... 27

Figure 1.4: Histone tails can be modified by the addition of a number of different molecules to facilitate recruitment or binding of downstream factors. 32

Figure 1.5: Enzymes responsible for the methylation and demethylation of histone H3 lysine 36 38

Figure 1.6: Schematic of the role of WEE1 in the DNA damage response..... 42

Figure 1.7: Loss of H3K36me3 is synthetic lethal with inhibition of WEE1 43

Figure 3.1 Volcano plot of the differentially expressed genes in U2OS SETD2 CRISPR cells relative to wildtype. 67

Figure 3.2: Enriched KEGG pathways of genes upregulated in SETD2 CRISPR U2OS 72

Figure 3.3: p53 target genes are upregulated in SETD2 CRISPR U2OS. 73

Figure 3.4: E2F target genes are differentially expressed in SETD2 deficient cells . 77

Figure 3.5: Enriched KEGG pathways of genes downregulated in SETD2 CRISPR U2OS 79

Figure 3.6: Plot showing distributed of differentially expressed genes after H3K36me3 loss 81

Figure 3.7: Volcano plot of the differentially expressed genes in U2OS wildtype and SETD2 CRISPR cells treated with 200nM AZD1775 relative to untreated. 83

Figure 3.8: Venn diagram of genes affected by AZD1775 treatment 84
Figure 3.9: Differentially expressed genes in cells treated with AZD1775 (a) Venn diagram of genes upregulated after AZD1775 treatment 94
Figure 4.1: Validation of E2F target gene depletion in SETD2 deficient cells..... 109
Figure 4.2: Complementation of SETD2 CRISPR U2OS with SETD2 plasmid 110
Figure 4.3: Depletion of HDAC2 leads to impaired E2F target gene expression.... 113
Figure 4.4: Depletion of H3K36me3 readers does not lead to impaired E2F target gene expression..... 114
Figure 4.5: SETD2 and HDAC2 co-depletion is not epistatic 115
Figure 4.6: SETD2 deficient cells show impaired G1/S progression 117
Figure 4.7: SETD2 deficient cells have increased p53 and p21 levels..... 120
Figure 4.8: Increased endogenous damage in SETD2 deficient cells 123
Figure 4.9: Exogenous nucleoside treatment partially rescues DNA damage in SETD2 deficient cells 124
Figure 4.10: Decreased replication fork speed in SETD2 deficient cells 125
Figure 4.11: Increased G1 53BP1 bodies upon depletion of SETD2 128
Figure 4.12: Loss of SETD2 leads to increased replication stress 131
Figure 4.13: Increased replication stress associated anaphase bridges in SETD2 deficient cells..... 132
Figure 4.14: Loss of SETD2 leads to increased levels of micronuclei formation 134
Figure 4.15: Replication stress induced E2F target gene expression is impaired after loss of SETD2 137
Figure 4.16: Replication stress induces H3K36me3 at E2F target gene promoters 138
Figure 4.17: KDM4A protein levels are not affected by replication stress 141

Figure 4.18: Independent roles for SETD2 in replication stress and DNA damage repair 145
Figure 4.19: Model of the role H3K36 trimethylation in the replication stress checkpoint response 146
Figure 5.1: SETD2 depletion does not further sensitise H1299 cells to AZD1775 . 152
Figure 5.2: Cell cycle profile of H1299 cells 154
Figure 5.3: RRM2-T33A expression in p53 deficient cells 156
Figure 5.4: p53 CRISPR MCF7 cell sensitivity to AZD1775 158
Figure 5.5: p53 point mutant MCF7 cell sensitivity to AZD1775 161
Figure 5.6: DNA damage markers visualised in p53 deficient cells treated with AZD1775 162
Figure 5.7: p53 depletion does not sensitise RPE-1 cells to AZD1775 164
Figure 5.8: Schematic overview detailing key steps in the siRNA screen protocol. 168
Figure 5.9: Viability assay of U2OS cells after treatment with indicated concentrations of AZD1775 for 48 hours relative to DMSO control 175
Figure 5.10: Cell cycle distribution of U2OS cells treated with DMSO or 300nM AZD1775. Cells were treated for 48hrs and cell cycle profile measured by flow cytometry 176
Figure 5.11: BrdU incorporation in U2OS cells treated with DMSO or AZD1775 ... 177

List of Tables

Table 3.1: Selected overrepresented GO terms of upregulated genes in SETD2 CRISPR U2OS cells compared to SETD2 wildtype 70

Table 3.2: Selected overrepresented GO terms of downregulated genes in SETD2 CRISPR U2OS cells compared to SETD2 wildtype 77

Table 3.3: Top 20 GO terms upregulated in both SETD2 CRISPR U2OS and wildtype after AZD1775 treatment 86

Table 3.4: KEGG pathways upregulated in both SETD2 CRISPR U2OS and wildtype after AZD1775 treatment 88

Table 3.5: Top 20 GO terms downregulated in both SETD2 CRISPR U2OS and wildtype after AZD1775 treatment 90

Table 3.6: KEGG pathways downregulated in both SETD2 CRISPR U2OS and wildtype after AZD1775 treatment 92

Table 3.7: Top 20 GO terms upregulated in SETD2 CRISPR U2OS compared to wildtype after AZD1775 treatment 96

Table 3.8: KEGG pathways upregulated in SETD2 CRISPR U2OS compared to wildtype after AZD1775 treatment 98

Table 3.9: Top 20 GO terms downregulated in SETD2 CRISPR U2OS compared to wildtype after AZD1775 treatment 100

Table 3.10: Top 20 KEGG pathways downregulated in SETD2 CRISPR U2OS compared to wildtype after AZD1775 treatment 102

Table 5.1: List of genes from the Cell Cycle and DNA Damage Response siRNA libraries whose knockdown was found to sensitise U2OS cells to AZD1775 treatment. 169

Table 5.2: GO terms enriched in the subset of genes whose knockdown resulted in sensitisation to AZD1775. 170
Table 5.3: Sensitivity of tumour suppressors screened to AZD1775 172

Abbreviations

°C	degree Celsius
µg	micrograms
µl	microlitre
µM	micromolar
bp	base pairs
BSA	bovine serum albumin
CDK	cyclin dependent kinase
DDR	DNA damage response
DNA	deoxyribonucleic acid
DTT	dithiothreitol
FACS	fluorescence activated cell sorting
g	grams
GFP	green fluorescent protein
GO	gene ontology
H3K36me3	Histone H3 lysine trimethlyation
HAT	histone acetyl transferase
HDAC	histone deacetylase
HR	homologous recombination
HU	hydroxyurea
IR	ionising radiation
Kb	kilobase
kDa	kilodalton
KDM4A	Lysine-specific demethylase 4A
KDM5C	Lysine-specific demethylase 5C
KMT2D	Lysine methyltransferase 2D
L	litre
M	molar
MBF	Mlu1-box binding factor
mg	milligrams
ml	millilitre
mM	millimolar
ng	nanograms
NHEJ	non-homologous end joining
p	p-value for student’s T-test
PBS	phosphate buffered saline
PCR	polymerase chain reaction
RPA	replication protein A
SD	standard deviation
SDS	sodium lauryl sulphate
SDS-PAGE	sodium lauryl sulphate-polyacrylamide gel electrophoresis
SETD2	SET Domain Containing 2
ssDNA	single stranded DNA
Ub	ubiquitin

Chapter 1

Introduction

1.1 Cancer

In 2018 there were over 18 million new cases of cancer, and over 9 million deaths from cancer worldwide (Ferlay et al., 2019). Although survival rates have continued to rise over the last 40 years, cancer is still a leading cause of death and it is imperative to increase our understanding of the disease in order to develop more effective treatments.

1.1.1 The cell cycle in cancer

Cancer is characterised by uncontrolled cell proliferation resulting from inappropriate activity of the proteins that regulate cell division. Activating mutations in pro-cell cycle signalling networks, along with loss of function mutations in tumour suppressor genes, drives oncogenic cell cycle progression. Unscheduled proliferation can lead to genomic instability and accumulation of further mutations (Kastan and Bartek, 2004). The cell cycle itself can be broadly divided into S phase, where DNA replication occurs, and mitosis, where replicated chromosomes are segregated into daughter cells (Norbury and Nurse, 1992), separated by the gap phases G1 and G2. The transition between cell cycle phases is carefully regulated, and dependent on the expression of the regulatory cyclins and cyclin-dependant kinases. Cyclins are cell cycle regulated proteins that bind and allosterically activate cyclin-dependant kinases, which are then able to phosphorylate downstream targets to drive cell cycle

progression (Kobayashi et al., 1991). Additionally, the cell cycle has multiple checkpoints in place to ensure that progression to the next phase does not occur prior to completing the previous phase (Johnson and Walker, 1999).

1.2 Cell cycle regulation

1.2.2 G1 and the E2F transcriptional network

The G1 phase of the cell cycle is the period when cells prepare to initiate DNA replication, and is the point at which cells commit to entering a new cell cycle. During this phase cells are able to enter a quiescent state (G0), where they do not progress further through the cell cycle. Progression through G1 is controlled by the D-type family of cyclins (D1, D2, and D3), which complex with CDK4 or CDK6, and the cyclin E-CDK2 complexes. Together these cyclin-CDK complexes act to phosphorylate the retinoblastoma (RB) family of tumour suppressors (Rb, p107, p130). The RB family are transcriptional co-repressors that regulate a number of genes involved in cell cycle control and progression. These include the E2F family of transcription factors, which control the expression of a key set of genes required for DNA replication and cell cycle progression. The E2F family are divided into activators (E2F1, E2F2 and E2F3A) which activate expression of pro-cell cycle genes, and repressors (E2F3B, E2F4, E2F5, E2F6, E2F7 and E2F8), which negatively regulate the activator E2Fs.

In early G1 the activator E2Fs are bound and repressed by RB (Helin et al., 1993), while E2F4 binds p107 and p130 at E2F target gene promoters to block their expression (Beijersbergen et al., 1994; Gaubatz et al., 2000; Takahashi et al., 2000). Upon hyper-phosphorylation by the cyclin D-CDK4/6 and cyclin E-CDK2

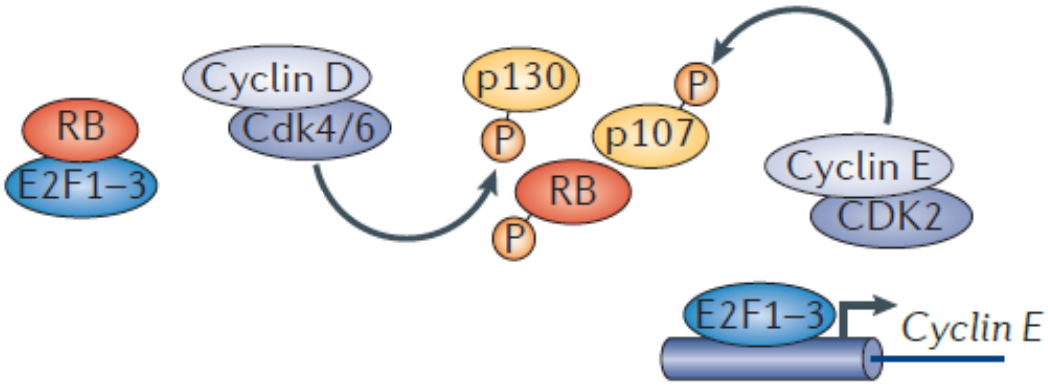


Figure 1.1: Regulation of the E2F family of transcription factors by pRB and the pocket proteins. Adapted from (Bertoli et al., 2013b)

complexes RB dissociates from the activator E2Fs. p107 and p130 are also phosphorylated, releasing E2F4 from target gene promoters, and allowing the activator E2Fs to bind and initiate transcription. E2F target genes include the components of the pre-replication complex (PRC), which forms the origin of replication and is required for the initiation of DNA replication.

1.2.3 Replication origin licensing and initiation

The origin recognition complex (ORC), a six sub-unit complex formed of ORC1-6, binds to the replication origin site. In contrast to yeast, where the ORC recognises a specific DNA sequence (Bell and Stillman, 1992), the mammalian ORC does not appear to have a specific recognition sequence, rather binding non-specifically to open regions containing chromatin modifications such as H3 acetylation and H3K4 methylation (Miotto et al., 2016). ORC binding facilitates the recruitment of CDC6, and together ORC and CDC6 act to recruit CDT1 and the MCM2-7 helicase subunits (Remus et al., 2009).

The MCM2-7 proteins form a double hexameric ring which encircles the DNA strand, with two hexamers loaded at each origin site (Evrin et al., 2009; Remus et al., 2009). MCM hexamers are loaded on to DNA in excess, which helps to protect cells under replication stressed conditions (Ibarra et al., 2008) by allowing cells to activate dormant origins and continue replication even in the presence of stalled forks. Replication is initiated by activation of the MCM helicase, which then begins to unwind the DNA double helix. Activation of the MCM helicase requires binding two additional factors, CDC45 and GINS (Ilves et al., 2010; Moyer et al., 2006), along

with phosphorylation by CDK and DDK (Dbf4-dependent kinase) (Deegan et al., 2016).

The increase in CDK activity required to activate origin firing also acts to prevent re-replication. High CDK activity inhibits assembly of the pre-replication complex meaning that once an origin has been fired, it cannot be relicensed until the following G1 phase, preventing origins from firing more than once per cell cycle (Dahmann et al., 1995).

1.2.4 Regulation of the G1/S transition

The transition from G1 to S phase is typically the point at which a cell commits to completion of another round of cell division, and as such is highly regulated to prevent inappropriate cell cycle progression. Disruption of the checkpoint mechanisms that block S phase entry can lead to replication stress, genome instability, and subsequently to oncogenesis.

Regulation of the E2F transcription factors by RB and the pocket proteins (Figure 1.1) acts to prevent transcription of S phase promoting genes in the absence of mitogenic signalling. Mitogen-induced cyclin D activation leads to phosphorylation of RB and E2F transcription as discussed previously. E2F target genes include cyclin E, and the S phase A type cyclins. These drive expression of pro-S phase genes, generating a positive feedback loop which helps to ensure commitment to cell cycle entry. Another E2F target gene, EMI1, inhibits the APC^{CDH1} complex, which is responsible for the degradation of the A and B type cyclins during G1. APC^{CDH1} acts to keep CDK levels low during G1 to facilitate the binding of pre-replication complexes (PRC) to DNA (Miller et al., 2006). Inhibition of APC^{CDH1} activity facilitates

the increase of CDK activity required for activation of the MCM helicase and DNA replication (Li and Zhang, 2009). Additional negative regulation of G1/S progression is provided by the INK4 (p15, p16, p18, p19) CDK inhibitors, which allosterically inhibit the formation of cyclin D-CDK4/6 complexes. Cyclin E-CDK2 inhibition is carried out by the CIP/KIP class of proteins, which include the CDK inhibitors p21 and p27 (Sherr and Roberts, 1999).

DNA replication origin licensing is also required for the G1/S transition. Insufficient origin licensing triggers G1 arrest through reduced cyclin E-CDK2 activity and Rb phosphorylation (Liu et al., 2009; Nevis et al., 2009) and increased activity of p21 and p27 (Machida et al., 2005) in a p53 dependent manner (Nevis et al., 2009). p53 also acts to block the G1/S transition in response to DNA damage through transcription of CDK inhibitors (Agarwal et al., 1995; Giono and Manfredi, 2006).

S phase entry triggers the inactivation of E2F transcription to prevent continued production of replication factors. The cyclin A/CDK2 complex phosphorylates the activator E2Fs, inhibiting DNA binding and blocking their transcriptional activity (Krek et al., 1995; Xu et al., 1994). Phosphorylation of E2Fs also triggers SKP2 mediated ubiquitylation and thus subsequent degradation by the ubiquitin-proteasome system (Hateboer et al., 1996). During G1 this degradation is blocked by the interaction between E2F and retinoblastoma protein, protecting E2F from premature degradation (Hofmann et al., 1996).

In addition to direct regulation of the E2F transcription factors, target gene promoters are also subject to negative regulation during S phase. The repressor E2Fs (E2F4, E2F5, E2F6, E2F7, E2F8) are themselves E2F target genes and accumulate throughout G1. They possess lower DNA binding affinity than the activator E2Fs,

suggesting they bind to DNA when the levels of other E2Fs are reduced. E2F4 and 6 have been found to bind and repress E2F target genes during S phase (Bertoli et al., 2013a; Giangrande et al., 2004), while E2F7 and 8 have been shown to negatively regulate genes characteristic of the G1/S transition (Li et al., 2008; Westendorp et al., 2012).

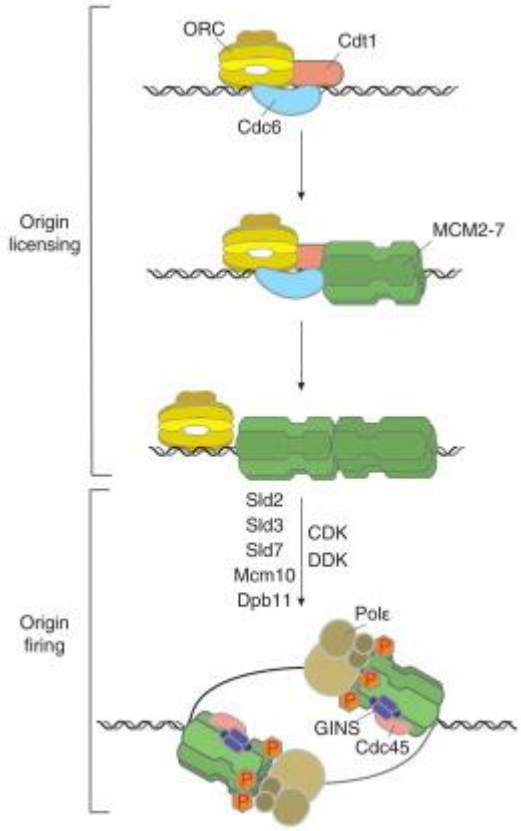


Figure 1.2: Model of replication origin initiation and firing in *Saccharomyces cerevisiae*. ORC, Cdc6 and Cdt1 load the MCM2-7 helicase on to DNA. Origin firing is activated by CDK and DDK dependent phosphorylation, together with several firing factors, including Sld2, Sld3, Sld7, Mcm10, Dpb11 and DNA polymerase ε, which aid the recruitment of Cdc45 and GINS to form the CMG complex, which then activates the helicase activity of the MCM2-7 complex. Adapted from (Hills and Diffley, 2014)

1.2.5 The intra-S checkpoint

Upon commitment to cell cycle entry, cells initiate DNA replication and progress into S phase. During S phase there are 2 main checkpoints through which cells maintain their genomic integrity and protect themselves from DNA damage – the DNA replication checkpoint and the DNA damage checkpoint. These checkpoints are primarily regulated by two checkpoint kinases, ATM (Ataxia Telangiectasia Mutated) and ATR (ATM and Rad3-related). Canonically ATM responds to double-strand DNA breaks, while ATR is activated by the presence of single-stranded DNA, which may result from a wide array of DNA lesions (Cimprich and Cortez, 2008; Harper and Elledge, 2007; Zou, 2007). However, there is extensive crosstalk between the ATM and ATR pathways. As one example, ATR has been shown to be activated in response to double-strand breaks in an ATM-dependent manner (Jazayeri et al., 2006).

In mammalian cells the effector kinases CHK1 and CHK2 function downstream of ATM and ATR, with CHK1 primarily activated by ATR and CHK2 primarily activated by ATM. Upon checkpoint activation the effector kinases phosphorylate multiple targets to block cell cycle progression. CHK1 phosphorylates the cyclin E-CDK2 phosphatase CDC25A, thereby reducing the level of CDK2 activity. Additional negative regulation of CDK2 is provided by direct inhibitory phosphorylation by the WEE1 kinase. Reduced CDK2 activity inhibits CDC45 loading onto pre-replication complexes, preventing the firing of new origins and reducing the rate of DNA replication (Sorensen et al., 2003). Although global activation of late-origin firing is inhibited in response to checkpoint activation to prevent further replication stress

(Yekezare et al., 2013), a large number of dormant origins are activated (Karnani and Dutta, 2011; McIntosh and Blow, 2012). These are origins licensed during the G1 phase of the cell cycle, but not fired during an unperturbed cell cycle. Activation of dormant origins allows completion of replication in the vicinity of stalled forks and so mitigates the consequences of fork arrest.

In both mammals and yeast the intra-S checkpoint also functions to maintain transcription of the G1/S genes that are normally turned off upon S phase entry (Bertoli et al., 2013a; Dutta et al., 2008), which is thought to facilitate re-activation of replication upon resolution of the checkpoint. In *Schizosaccharomyces pombe* this checkpoint induced transcription of MBF genes (the E2F homologue) is dependent on the H3K36 histone methyltransferase, Set2 (Pai et al., 2017).

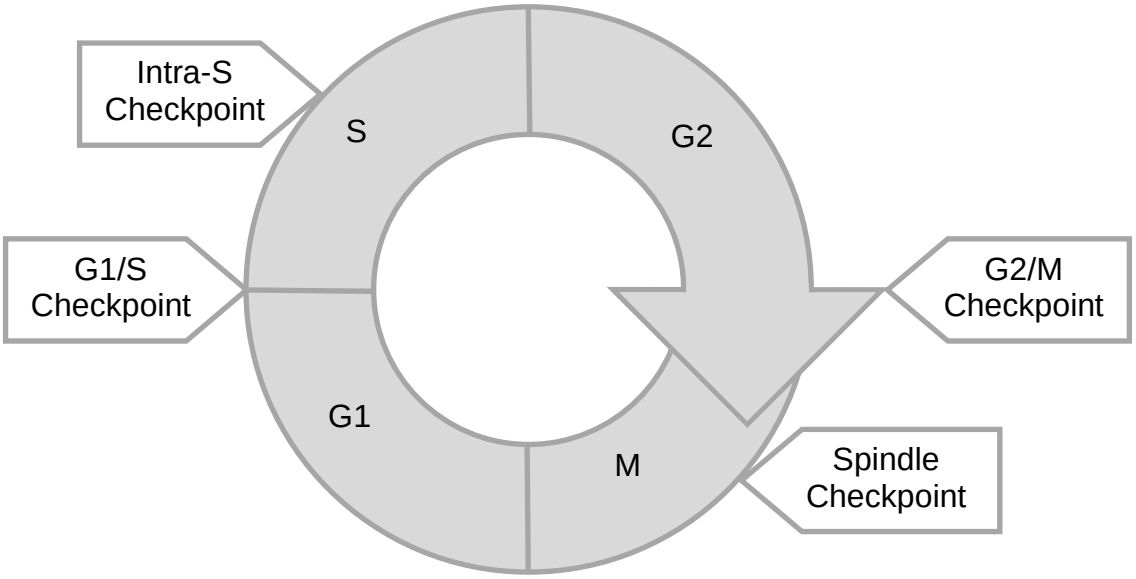


Figure 1.3: A model of canonical cell cycle checkpoints

1.3 DNA replication stress

A consequence of disruption to normal replication is the induction of replication stress. DNA replication stress is a broad term that typically describes the slowing, stalling, or collapse of the replication fork. Replication stress may arise from a variety of sources, including unrepaired DNA lesions, depletion of nucleotide pools, difficult to replicate regions of DNA or collisions between transcription and replication machinery.

Replication stress is a common result of oncogene activation, and present in many cancers. Overexpression of cyclin E, which complexes with CDK2 to drive S phase entry, is a feature of many cancers. In G1. this leads to a reduction in replication origin licensing by driving cells into S phase before licensing has been completed. Increased cyclin E expression in S phase can result in replication stress though over-usage of replication origins, possibly through exhaustion of nucleotide pools.

1.3.1 Replication factor shortage

Insufficient nucleotide supply results in a global inhibition of DNA replication, and consequently stalling of replication forks. ssDNA at stalled forks triggers activation of the S phase checkpoint (Sogo et al., 2002), as discussed in section 1.2.5. Depletion of dNTP pools can also lead to incorporation of rNTPs (ribonucleoside triphosphates) (Reijns et al., 2012), as the cellular concentration of rNTPs is much greater than that of dNTPs. Incorporation of rNTPs leads to stalling of the replication fork (Yao et al., 2013), and further sensitises cells to replication stress (Lazzaro et al., 2012), ultimately leading to genomic instability (Nick McElhinny et al., 2010).

Insufficiency is not restricted to nucleotide pools, and replisome proteins can also become limiting. CDC45 has been found to be rate limiting for replication initiation

(Kohler et al., 2016; Tanaka et al., 2011), and its overexpression results in exhaustion of replication protein A (RPA), the single-stranded DNA binding protein. This in turn can lead to an increase in exposed single-stranded DNA, replication fork collapse, and double-strand DNA breaks (Toledo et al., 2013). CDC45 is a target of the proto-oncogene MYC (Srinivasan et al., 2013), which is frequently overexpressed cancer, demonstrating another mechanism through which replication stress may arise in cancers.

1.3.2 Replication-transcription conflicts

Increased replication origin firing also increases the possibility of collisions between replication and transcription machinery. As transcription and replication occur simultaneously along the same DNA template, conflicts between the two processes are inevitable. Head-on collisions between the replisome and the transcription machinery may result in stalling of the RNA polymerase and slowing of the replication fork (Pomerantz and O'Donnell, 2010). Collisions are also associated with increased levels of DNA:RNA hybrids termed R-loops (Huertas and Aguilera, 2003; Wahba et al., 2011), which induce genomic instability, possibly by impeding progression of the replication fork (Gan et al., 2011; Macheret and Halazonetis, 2018).

1.4 Post-translational histone modifications

In eukaryotic cells, DNA is packaged into compact units called nucleosomes by wrapping around small, highly alkaline proteins called histones. There are four core histone proteins (H2A, H2B, H3 and H4) and two linker histones (H1 and H5). The

core histones form a H3/H4 tetramer that associates with two H2A/H2B dimers to form the octamer that comprises(Li et al., 2015; Yang et al., 2016) the core particle of the nucleosome (Kornberg, 1974; Kornberg and Thomas, 1974). The core histones have a tail-like structure that protrudes from the core octamer, which are the location of various post-translational modifications (Figure 1.4).

Post-translational histone modifications play a key role in the regulation of gene expression, cell cycle progression and genome stability. Histones can be subject to a wide variety of modifications including methylation, acetylation, ubiquitylation and phosphorylation (Bannister and Kouzarides, 2011), impacting a wide range of DNA processes. Histone modifications have also been associated with cancer (Audia and Campbell, 2016), with mis-regulation leading to oncogenic changes in gene expression (Varier and Timmers, 2011), impaired recruitment of DNA repair genes (Hauer and Gasser, 2017; Jeggo et al., 2017), and dysregulated cell cycle progression.

1.4.1 The histone code

The modifications present on histone tails may also function as binding sites for effector proteins, which are then able to affect transcription or chromatin structure, known as the histone code hypothesis. The first protein domain shown to interact with a covalent histone modification is the bromodomain, which recognises an acetylated lysine residue (Dhalluin et al., 1999; Winston and Allis, 1999). Bromodomains are found in over forty different proteins with diverse functions, including transcription factors and co-regulators, protein scaffolds, or chromatin-remodelling proteins (Fujisawa and Filippakopoulos, 2017).

Several domains capable of binding histone methyl-lysine residues have been identified, the first of which was the chromodomain (Bannister et al., 2001; Lachner et al., 2001). Chromodomain containing proteins recognise methylated H3K9 and H3K27, and other, related domains that interact with other lysine residues have since been identified (Kim et al., 2006; Qin and Min, 2014). As with proteins that recognise acetylated lysine residues, methyl-lysine binding proteins are involved in a wide range of processes, including DNA methylation (Dhayalan et al., 2010), DNA repair factor recruitment (Botuyan et al., 2006; Charier et al., 2004), and histone demethylation (Huang et al., 2006).

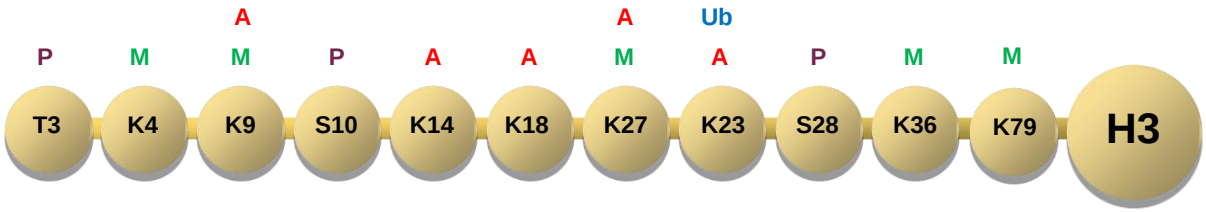


Figure 1.4: **Histone tails can be modified by the addition of a number of different molecules to facilitate recruitment or binding of downstream factors.** Several examples of common physiological post-translational modifications of the tail of histone H3 are shown. A = acetylation, M = methylation, P = phosphorylation, Ub = ubiquitylation

1.4.2 Histone modifications in cell cycle regulation

It has long been known that histone modifications change throughout the cell cycle, and the levels of many histone modifying enzymes fluctuate throughout the cell cycle. However, in many cases cell cycle progression itself is dependent on the chromatin landscape and timely histone modifications. As a consequence of this, disruption of the normal histone modification profile can be a key factor in oncogenesis (Sawan and Herceg, 2010).

1.4.2.1 Histone acetylation

Acetylation is a reversible modification of lysine residues in the tails of the core histones. Histone acetyltransferases catalyse the transfer of an acetyl group from acetyl coenzyme-A (acetyl CoA) to the histone tail, which can be removed by a family of enzymes called histone deacetylases (HDACs).

Histone acetylation is a major determinant of local chromatin conformation, and functions to regulate the folding and compaction of chromatin (Shahbazian and Grunstein, 2007). A more open chromatin state facilities access for transcriptional machinery, and so histone acetylation is canonically associated with actively transcribed chromatin, while deacetylation is usually indicative of transcriptional repression.

One example of this is the histone deacetylase HDAC1, which is recruited by pRB to repress transcription by the E2F transcription factors and block G1 progression (Brehm et al., 1998; Magnaghi-Jaulin et al., 1998). Interestingly, depletion of HDAC1 and 2 in combination leads to G1 arrest, indicating additional roles for HDAC1 during G1 (Yamaguchi et al., 2010).

Along with HDACs 1 and 2, numerous other histone deacetylases have been found to be involved in the G1/S transition. siRNA depletion of HDAC3 (Bhaskara et al., 2008), HDAC5 (Peixoto et al., 2012), HDAC6 (Namdar et al., 2010), HDAC7 (Zhu et al., 2011), HDAC8 (Dasgupta et al., 2016) and HDAC9 (Zhang et al., 2016) have all been found to lead to impaired G1 progression and S phase entry, while depletion of HDAC4 leads to increased cell cycle progression (Majdzadeh et al., 2008). Loss of HDAC10 has been shown to lead to both G1 and G2/M arrest (Li et al., 2015; Yang et al., 2016), suggesting other HDACs may also have roles at multiple stages of the cell cycle.

1.4.2.2 Histone methylation

In addition to histone acetylation, other modifications can also direct cell cycle progression. Histone methylation occurs on basic residues: lysine, arginine and histidine, although lysine methylation is by far the most well studied. Lysine residues can be reversibly mono, di, or tri methylated by two main families of histone methyltransferases. The SET-domain containing proteins (Rea et al., 2000) are grouped by the presence of a catalytic SET domain, while the DOT1-like proteins instead have a different catalytic domain (Feng et al., 2002; Min et al., 2003).

Lysine residues methylated by both groups of enzymes have been implicated in cell cycle regulation. H3K4 methylation by the COMPASS (Complex Proteins Associated with Set1) complex has been found to be involved in mitotic spindle assembly, as well as expression of genes involved in the G1/S transition (Beilharz et al., 2017). Depletion of two other H3K4 methyltransferases, MLL1 and MLL5, resulted in

decreased expression of E2F target genes and G1 arrest (Tyagi et al., 2007; Zhou et al., 2013), suggesting correct methylation of H3K4 is important for G1/S progression.

Methylation at H3K9 has been shown to have several important roles in regulating cell cycle progression. H3K9 trimethylation (in combination with H4K20 methylation) is required for proper chromosome condensation (Park et al., 2011), while the mono-methyltransferase SUV39H1 acts to repress E2F activity in concert with Rb during G1 (Vandel et al., 2001), and to co-ordinate chromosome segregation in mitosis (Heit et al., 2009; Melcher et al., 2000).

H3K27 methylation is another mark that has a strong connection to the G1 phase of the cell cycle. pRB and the pocket proteins are required H3K27 trimethylation by the methyltransferase EZH2, which then also methylates the CDK inhibitor p16 to help drive cell cycle progression (Kotake et al., 2007). Consistent with this, as cells progress through G1 H3K27me3 levels increase, and this is required for progression into S phase (Aoto et al., 2008).

DOT1L catalyses the methylation of H3K79, and has been implicated in the regulation of several different cell cycle phases. Loss of DOT1L blocks cell cycle progression, leading to accumulation of cells in G1 phase (Kim et al., 2012b; Schulze et al., 2009). DOT1L deficiency has also been seen to result in re-initiation of replication (Fu et al., 2013), suggesting a role for H3K79 methylation in determining replication timing. Depletion of DOT1L was also found to result in aneuploidy, which may indicate a role in chromosomal stability or regulation of cell division (Barry et al., 2009; Jones et al., 2008).

Timely removal of histone methylation has also been found to be required for normal cell cycle progression. Depletion of several different histone demethylases results in

cell cycle arrest at the G1/S boundary including KDM3A (Cho et al., 2012), KDM4B (Duan et al., 2015), KDM5B (Wang et al., 2016), and PHF8 (Liu et al., 2010).

1.4.3 Histone H3K36 Trimethylation

1.4.3.1 H3K36me3 in cancer

H3K36 trimethylation (H3K36me3) is a histone mark that has been strongly implicated in oncogenesis, although its role in the cell cycle is still unclear. In humans H3K36 mono and dimethylation is catalysed by seven enzymes (NSD1 (Rayasam et al., 2003), NSD2 (Kuo et al., 2011), NSD3 (Angrand et al., 2001), SETMAR (Lee et al., 2005), ASH1L (Tanaka et al., 2007), SETD3 (Kim et al., 2011)), while SETD2 (the human homologue of Set2) is the only characterised trimethlytransferase for H3K36 in the somatic cell cycle (Edmunds et al., 2008; Sun et al., 2005). During meiosis H3K36 can also be trimethylated by the PRDM9 methyltransferase (Diagouraga et al., 2018; Eram et al., 2014; Powers et al., 2016). The SETD2 protein consists of a WW domain (Gao et al., 2014), an SRI domain (Li et al., 2005), and the catalytic SET domain. The SRI domain mediates the interaction between SETD2 and the C-terminal domain of RNA Pol II (Li et al., 2002), although it is not required for catalytic activity of SETD2 (Hacker et al., 2016).

Mutations in SETD2 have been identified in a number of different cancer types including kidney, breast, lung, ALL (acute lymphoblastic leukaemia) and high-grade glioma (Al Sarakbi et al., 2009; Duns et al., 2010; Fontebasso et al., 2013; Gerlinger et al., 2012; Hakimi et al., 2013; Li et al., 2016b; Newbold and Mokbel, 2010; Zhang et al., 2012). These mutations are typically found within the SET or SRI domains of

SETD2, and predominantly lead to a non-functional or truncated protein and loss of H3K36me3 (Hacker et al., 2016).

Demethylation of H3K36me3 is catalysed by the KDM4 (also known as JMJD2) family of demethylases (Whetstine et al., 2006), overexpression of which has also been associated with various cancer types (Berry and Janknecht, 2013). Additionally, mutations in histone H3.3 that reduce the levels of H3K36me3 (G34R/V, K36M) have been identified in paediatric gliomas and bone malignancies (Behjati et al., 2013; Fontebasso et al., 2013; Wu et al., 2012) leading to alterations in the histone methylation landscape and gene expression profile (Bjerke et al., 2013; Chan et al., 2013; Fang et al., 2016).

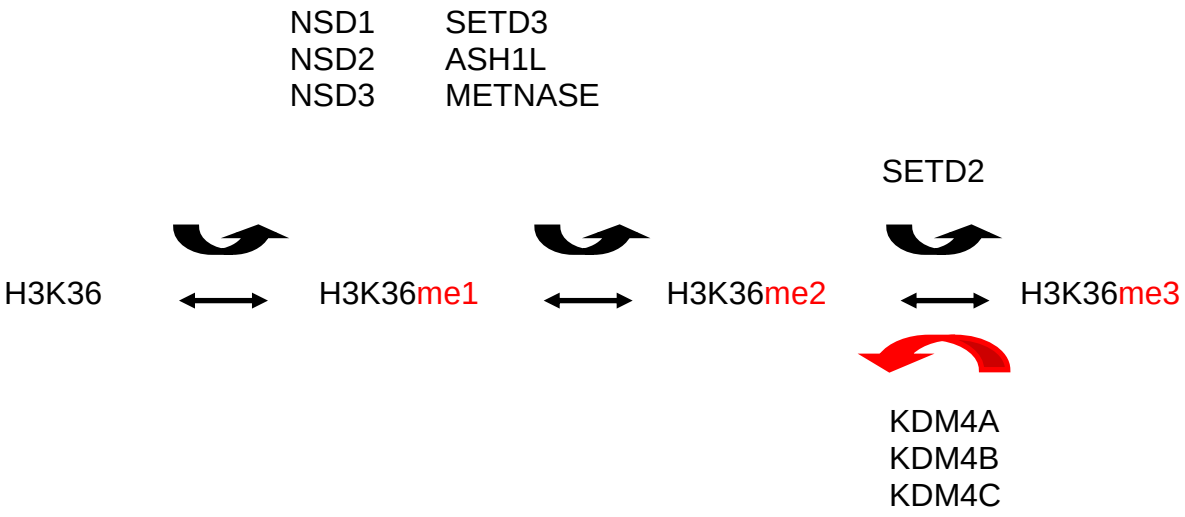


Figure 1.5: Enzymes responsible for the methylation and demethylation of histone H3 lysine 36

1.4.3.2 H3K36 methylation in DNA repair

As with a number of other histone modifications, H3K36 methylation has been shown to have important roles in the activation and regulation of DNA repair pathways. In *Schizosaccharomyces pombe,* the H3K36 methylation state is associated with double-strand break repair pathway choice (Pai et al., 2014). In mammalian cells, H3K36me2 levels are increased at sites of double-strand breaks, and act to promote non-homologous end joining (NHEJ) (Fnu et al., 2011), while H3K36 trimethylation is required for repair by homologous recombination (HR) (Carvalho et al., 2014; Pfister et al., 2014). As H3K36me3 is typically found in actively transcribed genes (Bannister et al., 2005; Edmunds et al., 2008), double-strand breaks in transcriptionally active regions are preferentially repaired by the more accurate homologous recombination, while other regions are repaired by NHEJ (Aymard et al., 2014). In addition to its role in repair of double-strand breaks, H3K36 trimethylation has also been implicated in DNA mismatch repair through an interaction with hMutSα (Li et al., 2013), while in yeast it has been found to recruit nucleotide excision repair factors (Lim et al., 2018).

1.4.3.3 H3K36 methylation in DNA replication

In addition to described roles in regulation of gene expression and recruitment of DNA repair factors, a role for H3K36me3 in DNA replication has been suggested. In both yeast and humans H3K36me3 is cell cycle regulated, peaking during the G1 phase of the cell cycle, before declining upon S phase entry (Li et al., 2013; Pai et al., 2014).

In *Schizosaccharomyces pombe,* the H3K36 methyltransferase set2 is thought to regulate origin firing though regulation of Cdc45 binding to replication origins (Pryde

et al., 2009). Set2 is also required for transcription of MluI cell-cycle box (MCB) binding factor (MBF) target genes, including ribonucleotide reductase (RNR), and loss of Set2 leads to reduced levels of dNTP synthesis and subsequently to delayed S phase progression (Pai et al., 2017).

Consistent with a potential conserved role in DNA replication, loss of human SETD2 leads to decreased replication fork speed and induction of replication stress (Kanu et al., 2015; Pfister et al., 2015). However, the role of SETD2 in mammalian DNA replication has not yet been fully explored.

1.5 Synthetic lethality with WEE1 inhibition

1.5.1 SETD2 and WEE1

As SETD2 has been identified as a key tumour suppressor in a range of cancers, potential methods to target cancers deficient in H3K36me3 have been investigated. A synthetic lethal interaction was discovered between loss of H3K36me3 and inhibition of the cell cycle kinase WEE1. Synthetic lethality describes a situation where loss of either of a pair of genes does not impact cell viability, but loss of both in combination leads to cell death. Loss of either WEE1 or SETD2 alone leads to depletion of the ribonucleotide reductase subunit RRM2, and loss of both together results in insufficient nucleotide pools and subsequent replication catastrophe (Figure1.7) (Pfister et al., 2015).

1.5.2 The WEE1 kinase

WEE1 is a protein kinase that is responsible for inhibitory phosphorylation of the cyclin-dependent kinases CDK1 and CDK2 at T14 and Y15 (Den Haese et al., 1995). Inhibition of CDK1 results in cell cycle arrest, and so WEE1 plays a key role in regulating cell cycle progression. WEE1 is activated in response to DNA damage during both G1 and G2, blocking further progression until the damage has been resolved (Beck et al., 2012; Rhind and Russell, 2001).

Disruption of the DNA damage checkpoints results in unchecked cell cycle progression with unrepaired damage, leading to mitotic or replication catastrophe. Cancer cells typically harbour high levels of endogenous DNA damage (Tubbs and Nussenzweig, 2017) and deficiency in one or more checkpoints (Laiho and Latonen, 2003), and so cancer cells may be more susceptible to WEE1 inhibition than non-transformed cells.

As a result, WEE1 has become an attractive target for potential cancer therapies. The WEE1 inhibitor AZD1775 (formerly MK1775) was first developed to target specifically p53 deficient cancers (Hirai et al., 2009; Mizuarai et al., 2009), although it has since been expanded to target other cancers, including those deficient in SETD2.

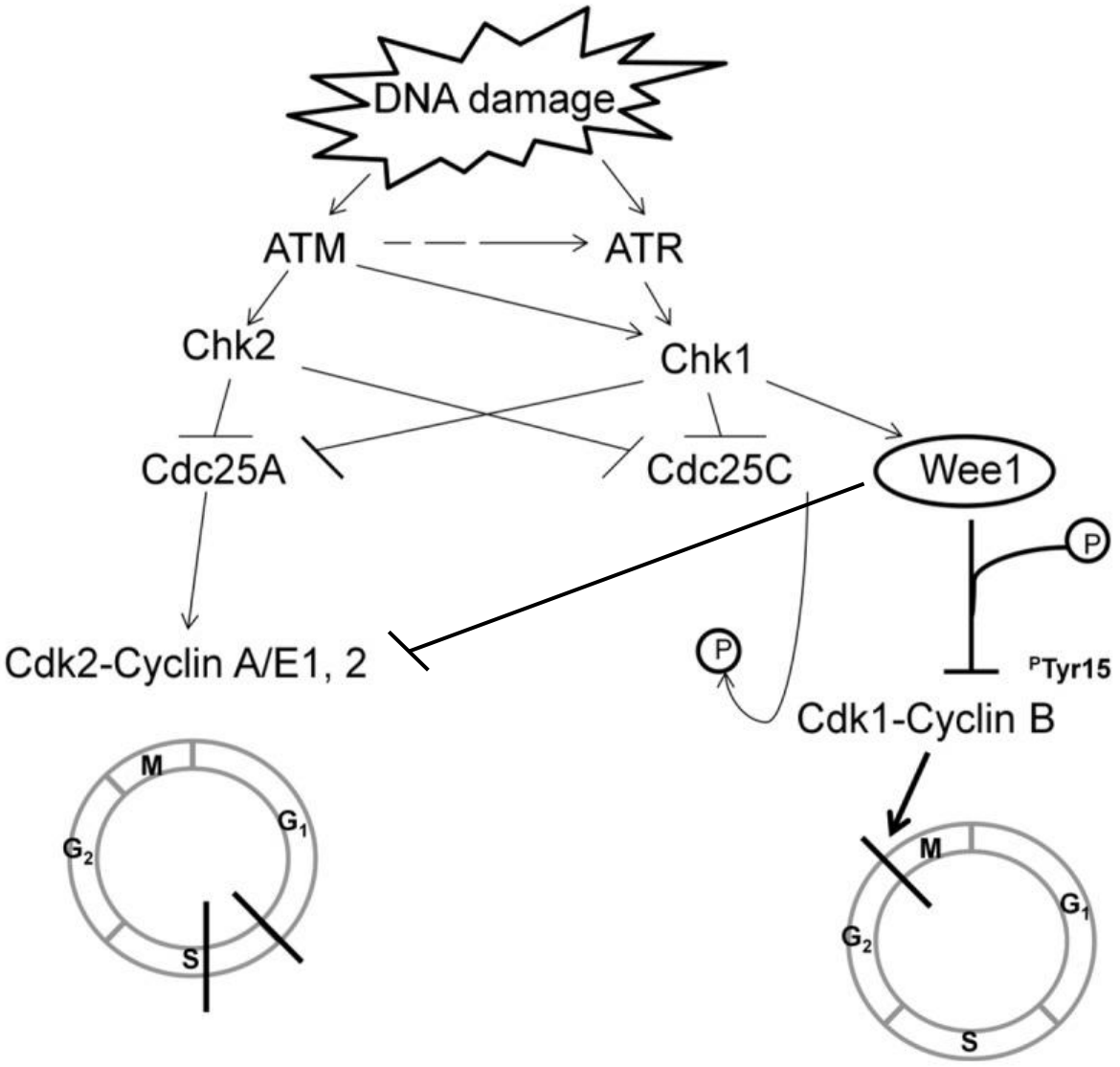


Figure 1.6: Schematic of the role of WEE1 in the DNA damage response. WEE1 is activated as part of the ATM/ATR pathway and functions to inhibit the activity of CDK1 and CDK2. Adapted from (Do et al., 2013)

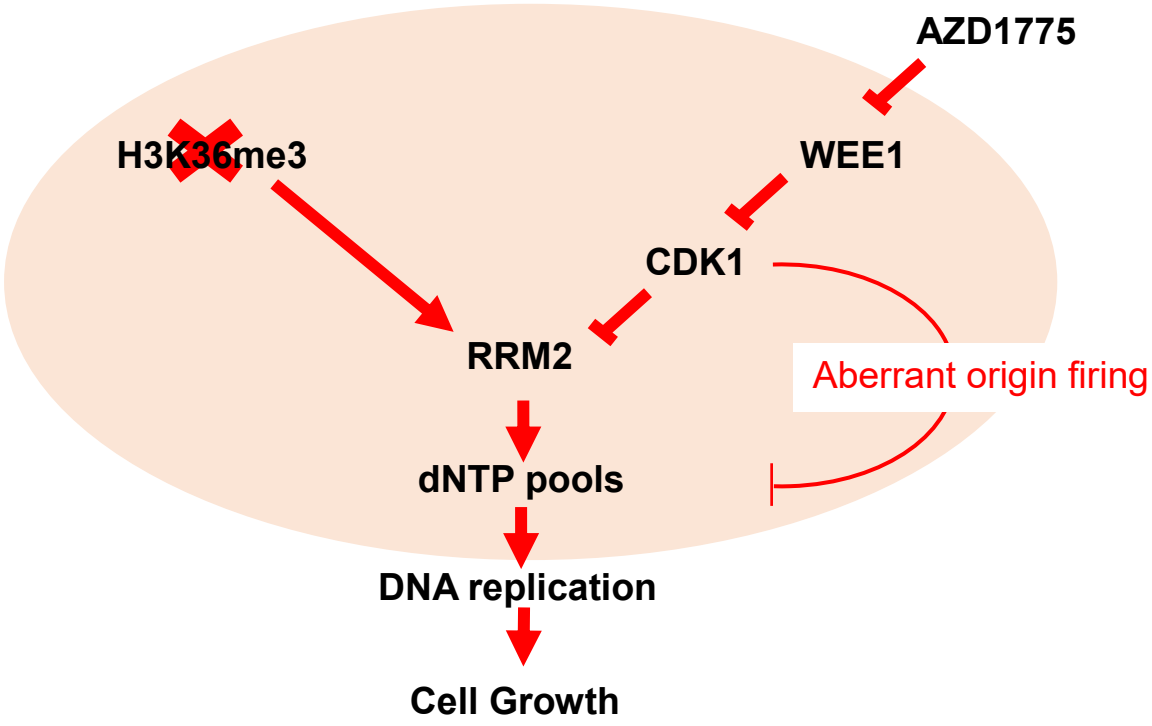


Figure 1.7: Loss of H3K36me3 is synthetic lethal with inhibition of WEE1. Depletion of both H3K36me3 and WEE1 leads to mutual depletion of RRM2, leading to depletion of nucleotide pools and replication fork stalling.

1.6 Thesis aims

1.6.1 Understanding the how SETD2 regulates RRM2

In both yeast and humans H3K36me3 and its methyltransferase have been identified as key regulators of nucleotide pools and DNA replication. A conserved synthetic lethality exists between loss of H3K36me3 and loss of WEE1, leading to nucleotide pool exhaustion and S phase arrest.

In yeast, loss of Set2 regulates expression of the ribonucleotide reductase subunit Cdc22 though the MBF transcription factor complex. In mammalian cells, expression of the Cdc22 homologue RRM2 is reduced in SETD2 deficient cells, and so the first aim of this thesis was to investigate the hypothesis that H3K36me3 regulates E2F target gene expression in humans.

1.6.2 Investigating a role for SETD2 in the replication stress response

In addition to regulating MBF target gene expression under normal cell cycle conditions, Set2 also facilitates MBF-dependent transcription in response to genotoxic stress to help prevent induction of DNA damage. As loss of SETD2 has been found to result in increased levels of replication stress, the second aim of this thesis was to explore a potential role for SETD2 and H3K36me3 in the replication stress response.

1.6.3 Exploring synthetic lethal interactions with WEE1 inhibition

As promising results have been seen with WEE1 inhibition in SETD2 deficient cancers, it is desirable to identify additional mutations that may be targetable with WEE1 inhibition. The final aim of this thesis was to explore potential novel synthetic lethalities with WEE1 inhibition.

Chapter 2

Methods

2.1 Resuscitation of frozen cell lines

Cells stored in liquid nitrogen were rapidly thawed at 37°C for 3 minutes. The cells were washed once with 10 ml complete media to remove DMSO from the freezing media, and pelleted by centrifugation at 1300 rpm for 3 minutes. The supernatant was removed and the cell pellet was resuspended in 5ml complete media and transferred to a T25 tissue culture flask.

2.2 Maintenance of cell lines

All cell lines were maintained in complete media consisting of Dulbecco's modified minimal essential media (DMEM) (Invitrogen) supplemented with 10% foetal bovine serum (FBS) (Invitrogen), 100U penicillin and 0.1 mg/ml streptomycin (Sigma). All cells were grown at 37°C in a humidified incubator with 5% carbon dioxide. Cells were passaged every 3 days, where cells were washed with phosphate buffered saline (PBS) and then incubated with Trypsin-EDTA for 5-10 minutes at 37°C. Trypsinised cells were re-suspended in complete media and re-plated at a 1:5 dilution. U2OS KDM4A FLIPIN TREX cells were maintained in selection media (100 µg/ml Hygromycin and 15 µg/ml Blasticidin S) and overexpression induced by addition of 5 µM Doxycycline.

2.3 Cryopreservation of cell lines

Log-phase growing cells were trypsinised as described above. 1 x 10^6 cells were spun down at 1300 rpm for 3 minutes and re-suspended in 1 ml freezing media (FBS containing 10% (v/v) tissue culture ready DMSO (Sigma)). The suspension was transferred to a cyrovial and frozen at -80C overnight before being transferred into liquid nitrogen for long-term storage.

2.4 Cell lines

The U2OS cell line was derived from human osteosarcoma and obtained from ATCC (ATCC number HTB-96).

The U2OS SETD2 CRISPR cell line was generated by Dr Sovan Sarkar and Dr Sophia Pfister.

The H1299 cell line was derived from human non-small cell lung carcinoma and obtained from the lab of Dr Andy Ryan.

The MCF7 cell line was derived from human metastatic breast cancer and obtained from the lab of Dr Ross Chapman

The MCF7 p53 CRISPR cell line was generated in the lab of Dr Ross Chapman

The RPE cell line was derived from human retinal pigment epithelium and obtained from the lab of Dr Ross Chapman.

The RPE p53 CRISPR cell line was generated in the lab of Dr Ross Chapman

The T98G cell line was derived from human glioblastoma and obtained from the lab of Dr Rob De Bruin.

2.5 Cell Cycle Synchronisation

Synchronisation of T98G cells in G1 was achieved by culturing cells in FBS free DMEM for 40-48 hours. Cells were released from G1 arrest by addition of complete media. U2OS cells were synchronised by addition of 40 μM lovastatin, and released by addition of 4mM mevalonate.

2.6 Bacterial transformation

Chemically competent E. coli DH5α cells (produced in-house by Carol Walker) were used for plasmid amplification. 1.5 μl of plasmid DNA (1 pg-100 ng) was added to 50μl of competent cells. The mixture was incubated on ice for 30 minutes, heat-shocked at 42^{o}C for 30 seconds, left on ice for 5 minutes and allowed to recover in 1 ml super optimal broth for 1 hour at 37^{o}C with shaking. 50-100 μl of the mixture was plated onto a selection plate and incubated overnight at 37^{o}C. Depending on the plasmid backbone, selection of the plasmid-carrying bacteria clones was achieved by adding either 100 μg/ml ampicillin or 50 μg/ml kanamycin to the LB agar plates.

2.7 Plasmid purification

Plasmid purification from bacterial cultures was performed using QIAprep spin miniprep kits (Qiagen) according to the manufacturer's instructions. The QIAprep columns contain a silica membrane that binds DNA in the presence of a high concentration of chaotropic salt, and allows DNA elution in low-salt buffer or water. In summary, following overnight growth in 5ml of selective LB in a 50 ml tube, bacterial cells were harvested by centrifugation at 4000g for 20 minutes. The pellet was re-

suspended in 250µl P1 buffer (containing RNase A) and cells were lysed by addition of 250µl P2 buffer and inverting. The lysis buffer was neutralised by adding 350µl of P3 buffer. Cell debris and genomic DNA were precipitated from the solution by centrifugation at 13,000rpm for 10 minutes at room temperature. The supernatant (containing plasmid DNA) was pipetted into a QIAprep spin column and centrifuged for 1 minute at 13,000rpm, and the flow-through was discarded. The plasmid DNA bound to the silica membrane was washed with 0.75ml PE buffer to remove impurities. The plasmid DNA was eluted by incubating 50 µl H2O in the column for 1 minute before centrifugation into a collection tube.

2.8 siRNA transfection

All siRNAs (20nM final concentration) were delivered to the cells by RNAiMAX (Invitrogen) according to manufacturer's instructions. Cells were treated with the siRNA/RNAiMAX mixture in suspension (reverse transfection). The media was changed after 48 hours and knockdown efficiency determined by western blotting.

siSETD2 (Dharmacon): UAAAGGAGGUAUAUCGAAU

E2F7 (Dharmacon): AAAGGTACGACGCCTCTATGA

Rb (Dharmacon): L-003296

CDC6 (Dharmacon): L-003233

E2F1 (Santa Cruz): ACUGACCAUCAGUACCUGGUU

CDKN1A (Dharmacon): L-003471

ZMYND11 (Dharmacon): L-006936

MORF4L (Dharmacon): L-006379

HDAC2 (Dharmacon): L-003495

ON-Target *plus* SMART pool siRNA library - Cell Cycle Regulation (Dharmacon): G-103200

ON-Target *plus* SMART pool siRNA library - DNA Damage Response (Dharmacon): G-106005

Custom ON-Target plus SMART pool siRNA of Tumour Suppressor Genes (Dharmacon): Full Sequences are listed in the appendix

2.9 Western blots

Cells were lysed in lysis buffer (50 mM Tris HCl pH7.5, 150 mM NaCl, 1% Triton X-100, supplemented with protease and phosphatase inhibitors) for 30 minutes on ice (with intermittent vortexing). The lysate was centrifuged for 10 minutes at 13,000 rpm to pellet cellular debris. The supernatant was transferred to fresh tubes and protein concentrations determined using the Bradford assay. 25µg of protein was mixed with the NuPAGE LDS loading buffer (Invitrogen) and the reducing agent Dithiothreitol (DTT), and denatured by boiling at 95°C for 5 minutes. Samples and molecular weight ladder (Invitrogen) were loaded onto pre-cast NuPAGE gels (Invitrogen) and electrophoresis was performed according to the manufacturer's instructions. Proteins were transferred onto a PVDF or nitrocellulose membrane (0.2 or 0.45µm pore size) in a transfer unit (Invitrogen) at 30V for 2 hours according to manufacturer's instructions. The membrane was blocked in blocking buffer (PBS containing 5% skimmed milk and 0.1% Tween) for 1 hour at room temperature before incubating

with the primary antibody diluted in the blocking buffer at 4°C overnight. After washing at least three times with PBS-T (PBS containing 0.1% Tween), the membrane was incubated with a HRP-conjugated secondary antibody diluted 1:4000 in the blocking buffer for 1 hour at room temperature. After again washing with PBS-T, the proteins on the membrane were visualised with the ECL Chemiluminescence substrates (Thermo Scientific) according to the manufacturer's instructions.

The following antibodies were used (Unless otherwise specified antibodies were used at a dilution of 1:1000):

H3K36me3 (Abcam, 9050), Histone H3 (Abcam,10799), RRM2 (Santa Cruz), p53 (Santa Cruz), GAPDH (Novus, 1:10000), p21 (Cell Signalling), Flag Tag (Sigma), Tubulin (Santa Cruz), E2F1 (Santa Cruz), CDC6 (Santa Cruz), MCM2 (Cell Signalling), KDM4A (Abcam)

2.10 Inhibitors

Concentrations indicated in figure legends

WEE1 - AZD1775 (Sigma)

ATR - VE822 (Sigma)

Hydroxyurea (Sigma)

2.11 Resazurin assay for cell viability

Equal numbers of cells were seeded in a 96-well plate 24 hours before inhibitor treatment. DMSO was used as a negative control and as a solvent for the inhibitors. 48 hours after addition of inhibitors the media were removed and fresh media containing Resazurin was added to each well. Resazurin is a nonfluorescent dye, which is converted by redox reaction to red fluorescent resorufin by living cells. The fluorescent signal is proportional to the number of living cells, and was measured by a fluorescence plate reader (BMG Lab-tech).

2.12 Cell cycle analysis by BrdU incorporation

Cells were incubated in media containing 20μM BrdU for 20 minutes at37◦C. Cells were then collected by trypsinisation and fixed in cold 70% ethanol. Cells were incubated for 20 minutes at room temperature in 2 m HCl (which denatures double-stranded DNA), containing 0.1 mg/ml pepsin (which digests nuclear proteins to expose DNA). Cells were then washed in PBS, and washed in PBS containing 0.5% FBS and 0.5% Tween. Cells were incubated in the blocking buffer (PBS with 2% FBS) containing the anti-BrdU monoclonal antibody (BD Biosciences) (1:100 dilution) for 90 minutes at room temperature. Cells were washed twice with PBS and incubated in blocking buffer containing the Alexa Fluor 488 secondary antibody (Invitrogen, 1:200 dilution) for 60 min at room temperature protected from light. Cells were then washed in PBS and resuspended in PBS containing 0.1 mg/ml propidium iodide, and analysed by FACS Scan (Becton Dickinson).

2.13 RNA extraction

RNA was extracted using RNeasy mini kit (Qiagen) according to the manufacturer's instructions. RNA concentration and 260/280 ratio were determined using a NanoDrop, ND-1000 spectrophotometer (Thermo Scientific).

2.14 RNA-Seq Library preparation and Illumina sequencing

Library preparation and Illumina sequencing was performed by technical staff at Novogene Co Ltd. Duplicate samples of wildtype and SETD2 CRISPR isogenic U2OS treated were treated with 200nM AZD1775 or 2nM hydroxyurea for 48 hours. A total amount of 3 μg RNA per sample was used as input material for the RNA sample preparations. Ribosomal RNA was removed using the Epicentre Ribo-zeroTM rRNA Removal Kit (Epicentre, USA) according to the manufacturer's instructions, and rRNA free residue was cleaned up by ethanol precipitation. Subsequently, sequencing libraries were generated using the rRNA-depleted RNA by NEBNext® UltraTM Directional RNA Library Prep Kit for Illumina® (NEB, USA) following manufacturer's recommendations. Briefly, fragmentation was carried out using divalent cations under elevated temperature in NEBNext First Strand Synthesis Reaction Buffer(5X). First strand cDNA was synthesized using random hexamer primer and M-MuLV Reverse Transcriptase (RNaseH-). Second strand cDNA synthesis was subsequently performed using DNA Polymerase I and RNase H. In the reaction buffer, dNTPs with dTTP were replaced by dUTP. Remaining overhangs were converted into blunt ends via exonuclease/polymerase activities. After adenylation of 3' ends of DNA fragments, NEBNext Adaptor with hairpin loop structure were ligated to prepare for hybridization. In order to select cDNA fragments of preferentially 150~200 bp in length, the library fragments were purified with

AMPure XP system (Beckman Coulter, Beverly, USA). Then 3 µl USER Enzyme (NEB,USA) was used with sizeselected, adaptor-ligated cDNA at 37°C for 15 min followed by 5 min at 95°C before qRT-PCR. Then qRT-PCR was performed with Phusion High-Fidelity DNA polymerase, Universal PCR primers and Index (X) Primer. Finally, products were purified (AMPure XP system) and library quality was assessed on the Agilent Bioanalyzer 2100 system. Clustering of the index-coded samples was performed on a cBot Cluster Generation System using HiSeq PE Cluster Kit cBot-HS(Illumina) according to the manufacturer's instructions. After cluster generation, the library preparations were sequenced on an Illumina Hiseq platform and paired-end reads were generated. Cuffdiff (v2.1.1) was used to calculate FPKMs of both lncRNAs and coding genes in each sample. Gene FPKMs were computed by summing the FPKMs of transcripts in each gene group. FPKM means fragments per kilo-base of exon per million fragments mapped, calculated based on the length of the fragments and reads count mapped to this fragment.

2.15 qRT-PCR (Quantitative reverse transcription polymerase chain reaction)

qRT-PCR was performed to analyse the relative levels of a specific RNA sequence, in this case to measure the changes in mRNA levels. Total RNA was purified using the RNeasy kit (Qiagen) and cDNA was prepared using the SuperScript III RT-PCR system (Invitrogen). Quantitative RT-PCR was performed using Absolute Blue QPCR SYBR Green (Thermo Scientific) according to the manufacturer's protocol. Reactions were carried out in duplicates for each target transcript using a 7500 Fast Real-Time PCR System (Applied Biosystems). The comparative CT method was applied for quantifying the gene expression, and values were normalised against

GAPDH as a control. Results were expressed as fold changes compared to the control condition. The following primers were used (all primers depicted 5’ to 3’):

MORF4L1 Forward	AGCAATGTTGGCTTATACACCTC
MORF4L1 Reverse	AGCTTTCCGATGGTACTCAGG
ZMYND11 Forward	ATGGCACGTTTAACAAAAAGACG
ZMYND11 Reverse	CGGTCAATGTTGGCAATCTGC
PFH1 Forward	CTGATGGGCTGCTATACTTGG
PFH1 Reverse	GAAACTGCGAATCATCCTCAAAC
HDAC1 Forward	CTACTACGACGGGGATGTTGG
HDAC1 Reverse	GAGTCATGCGGATTCGGTGAG
HDAC2 Forward	ATGGCGTACAGTCAAGGAGG
HDAC2 Reverse	TGCGGATTCTATGAGGCTTCA
E2F1 Forward	ACGCTATGAGACCTCACTGAA
E2F1 Reverse	TCCTGGGTCAACCCCTCAAG
E2F2 Forward	CGTCCCTGAGTTCCCAACC
E2F2 Reverse	GCGAAGTGTCATACCGAGTCTT
Cyclin D1 Forward	GCTGCGAAGTGGAAACCATC
Cyclin D1 Reverse	CCTCCTTCTGCACACATTTGAA
Cyclin E2 Forward	AAGGAGCGGGACACCATGA
Cyclin E2 Reverse	ACGGTCACGTTTGCCTTCC

CDC6 Forward	TGTTCTCCTCGTGTAAAAGCC
CDC6 Reverse	GGGGAGTGTTGCATAGGTTGT
CDT1 Forward	CGGTGGACGAGGTTTCCAG
CDT1 Reverse	CTGCCGGGGTGGATTTCTT
MCM2 Forward	CCGTGACCTTCCACCATTTGA
MCM2 Reverse	GGTAGTCCCTTTCCATGCCAT
CDKN1A Forward	TGTCCGTCAGAACCCATGC
CDKN1A Reverse	AAAGTCGAAGTTCCATCGCTC
SETD2 Forward	CCTGGGGAATTCAACCCTGC
SETD2 Reverse	ATGTTTCAGGTTCAGGGGGAG
MGA Forward	GTCATCGGGTCCGTCTTACAG
MGA Reverse	TGAGGCTACACGGGAGTCAT
ZMYM3 Forward	TTCCCCAGTCCATTTGACCC
ZMYM3 Reverse	GGATTCCAGTAGATCCTCTCCAA
MSH6 Forward	CCAAGGCGAAGAACCTCAAC
MSH6 Reverse	ACCAGGGGTAACCCTCCATC
ZFHX3 Forward	CAAGTTCACGACGGACAACCT
ZFHX3 Reverse	GCTTGCACTGGTATGAGTCCC
SCAF4 Forward	TGCGACAGTCTCGTCATCAG
SCAF4 Reverse	AAAGGTTCAGCACACGAACTATT

LATS1 Forward	AATTTGGGACGCATCATAAAGCC
LATS1 Reverse	TCGTCGAGGATCTTGGTAACTC
TXNIP Forward	GGTCTTTAACGACCCTGAAAAGG
TXNIP Reverse	ACACGAGTAACTTCACACACCT
ATF7IP Forward	AAGGCTCGAAAAACGATGAGAG
ATF7IP Reverse	GCCATTTAACAGCTTGACATCAG
KDM5C Forward	GGGTCCGACGATTTCCTACC
KDM5C Reverse	ATGCCCGATTTCTCTGCGATG
KMT2D Forward	GAGCTACGGCGCTTTGAGTT
KMT2D Reverse	AGGGAAACCAATCTGTGATAGGT
SIN3A Forward	ACCATGCAGTCAGCTACGG
SIN3A Reverse	CACCGCTGTTGGGTGATGA
LATS2 Forward	ACTTTTCCTGCCACGACTTATTC
LATS2 Reverse	GATGGCTGTTTTAACCCCTCA

2.16 Immunofluorescence

Cells were seeded on to glass coverslips and treated with AZD1775 or DMSO control. For visualisation of foci cells were pre-extracted on ice for 2 min (10 mM PIPES, pH 6.8, 300 mM Sucrose, 100 mM NaCl, 1.5 mM MgCl2 and 0.5% TritonX-100) and fixed with 4% paraformaldehyde in PBS for 10 min at room temperature. Coverslips were washed 3 times in PBS, and subsequently blocked in PBS, 0.1%

Triton, 1% BSA and 1% goat serum for 1 hr. Coverslips were then incubated with primary antibody in 1% BSA and 1% goat serum or FBS in PBS overnight at 4°C. Unbound primary antibody was removed by washing 3 times for 5 min in PBS at room temperature, followed by incubation with the indicated secondary antibody for 60 min at room temperature. Slides were then washed 3 times for 5 min in PBS (final wash contained 1:1000 Hoechst 33342) before mounting with Vectashield mounting medium (Vector Laboratories).

The following antibodies were used at a dilution of 1:300:

cGAS (Cell Signalling), γH2AX (Novus), 53BP1 (Genetex), PICH (Abnova), FANCD2 (Novus)

2.17 Anaphase bridges

Cells were seeded onto No:1.5 H cover glass and fixed with PFA buffer (250 mM HEPES, 1x PBS, pH7.4, 0.1% Triton X-100, 4% methanol-free paraformaldehyde) for 20 min at 4 °C. Samples were then incubated with primary antibodies at 37 °C for 90 minutes and rinsed with 1 × PBS followed by incubation of secondary antibodies in room temperature for 25 minutes. The cells were mounted using Vectashield containing DAPI. Anaphase cells with chromatin bridges were scored under Zeiss Axio Observer Z1 microscope.

2.18 High-resolution deconvolution microscopy

Image acquisition was carried out under a Zeiss AxioObserver Z1 epifluorescence microscopy system with 100 × /1.4 oil Plan-Aprochromat objective and a Hamamatsu ORCA-Flash4.0 LT camera. The system is calibrated and aligned by using 200 nm-diameter TetraSpeck microspheres (ThermoFisher). Z-stack images were acquired at 0.2 µm intervals covering a range from 3–8 µm by using ZEN blue software. Deconvolution was carried out using Huygens Professional deconvolution software (SVI) with a measured point-spread-function generated by 200 nm-diameter TetraSpeck microspheres. Classical maximum likelihood estimation method with iterations of 40–60 and signal-to-noise of 20–40 was applied.

2.19 Chromatin Immunoprecipitation (ChIP)

Approximately 1×10^8 T98G cells were grown on $15cm^2$ dishes and cross-linked by addition of formaldehyde (to 1% final concentration). Cross-linking was allowed to proceed at room temperature for 10 min before termination with glycine (final concentration 0.125 m). Cells were washed with PBS, trypsinized, and scraped into PBS. Cells were collected by centrifugation and resuspended in buffer containing 25mM Tris-Cl pH8, 2 mM EDTA, 150 mM NaCl, 1% Triton X-100, 0.1% SDS and protease inhibitors, and sonicated on ice to an average length of 700 base pairs. Chromatin was collected and incubated with a salmon sperm DNA/protein-A sepharose slurry (50% v/v beads in TE buffer supplemented with 0.2 mg salmon sperm DNA and 0.5mg BSA/ml) to avoid non-specific binding of protein-A sepharose. After preclearing, the beads were briefly centrifuged at 1000 rpm at 4oC for 1 min, the supernatants were collected and 1/10 of each sample was stored at 4oC as an input control. The supernatant fractions were then subjected to chromatin

immunoprecipitation overnight at 4ºC with 5µg of H3K36me3 or IgG antibody. Following incubation with antibody, 20µl of salmon sperm DNA/protein-A sepharose was added to each tube for 2hrs with rotation at 4ºC to isolate the immune complexes. The sepharose-antibody-chromatin complexes were then captured by centrifugation at 2000 rpm for 2 min at 4ºC and washed sequentially for 10 min, first in 25mM Tris-Cl pH8, 2 mM EDTA, 150 mM NaCl, 1% Triton X-100, and 0.1% SDS, then in 25mM Tris-Cl pH8, 2 mM EDTA, 500 mM NaCl, 1% Triton X-100, and 0.1% SDS, then in 250 mM LiCl, 1% NP-40, 1% sodium deoxycholate, 1 mM EDTA, 10 mM Tris-HCl pH8, then twice in TE (10 mM Tris-HCl pH8, 1 mM EDTA). Sepharose bound proteins were then eluted with 100µl elution buffer (1%SDS, 100 mM $NaHCO_3$). Samples were incubated at 65ºC overnight to remove crosslinks, before DNA was purified with QIAquick PCR purification kit according to manufacturer's instructions, and further analysed by PCR.

The following primers were used (all primers depicted 5' to 3'):

RRM2 Forward	GGCAAATCAGAAAGCCACATAG
RRM2 Reverse	GTACTACTCATTGGGCGTCAA
RAD51 Forward	TAAACTCGCGCAGGATCAAGTTCT
RAD51 Reverse	TTCAGAATTCCCGCCAAACCCTCT
CHK1 Forward	GGAAAGCATTTGTCTCCCACCTCA
CHK1 Reverse	AAATCACAATCGCCACTCCCAAGC
CTIP Forward	GATTTGGCACTCTGGTGAGGGAAA
CTIP Reverse	AGGTCAAATACCGCCTCCGAGATT

GAPDH Forward GGAGCGAGATCCCTCCAAAAT

GAPDH Reverse GGCTGTTGTCATACTTCTCATGG

The following antibodies were used at a concentration of 5 µg for 25 µg chromatin:

IgG (Abcam), H3K36me3 (Abcam)

2.20 DNA Fibre Assay

Cells were labelled for 20 minutes in media containing 25µM CldU, followed by 20 minutes in media containing 250µM IdU at 37^{o}C. Cell were collected by trypsinisation and resuspended in ice-cold PBS at the concentration of 2.5x10^{5} cells/ml. 2.5µl of the suspension was pipetted onto a microscope slide, and 7.5µl of the lysis buffer (200 mM Tris-HCl pH7.4, 50 mM EDTA, 0.5% SDS) was then added and mixed by gentle pipetting. The DNA was allowed to run down the slide slowly, air-dried and fixed in methanol/acetic acid (3:1) for overnight at 4^{o}C. Before staining, the slides were washed with PBS until the pH returned to neutral. The slides were incubated in the blocking buffer (2% BSA, 0.1% Tween 20, 1x PBS; 0.22 µm filtered) for 40 minutes, and incubated in the blocking buffer containing rat anti-CldU antibody (1:500 dilution) and mouse anti-IdU-FITC antibody (1:100 dilution) for 2.5 hours at room temperature. After rinsing in PBS-T (PBS containing 0.2% Tween), the slides were incubated in the blocking buffer containing the anti-rat Cy3 antibody (1:300 dilution) and the anti-Mouse AlexaFluor 488 antibody (1:300 dilution) for 1 hour at room temperature. After washing, the slides were mounted with Antifade Gold

(Invitrogen) and analysed using the Nikon Ni-E microscope. DNA fibre images were measured and counted using ImageJ.

2.21 Statistical Analysis

For the RNA Sequencing statistically significant differentially expressed genes were determined using Cuffdiff. Cuffdiff provides statistical routines for determining differential expression in digital transcript or gene expression data using a model based on the negative binomial distribution (Trapnell et al., 2010). Transcripts with a P-adjust <0.05 were assigned as differentially expressed.

Gene Ontology (GO) enrichment analysis of differentially expressed genes or lncRNA target genes was carried out using the GOseq R package, in which gene length bias was corrected. GO terms with a corrected P value of less than 0.05 were considered significantly enriched.

Differentially expressed genes were mapped to KEGG pathways using KOBAS (Mao et al., 2005).The p value for the pathway is calculated with the following equation:

Where N represents the total number of genes in the genome, M represents the genes in a designated KEGG pathway, *n* is the set of differentially expressed genes, and *m* is the differentially expressed genes involved in the given KEGG pathway.

For synthetic lethality screens, genes whose depletion sensitised cells to WEE1 inhibition were identified through Z-score analysis. First each well was normalised to a non-transfected control, and the normalised values for each replicate were then averaged. Z-scores were calculated from the non-targeting control wells using the formula:

$$\text{Z-score} = [(\text{Normalised mean of Well X}) - (\text{Normalised mean of NT wells})]/(\text{SD of NT wells})$$

The Z-score for the DMSO control wells was then subtracted from the Z-score of the AZD1775 treated wells. This difference in Z-scores represents the change in number of standard deviations from the mean upon treatment with AZD1775.

Chapter 3

RNA sequencing of SETD2 parental and CRISPR cell lines

3.1 Introduction

H3K36me3 is canonically associated with actively transcribed genes, and so it was predicted that its loss may result in broad changes in the transcriptional profile. In order to identify genes potentially linking H3K36me3 and *RRM2* expression levels, RNA-Seq analysis was carried out in U2OS parental and U2OS SETD2 CRISPR isogenic cell lines. RNA sequencing allows analysis of the entire transcriptome, including low abundance transcripts, and differentially expressed genes can subsequently be grouped into by pathway, enabling identification of pathways affected by loss of H3K36me3. RNASeq was carried out with and without drug treatment to identify genes only affected under stressed conditions. Cells were treated with either the WEE1 inhibitor AZD1775 (200nM) or DMSO control for 48 hours. Two biological repeats were sequenced from independently extracted RNA.

3.2 Results

3.2.1 Global effects of loss of H3K36me3 on transcription

Although H3K36me3 is normally associated with active transcription, a greater number of upregulated genes than downregulated was observed in the SETD2 CRISPR U2OS cell line. 726 genes were upregulated and 575 were downregulated compared to the wildtype cell line (Figure 3.1). SETD2 has been shown to interact with the phosphorylated C terminal domain of RNA Pol II to recruit the FACT complex (Carvalho et al., 2013). This is thought to promote nucleosome disassembly and facilitate transcription (Orphanides et al., 1998). It was therefore initially predicted that a global decrease in transcription would occur after SETD2 deletion. One possible explanation for the greater number of upregulated genes may be the presence of H3K36me3 at regions of facultative heterochromatin. Loss of H3K36me3 from these regions may allow transcription machinery to access regions that would otherwise be silenced (Chantalat et al., 2011a).

SETD2 has also been implicated in regulation of splicing machinery and suppression of cryptic transcription (Carvalho et al., 2013; Neri et al., 2017), although this has also been disputed (Kanu et al., 2015). An increase in cryptic transcription could result in greater numbers of incomplete transcripts, which may be recognised as gene upregulation by RNA-Seq.

Additionally, SETD2 is thought to play a role in regulation of transcriptional termination. Disruption of termination upon SETD2 deletion may allow RNA Pol II to continue transcription inappropriately in the absence of SETD2 (Proudfoot, 2016), resulting in aberrant transcription and upregulated expression.

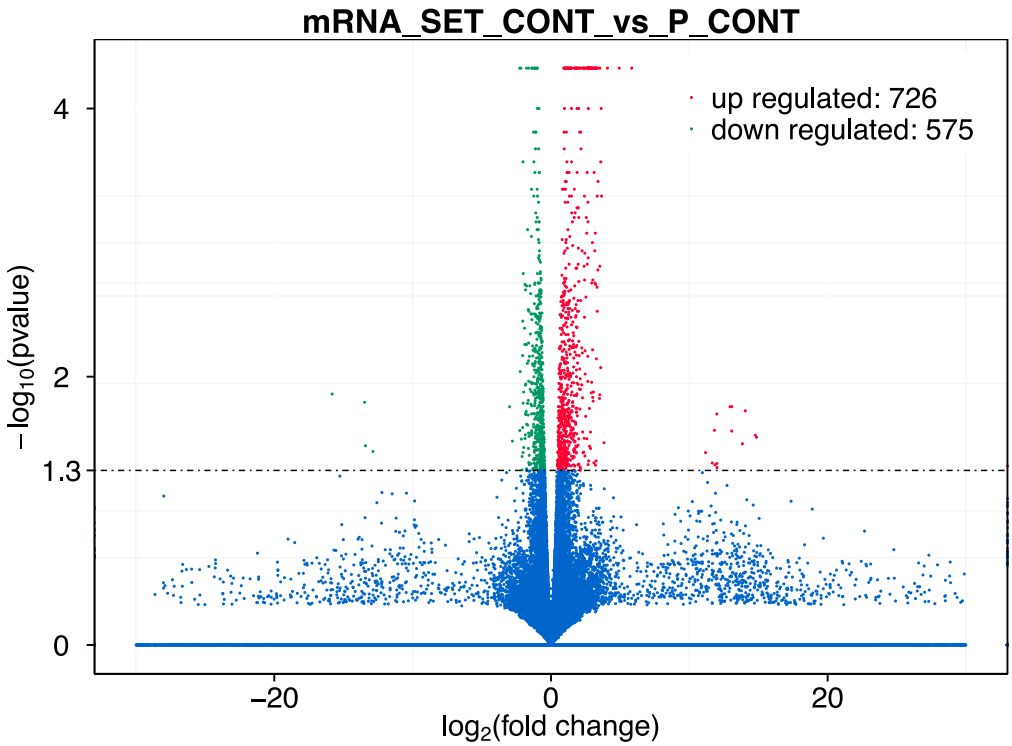


Figure 3.1 Volcano plot of the differentially expressed genes in U2OS SETD2 CRISPR cells relative to wildtype. The x axis represents the log2 of the fold change (FC) and the y axis represents the–log10 of the p-value. Red dots represent upregulated genes, green dots represent downregulated genes, and blue dots represent those genes whose fold change was non-significant.

3.2.2 Pathways of differentially expressed genes in SETD2 CRISPR U2OS compared to SETD2 parental

3.2.2.1 Upregulated GO terms

One method of identifying pathways up or downregulated in the RNA-Seq is to use gene ontology (GO) term enrichment. This makes use of the gene ontology classification system, where genes are grouped based on their functional characteristics. The gene ontology can be used to identify GO terms that appear more frequently than would normally be expected by chance. The GOseq R package (Young et al., 2010), was used to identify pathways associated with the differentially expressed genes identified by RNA-Seq.

24 GO terms were found to be upregulated with an adjusted p value of less than 0.05 in SETD2 CRISPR cells compared to parental U2OS (Table 1). Over 80% of these terms (20/24) contain multiple genes encoding collagenases, including COL1A1, COL4A4, COL5A1, COL5A3, COL6A3, COL7A1, COL12A1 and COL27A1. Although to date no link has been established between SETD2 and collagen transcription, SETD2 is a well-established tumour suppressor, and several collagen genes have also been associated with cancers (Li et al., 2016a; Rasmussen et al., 2015). As a number of different collagen genes were upregulated upon SETD2 loss it is possible that SETD2 is involved in the negative regulation of collagen genes. Interestingly, the collagen-related cancer chondroblastoma has been shown to have a very strong association with disruption of H3K36

trimethylation. Over 90% of chondroblastomas contain a mutation replacing lysine 36 with methionine (K36M) in the histone H3 variant H3.3, leading to a global decrease in levels of H3K36 methlyation (Behjati et al., 2013; Lewis et al., 2013). This change in H3K36me3 profile leads to a change cancer-associated gene expression, promoting tumourigenesis (Fang et al., 2016). This may suggest a potential tumour suppressor role for SETD2 in the regulation of collagen gene expression, although this needs to be explored further as the H3K36M mutation also blocks mono and dimethlyation.

Consistent with this idea, the majority of the upregulated GO terms appear to be involved in cell structure and organisation. SETD2 has previously been shown to methylate alpha-tubulin (Park et al., 2016) and may have further, presently unidentified roles in regulation of cell structure.

Additionally, two terms relating to insulin growth factor binding are upregulated, with the highest percentage of genes modified. However, there are very few genes within this GO term and so it is possible that the high significance of this association is an artefact.

GO Term	Corrected pValue	Percentage of Genes Differentially Expressed
extracellular region part	0.00014558	5.18
extracellular matrix organization	0.00069255	10.08
extracellular structure organization	0.00069255	10.05
extracellular space	0.00085927	6.12
nucleosome	0.0012841	14.71
insulin-like growth factor binding	0.0043899	32.00
vesicle	0.018607	4.92
extracellular matrix	0.018607	8.37
extracellular matrix disassembly	0.018607	13.08
collagen catabolic process	0.018607	16.88
membrane-bounded vesicle	0.018607	4.90
extracellular organelle	0.018607	5.05
extracellular membrane-bounded organelle	0.018607	5.05
extracellular vesicular exosome	0.018607	5.05
extracellular region	0.018607	4.63
multicellular organismal macromolecule metabolic process	0.020372	13.11
multicellular organismal catabolic process	0.026352	15.66
cell migration	0.033863	6.32
insulin-like growth factor II binding	0.03424	57.14
collagen metabolic process	0.036098	12.82
endoplasmic reticulum lumen	0.041521	10.42
response to oxygen levels	0.046054	8.64
multicellular organismal metabolic process	0.047611	11.85

Table 3.1: Selected overrepresented GO terms of upregulated genes in SETD2 CRISPR U2OS cells compared to SETD2 wildtype. Given are the term description, corrected p value and the percentage of genes within the GO term that are differentially expressed in SETD2 CRISPR U2OS.

3.2.2.2 Upregulated KEGG pathways

Another way to categorise differentially expressed genes is the Kyoto Encyclopaedia of Genes and Genomes (KEGG). KEGG is a collection of databases mapping the current knowledge of genomes, drugs, biological pathways, and other studies. The KEGG Pathway database is a collection of pathway maps, which can be used in a similar manner to the GO database to identify pathways that appear more frequently than would be expected. The differentially expressed genes were mapped to KEGG pathways using KOBAS (Mao et al., 2005), which identifies the most frequent and the most significantly enriched pathways in a given set of sequences.

14 KEGG pathways are significantly upregulated in SETD2 CRISPR U2OS compared to wildtype cells (Figure 3.2). One of the most strongly upregulated terms is the p53 signalling pathway, which is activated upon DNA damage. SETD2 has previously been shown to act as an important DNA repair factor (Kanu et al., 2015; Li et al., 2013; Pfister et al., 2014), and so it is possible that defective DNA damage repair in SETD2 deficient cells may result in activation of p53. Interestingly, it has also previously been suggested that SETD2 is required for activation of p53 and its downstream signalling pathway (Carvalho et al., 2014), however we observed clear upregulation of a number of p53 target genes after loss of SETD2.

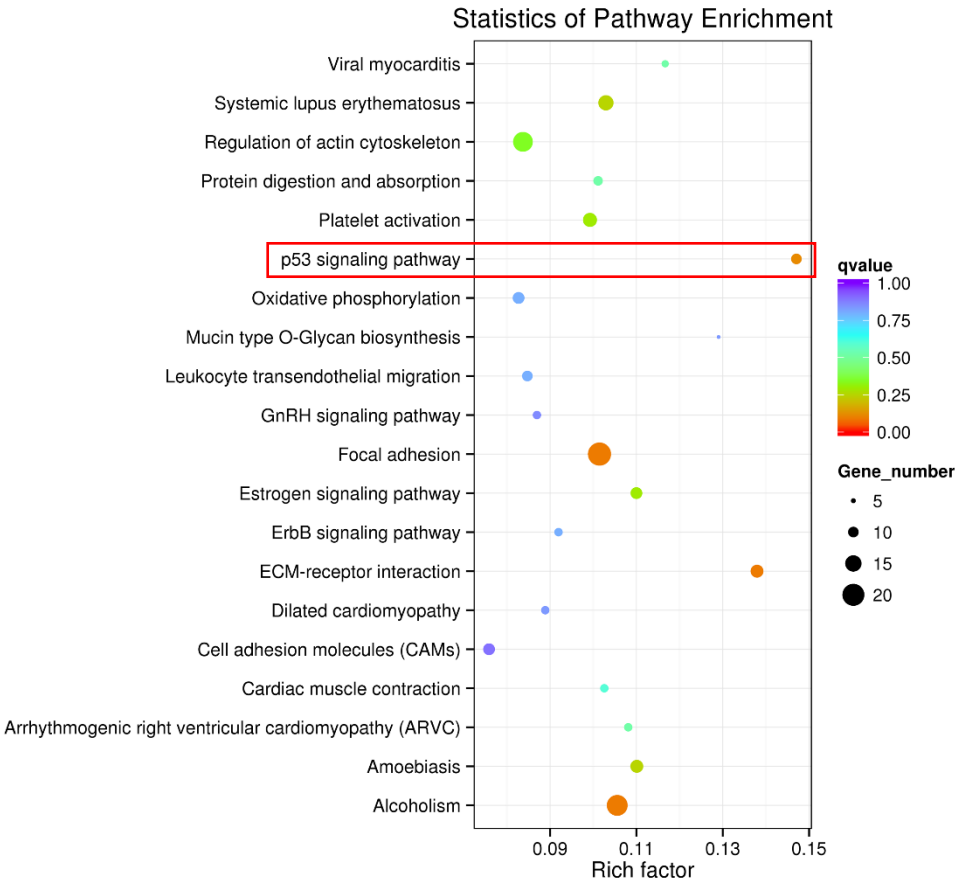


Figure 3.2: Enriched KEGG pathways of genes upregulated in SETD2 CRISPR U2OS. Rich factor represents the ratio of genes in the given pathway that are differentially expressed in SETD2 CRISPR U2OS to the total number of genes with in the pathway. A larger Rich factor indicates a greater degree of pathway enrichment. The q value is the corrected p value, where a lower value indicates a greater degree of pathway enrichment.

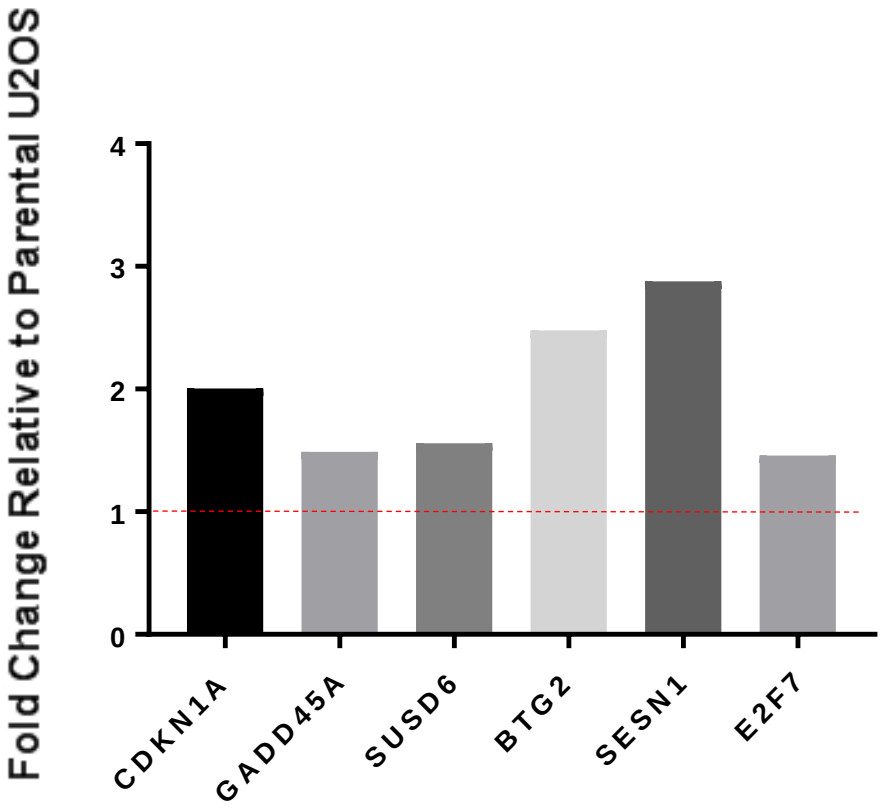


Figure 3.3: p53 target genes are upregulated in SETD2 CRISPR U2OS. Graph showing selected p53 target genes are significantly upregulated in SETD2 CRISPR U2OS relative to parental cells measured by RNA-seq. Data averaged from 2 independent biological replicates. For all genes shown $p<0.05$.

3.2.2.3 Downregulated GO terms

Although fewer genes were downregulated than upregulated after SETD2 loss, the pathways in the downregulated subset appear to have been more significantly altered than in the upregulated group. Only 24 GO terms had a p value below 0.05 in the upregulated subset, whereas there were over 200 such terms in the downregulated group. As such, only those terms with an adjusted p value below 0.001 are shown here (Table 3.2).

This group contains several terms consistent with what is already known about SETD2, including ‘transcription from RNA polymerase II promoter’. As discussed previously, SETD2 binds to the C-terminal domain of RNA pol II, coupling histone methylation to transcription. However, only a subset of genes transcribed by RNA pol II are downregulated upon loss of SETD2. One possible explanation for this is the cell cycle regulation of SETD2, which is degraded during the S and G2 phases of the cell cycle (Li et al., 2013). As such, it is unlikely that loss of SETD2 would affect genes transcribed in these phases of the cell cycle. It is also likely that a proportion of the genes within this GO term were not actively transcribed in the conditions this RNA-Seq was carried out in, and as such these genes would not be affected by loss of SETD2 either.

Several of the terms downregulated are related to differentiation, particularly of neural cells. Mutations in SETD2 or histone H3 resulting in a loss of H3K36me3 are frequently observed in brain tumours, particularly paediatric glioma (Fontebasso et al., 2013), suggesting a possible role for SETD2 and H3K36me3 in regulating genes involved in neural differentiation.

The ‘cell cycle’ and ‘transcription factor binding’ terms are of particular interest, as they are likely to include genes involved in RRM2 regulation, and could help to explain the mechanism through which SETD2 loss results in RRM2 downregulation. Both of these terms contained the transcription factors E2F1 and E2F2, which are required for G1/S progression (Bracken et al., 2004). Additionally, RRM2 is a known E2F target gene, suggesting that RRM2 downregulation upon SETD2 loss may occur through reduced E2F activity. Supporting this, there was a significant overlap between the genes downregulated in the SETD2 CRISPR cell line and known E2F1 target genes. This included other genes involved in replication, such as the licensing factors CDT1 and CDC6, components of the MCM helicase, and CCND1 (cyclin D).

It is notable that in the most significantly downregulated pathways only a small percentage of the genes were affected, typically around 5% of the genes in the GO term. This contrasts strongly with the upregulated subset, where at least 10% of the genes were affected (Table 1). This suggests that SETD2 loss results in downregulation of genes involved in a wide range of pathways, rather than a high percentage of the genes involved in one pathway. One possible explanation for this is that loss of SETD2 leads to downregulation of transcription factors which are involved in multiple pathways, such as E2F1 and 2, SRF, JUND and RELA.

GO Term	Corrected pValue	Percentage of Genes Differentially Expressed
intracellular organelle part	1.07E-08	3.87
organelle part	1.45E-08	3.83
nucleoplasm	6.76E-07	4.72
neurogenesis	9.18E-07	5.57
transcription factor binding	4.98E-06	8.15
generation of neurons	5.99E-06	5.46
nuclear lumen	5.99E-06	4.41
negative regulation of cellular process	6.48E-06	4.35
nuclear part	8.58E-06	4.27
organelle lumen	8.58E-06	4.21
membrane-enclosed lumen	1.19E-05	4.18
protein binding	1.19E-05	3.35
intracellular organelle lumen	1.19E-05	4.19
nervous system development	2.65E-05	4.68
negative regulation of biological process	3.76E-05	4.15
neuron differentiation	4.08E-05	5.34
response to external stimulus	5.76E-05	5.04
intracellular organelle	6.46E-05	3.36
chromatin binding	7.91E-05	7.63
intracellular membrane-bounded organelle	0.0001147	3.41
transcription from RNA polymerase II promoter	0.0001147	4.88
non-membrane-bounded organelle	0.0001516	4.11
intracellular non-membrane-bounded organelle	0.0001516	4.11
organelle	0.00019609	3.29
positive regulation of cellular process	0.00026632	4.00
regulation of developmental process	0.00029764	4.64
chromatin	0.00030766	7.76
cellular component organization or biogenesis	0.00030766	3.72
cytoplasm	0.00033027	3.37
positive regulation of cell differentiation	0.00040145	6.40
single-organism developmental process	0.0006838	3.88
positive regulation of biological process	0.00074546	3.88
system development	0.00076459	3.91
macromolecular complex	0.00076459	3.88
cell cycle	0.00078741	4.77

Table 3.2: Selected overrepresented GO terms of downregulated genes in SETD2 CRISPR U2OS cells compared to SETD2 wildtype. Given are the term description, corrected p value and the percentage of genes within the GO term that are differentially expressed in SETD2 CRISPR U2OS.

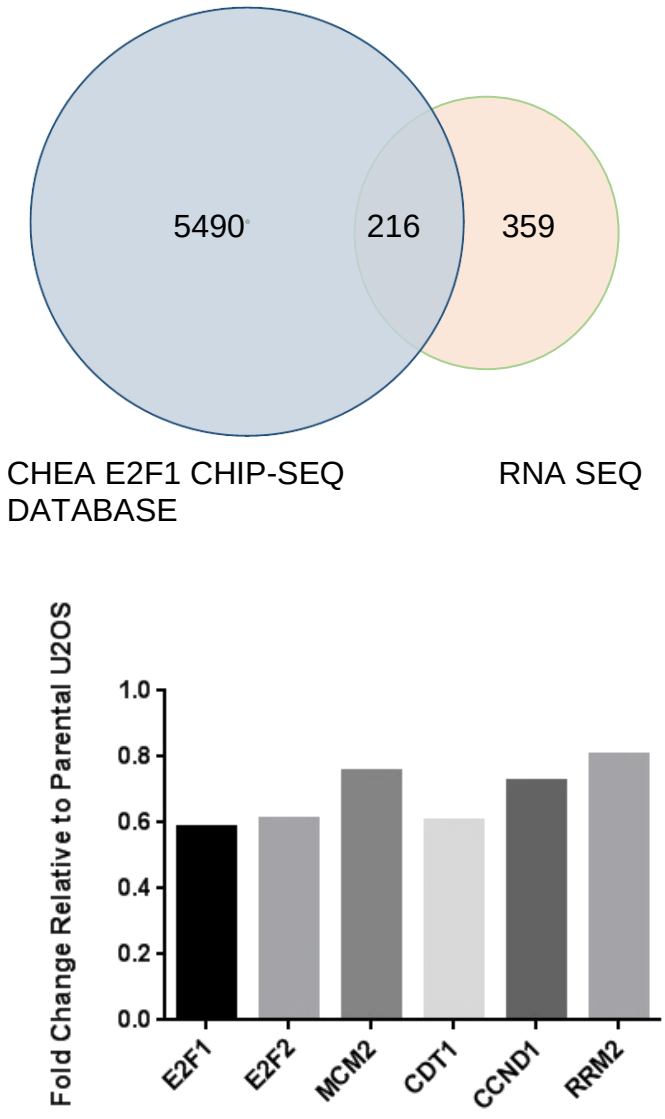


Figure 3.4: E2F target genes are differentially expressed in SETD2 deficient cells. (a) Venn diagram showing the overlap of genes downregulated in SETD2 CRISPR U2OS and the CHEA E2F1 ChIP-Seq database of known E2F1 target genes. **(b)** Selected E2F target genes downregulated in SETD2 CRISPR U2OS RNA-Seq relative to wildtype levels

3.2.2.4 Downregulated KEGG pathways

Overall the downregulated pathways showed more significant q values than the upregulated subset, but had little association with known SETD2 function. The ‘pathways in cancer’ pathway includes the transcription factors E2F1 and E2F2, which were also identified as downregulated through the GO terms. The ‘alcoholism’ term contains several genes associated with chromatin modifications, including the histone deacetylase gene HDAC5 and 8 genes encoding different histone variants. This may indicate that SETD2 has wider reaching impacts upon chromatin structure, potentially including regulation of histone variant expression. However, more work will need to be done to investigate the changes in the chromatin profile upon SETD2 loss.

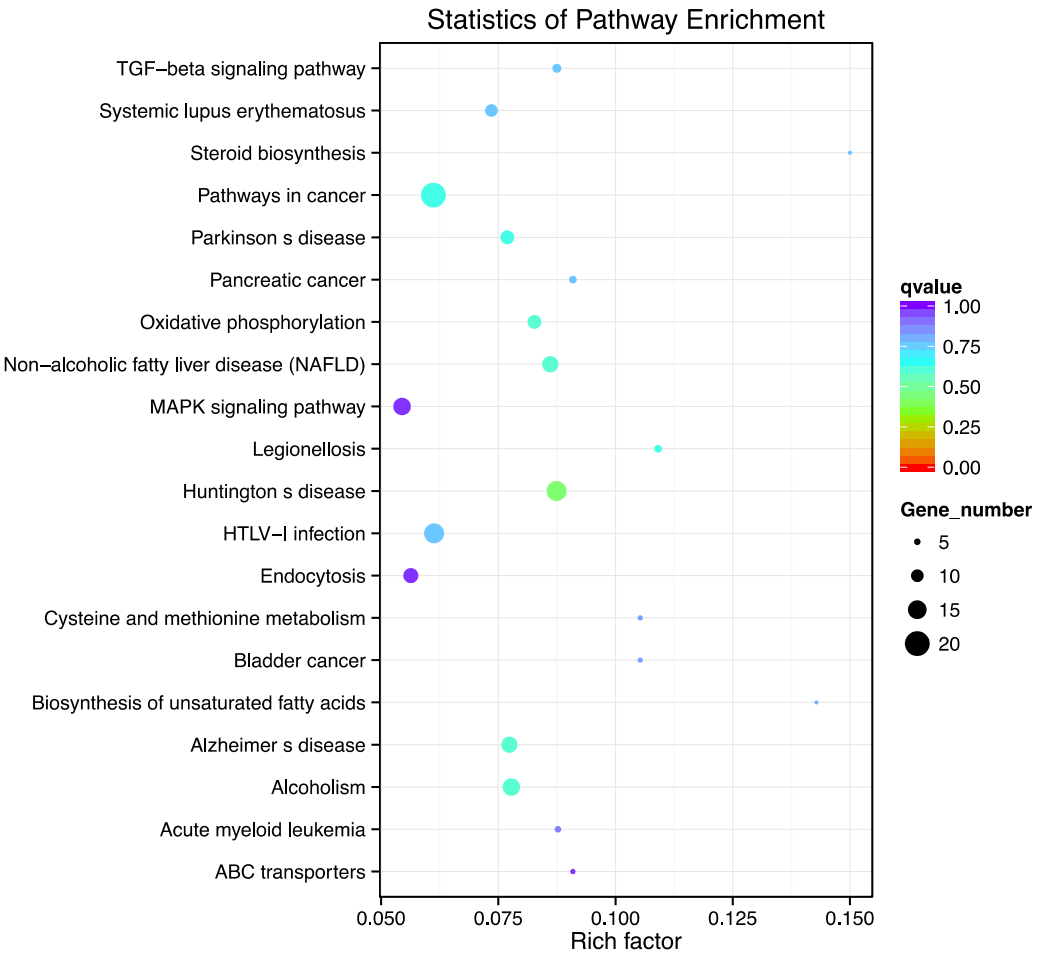


Figure 3.5: Enriched KEGG pathways of genes downregulated in SETD2 CRISPR U2OS. Rich factor represents the ratio of genes in the given pathway that differentially expressed in SETD2 CRISPR U2OS to the total number of genes with in the pathway. A larger Rich factor indicates a greater degree of pathway enrichment. The q value is the corrected p value, where a lower value indicates a greater degree of pathway enrichment.

3.2.2.5 Global distribution of differentially expressed genes after SETD2 loss

H3K36me3 has previously been shown to be associated with actively transcribed genes, and appears to be evenly distributed across all chromosomes. However, it is currently unknown whether loss of H3K36me3 affects all regions of the genome equally. To investigate whether specific chromosomal regions are more strongly affected by loss of H3K36me3, differentially expressed genes were mapped to their chromosomal location (Figure 3.6). Differentially expressed genes, both upregulated and downregulated, appear to be distributed across all chromosomes, with no regions appearing to be more strongly affected.

.

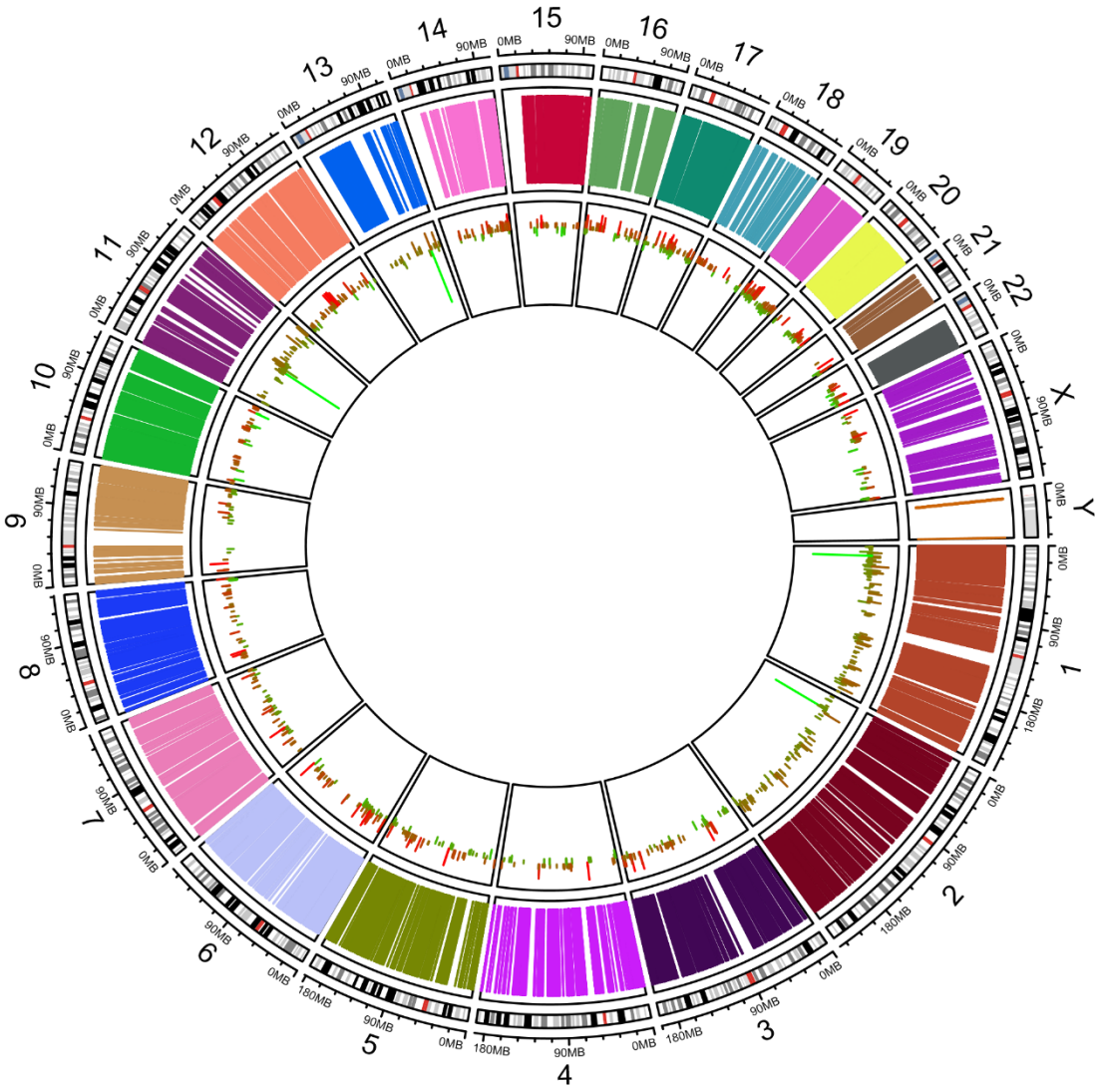


Figure 3.6: Plot showing distributed of differentially expressed genes after H3K36me3 loss. Green indicates reduced expression, red indicated increased expression relative to the length of the bar. Only those genes with a p value of less than 0.05 are shown.

3.2.3 Global effects of WEE1 inhibition of transcription

In order to investigate the effect of WEE1 inhibition on gene expression in both wildtype and SETD2-deficient cells, RNA-Seq was carried out on U2OS wildtype and SETD2 CRISPR isogenic cell lines after treatment with 200nM AZD1775.

Approximately 1000 genes were differentially expressed in the parental U2OS cell line after WEE1 inhibition, while expression of over 3000 genes was altered in the SETD2 deficient cell line (Figure 3.7), indicating that WEE1 inhibition has a much stronger impact on transcription in the absence of SETD2.

SETD2 CRISPR cells are significantly more sensitive to inhibition of WEE1 than the parental cells, which leads to accumulation of cells in non-replicating S phase in the absence of SETD2, while the cell cycle of the wildtype cell line does not appear to be significantly disrupted (Pfister et al., 2015). This accumulation of cells in S phase may result in altered expression of cell cycle regulated genes, leading to differential expression of a greater number in SETD2 deficient cells. It is also possible that transcription of a subset of genes is only affected in the absence of SETD2, which may also contribute to the difference in gene expression.

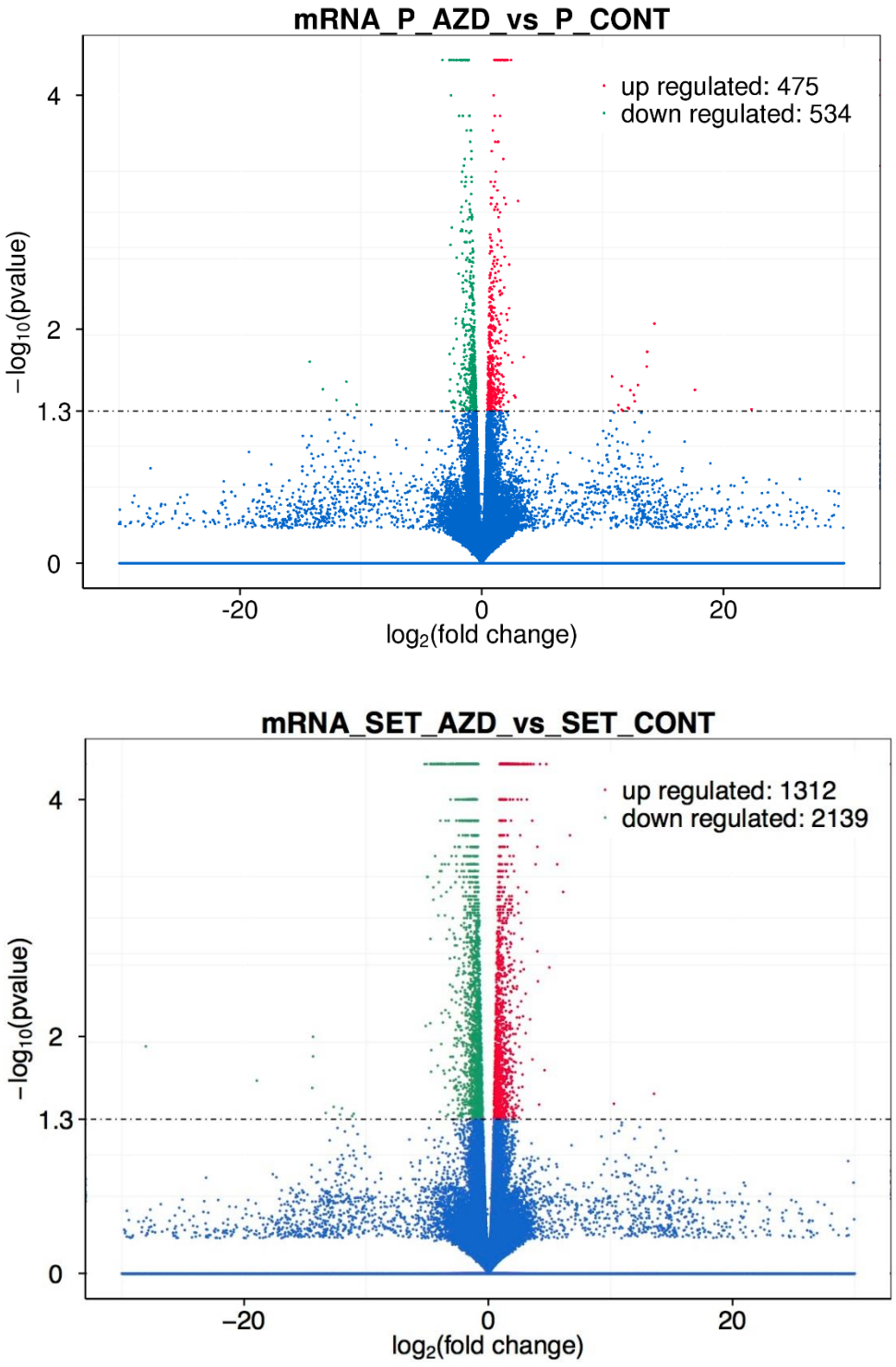


Figure 3.7: Volcano plot of the differentially expressed genes in U2OS wildtype and SETD2 CRISPR cells treated with 200nM AZD1775 relative to untreated. The x axis represents the log2 of the fold change (FC) and the y axis represents the–log10 of the p-value. Red dots represent upregulated genes, green dots represent downregulated genes, and blue dots represent those genes whose fold change was non-significant.

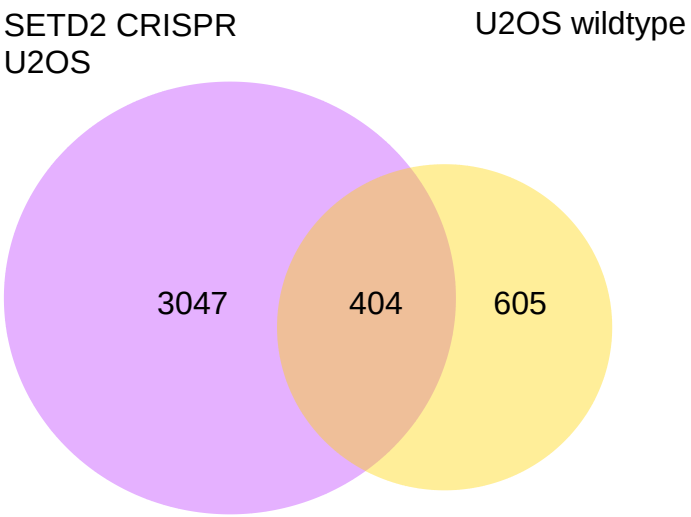


Figure 3.8: Venn diagram of genes affected by AZD1775 treatment. The purple circle indicates the total number transcripts affected by 200nM AZD1775 treatment for 48 hours in SETD2 CRISPR deleted U2OS. The yellow circle shows transcripts affected in wildtype cells.

Of the roughly 1000 genes whose expression was altered after WEE1 inhibition in parental U2OS, over 40% were also differentially expressed in SETD2 deficient cells. In contrast, only 12% of the differentially expressed genes in the SETD2 CRISPR U2OS cell line were also affected in the parental U2OS (Figure 3.8).

3.2.4 Pathways of genes differentially expressed in both U2OS parental and SETD2 CRISPR after WEE1 inhibition

3.2.4.1 Upregulated GO Terms

As in the comparison between untreated parental U2OS and SETD2 CRISPR cell lines, the main methods used to identify pathways affected by WEE1 inhibition are GO term and KEGG pathway enrichment. The GO terms upregulated after WEE1 inhibition in both parental and SETD2 CRISPR U2OS are primarily related to protein production and processing, and include SRP-dependent co-translational protein targeting to membrane, translation, translation initiation and tRNA aminoacylation for protein translation (Table 3.3). These findings suggest that WEE1 inhibition may impact on protein synthesis. Consistent with this, a relationship has been identified in yeast between protein synthesis and WEE1 protein levels, where WEE1 levels increased upon inhibition of protein synthesis to block cell cycle progression (Suda et al., 2000). This may explain the altered expression of genes involved in protein expression seen after WEE1 inhibition, although more work needs to be done to confirm if this is the case.

Term	P-Value
SRP-dependent cotranslational protein targeting to membrane	1.10E-09
translation	2.80E-09
viral transcription	6.20E-09
nuclear-transcribed mRNA catabolic process, nonsense-mediated decay	1.10E-08
translational initiation	4.30E-08
rRNA processing	2.70E-06
PERK-mediated unfolded protein response	7.10E-05
tRNA aminoacylation for protein translation	1.70E-04
response to endoplasmic reticulum stress	1.80E-04
cellular response to amino acid stimulus	3.30E-04
positive regulation of transcription from RNA polymerase II promoter in response to endoplasmic reticulum stress	3.10E-03
circadian regulation of gene expression	7.50E-03
cellular response to lipopolysaccharide	8.30E-03
gamma-aminobutyric acid metabolic process	1.40E-02
negative regulation of neuron apoptotic process	1.40E-02
cellular amino acid biosynthetic process	1.40E-02
liver development	1.50E-02
macroautophagy	1.60E-02
cellular response to glucose starvation	1.80E-02
cellular response to dexamethasone stimulus	1.80E-02

Table 3.3: Top 20 GO terms upregulated in both SETD2 CRISPR U2OS and wildtype after AZD1775 treatment

3.2.4.2 Upregulated KEGG pathways

Only 5 KEGG pathways were significantly upregulated in both U2OS parental and SETD2 CRISPR cell lines after WEE1 inhibition, with genes comprising ribosomal subunits making up the most strongly upregulated subset. All 5 upregulated pathways are involved in production of amino acids or translation, suggesting that inhibition of WEE1 may result in an upregulation of genes involved in protein production.

Interestingly, unpublished data from the Durocher lab found that deletion of the translation inhibitors GCN1 and GCN2 promotes resistance to AZD1775 treatment, further supporting a potential relationship between WEE1 and translation. Additionally, gcn2 in yeast has previously been shown to regulate cell cycle progression by delaying S phase entry after UV irradiation or methyl methanesulphonate (MMS) exposure (Krohn et al., 2008; Tvegard et al., 2007). Although the mechanism for this regulation is unclear, it may be related to delayed formation of the pre-replication complex, and may be another mechanism through which GCN2 could modulate sensitivity to WEE1 inhibition.

Term	P-Value
Ribosome	7.90E-08
Biosynthesis of amino acids	8.10E-04
Aminoacyl-tRNA biosynthesis	4.10E-03
Alanine, aspartate and glutamate metabolism	5.00E-03
Glycine, serine and threonine metabolism	6.70E-03

Table 3.4: KEGG pathways upregulated in both SETD2 CRISPR U2OS and wildtype after AZD1775 treatment

3.2.4.3 Downregulated GO terms

In both parental and SETD2 CRISPR U2OS cell lines more genes were downregulated than upregulated after WEE1 inhibition (Figure 3.7). Unsurprisingly, owing to WEE1's function in cell cycle regulation, many of the GO terms downregulated after WEE1 inhibition are involved in cell cycle progression. Although WEE1 inhibition in SETD2 deficient cells leads to increased S phase population, the majority of these are related to G1/S phase progression and DNA replication.

WEE1 deficient cells have previously been shown to have decreased replication fork speed (Dominguez-Kelly et al., 2011), indicating that there is a role for WEE1 in DNA replication. The genes downregulated within the DNA replication terms are primarily involved in origin licensing, such as CDC6, CDT1, ORC1, ORC6, MCM2, 3 and 4. Downregulation of these genes upon inhibition of WEE1 suggests WEE1 activity is required for efficient origin licensing. Origin licensing takes place throughout G1, and is inhibited by CDK activity. Increased levels of CDK activity results in inhibition of E2F transcription by targeting activator E2Fs for degradation by the ubiquitin-proteasome system, which may be the cause of the observed reduction in these DNA replication genes. It has also been shown that WEE1 inhibition results in accelerated S phase entry from G1 (Beck et al., 2012), which is another potential cause of reduced DNA replication gene expression.

Term	P-Value
G1/S transition of mitotic cell cycle	7.60E-18
DNA replication	6.10E-17
DNA replication initiation	6.90E-10
regulation of transcription involved in G1/S transition of mitotic cell cycle	7.80E-08
DNA synthesis involved in DNA repair	2.30E-05
strand displacement	1.20E-04
DNA strand elongation involved in DNA replication	4.00E-04
microtubule-based process	4.30E-04
regulation of cyclin-dependent protein serine/threonine kinase activity	5.90E-04
DNA duplex unwinding	9.40E-04
nucleosome assembly	1.20E-03
positive regulation of cyclin-dependent protein serine/threonine kinase activity	1.70E-03
positive regulation of cell migration	2.50E-03
DNA replication checkpoint	2.60E-03
telomere maintenance via recombination	3.90E-03
double-strand break repair	4.20E-03
DNA damage response, detection of DNA damage	5.40E-03
inner cell mass cell proliferation	6.10E-03
response to organonitrogen compound	8.30E-03
protein heterotetramerization	8.30E-03

Table 3.5: Top 20 GO terms downregulated in both SETD2 CRISPR U2OS and wildtype after AZD1775 treatment

3.2.4.4 Downregulated KEGG pathways

WEE1 dependent phosphorylation of CDK1 is one of the main mechanisms of negative regulation of G2/M progression, and so it was predicted WEE1 inhibition would result in cell cycle disruption. Consistent with the over-represented GO terms, the most significantly downregulated KEGG pathways were ‘cell cycle’ and ‘DNA replication’. This further suggests the presence of an important role for WEE1 during the G1 and S phases of the cell cycle.

Interestingly, the upregulated pathways and terms did not show any enrichment of mitotic genes, suggesting that WEE1 inhibition did not result in an increase in mitotic cells. It has previously been published that WEE1 inhibition results in a transient increase in the presence of mitotic cells, peaking after 4 hours (Chang et al., 2016). As the treatment here was for 48 hours it is likely that any transient increase in mitosis was not captured in the gene expression profile.

Term	P-Value
Cell cycle	7.00E-08
DNA replication	1.00E-04
Phagosome	4.10E-03
Gap junction	6.20E-03
Systemic lupus erythematosus	8.70E-03
Pyrimidine metabolism	1.20E-02
MicroRNAs in cancer	1.30E-02
Bladder cancer	1.70E-02
Small cell lung cancer	2.60E-02
Ribosome biogenesis in eukaryotes	2.80E-02
Purine metabolism	2.90E-02
Pathogenic Escherichia coli infection	3.00E-02
Alcoholism	3.00E-02
Mismatch repair	3.70E-02

Table 3.6: KEGG pathways downregulated in both SETD2 CRISPR U2OS and wildtype after AZD1775 treatment

3.2.5 Pathways of genes differentially expressed in only SETD2 CRISPR after WEE1 inhibition

In order to identify genes potentially leading to increased sensitivity to WEE1 inhibition after loss of SETD2, the 3047 genes that were differentially expressed only in SETD2 deficient cells after AZD1775 treatment were investigated. Over 1000 genes were upregulated uniquely in SETD2 CRISPR U2OS cells after WEE1 inhibition, compared to only 138 genes upregulated in both wildtype and SETD2 CRISPR cells (Figure 3.9).

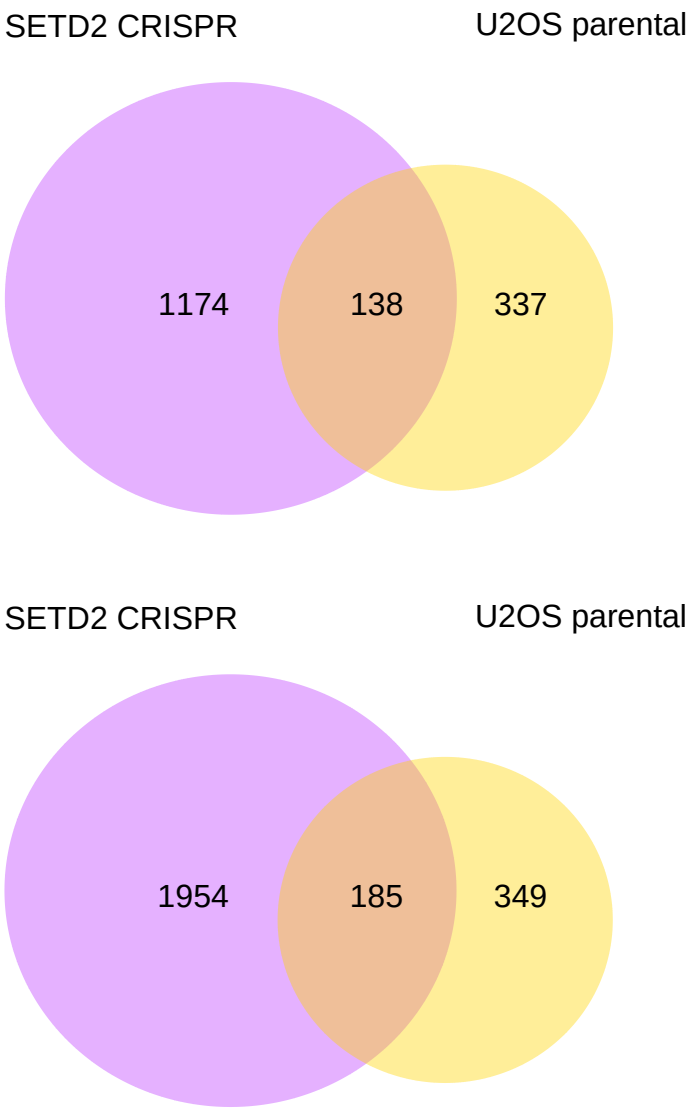


Figure 3.9: Differentially expressed genes in cells treated with AZD1775 (a) Venn diagram of genes upregulated after AZD1775 treatment. The purple circle indicates the total number transcripts affected by 200nM AZD1775 treatment for 48 horus in SETD2 CRISPR deleted U2OS. The yellow circle shows transcripts affected in parental cells. **(b)** Venn diagram of genes downregulated after AZD1775 treatment.

3.2.5.1 Upregulated GO Terms

The GO terms enriched in genes upregulated only in SETD2 CRISPR U2OS show a large degree of overlap with those enriched in both cell lines (Table 3.7). The most strongly enriched terms are again those involved in translation and protein production, including SRP-dependent co-translational protein targeting to membrane and translational initiation. SRP (signal recognition particle) interacts with a nascent polypeptide destined for the endoplasmic reticulum, and facilitates its localisation to the ER membrane (Egea et al., 2005). These terms were amongst the most strongly enriched in the set of genes upregulated in both U2OS parental and SETD2 CRISPR cell lines.

This suggests that WEE1 inhibition in SETD2 deficient cells results in upregulation of the same pathways as in wildtype cells, but a greater number of genes within these pathways are affected after depletion of SETD2.

Of particular interest in the GO terms that were enriched uniquely in the SETD2 CRISPR cell line is ‘apoptotic process’ (Table 3.7). Several of the genes within the apoptotic process term are also p53 target genes (Fischer, 2017), including FAS, TRAF4, TNFRSF10B, TNFRSF10C. This may indicate that WEE1 inhibition in SETD2 deficient cells results in increased apoptosis through induction of the p53 signalling pathway.

Term	P-Value
SRP-dependent cotranslational protein targeting to membrane	3.30E-34
translational initiation	1.80E-32
nuclear-transcribed mRNA catabolic process, nonsense-mediated decay	9.60E-32
viral transcription	7.00E-30
rRNA processing	2.00E-19
translation	3.40E-18
ribosomal small subunit assembly	4.30E-05
intracellular protein transport	4.60E-05
ribosomal large subunit assembly	9.00E-05
autophagy	1.30E-04
cytoplasmic translation	3.10E-04
response to oxidative stress	3.50E-04
macroautophagy	8.90E-04
apoptotic process	1.30E-03
ribosomal small subunit biogenesis	1.30E-03
positive regulation of I-kappaB kinase/NF-kappaB signaling	1.50E-03
regulation of apoptotic process	1.60E-03
cellular response to mechanical stimulus	1.70E-03
vesicle-mediated transport	1.80E-03
intrinsic apoptotic signaling pathway in response to endoplasmic reticulum stress	1.90E-03

Table 3.7: Top 20 GO terms upregulated in SETD2 CRISPR U2OS compared to wildtype after AZD1775 treatment

3.2.5.2 Upregulated KEGG pathways

'Ribosome' is the KEGG pathway most significantly enriched in the set of genes upregulated only in SETD2 CRISPR U2OS following treatment with AZD1775 (Table 3.8). This term was also the most significantly enriched term amongst genes upregulated in both cell lines (Table 3.4), indicating that transcription of genes encoding ribosomal subunits is upregulated independently of SETD2 status. However, a greater number of ribosomal genes are upregulated in SETD2 deficient cells after WEE1 inhibition than in parental, indicating that this term is more significantly impacted by WEE1 inhibition in the absence of SETD2. Several ribosomal genes have been associated with induction of apoptosis, which may explain why these genes are more strongly upregulated in the SETD2 CRISPR cell line (Naora et al., 1998; Neumann and Krawinkel, 1997).

The p53 signalling pathway was the most significantly enriched KEGG pathway that appeared only in SETD2 deficient cells after WEE1 inhibition (Table 3.8). Upregulated genes in this pathway included p21, GADD45A, BAX, MDM2, RRM2B, CCNG1, and CCND2. p53 target genes are canonically upregulated in response to DNA damage (Meek, 2004), suggesting that WEE1 inhibition results in induction of DNA damage in SETD2 deficient cells, but not in parental U2OS. This is consistent with the increased sensitivity to WEE1 inhibition observed in SETD2 deficient cells.

Term	P-Value	Fold Enrichment
Ribosome	3.10E-25	5.8
p53 signaling pathway	3.10E-06	4
Lysosome	2.10E-04	2.6
Protein processing in endoplasmic reticulum	2.30E-03	2
Glutathione metabolism	1.40E-02	2.8
FoxO signaling pathway	2.30E-02	1.9
Phagosome	3.40E-02	1.7
Amyotrophic lateral sclerosis (ALS)	3.80E-02	2.5
Arginine and proline metabolism	3.80E-02	2.5
Bladder cancer	4.40E-02	2.7

Table 3.8: KEGG pathways upregulated in SETD2 CRISPR U2OS compared to wildtype after AZD1775 treatment

3.2.5.3 Downregulated GO Terms

Almost twice as many genes were downregulated than upregulated in SETD2 CRISPR U2OS alone after WEE1 inhibition (Figure 3.9). Similar to those genes downregulated in both parental and SETD2 CRISPR U2OS, there is a clear downregulation of cell cycle genes, with the top seven enriched terms all related to cell cycle progression. Interestingly, although those genes downregulated in both cell lines were primarily involved in G1/S progression and DNA replication (Table 3.5), the genes downregulated in SETD2 deficient cells alone are largely involved in mitosis and cell division (Table 3.9). While this is in contrast with the general consensus that inhibition of WEE1 drives cells into mitosis, it is consistent with the mechanism of SETD2 lethality with AZD1775, where cells accumulate in a non-replicating S phase. This leads to a decreased mitotic population, and decreased transcription of genes involved in mitotic progression.

Term	P-Value
cell division	5.50E-30
sister chromatid cohesion	8.50E-27
mitotic nuclear division	1.40E-23
G2/M transition of mitotic cell cycle	1.30E-16
nucleosome assembly	9.80E-13
chromosome segregation	9.40E-12
DNA replication	4.70E-11
protein sumoylation	5.30E-11
mitotic nuclear envelope disassembly	1.30E-10
mitotic sister chromatid segregation	8.90E-10
cell proliferation	2.60E-09
gene silencing by RNA	3.40E-09
CENP-A containing nucleosome assembly	5.00E-09
viral process	9.00E-09
positive regulation of transcription, DNA-templated	3.60E-08
DNA replication-dependent nucleosome assembly	7.90E-08
negative regulation of transcription from RNA polymerase II promoter	1.50E-07
tRNA export from nucleus	6.20E-07
DNA repair	6.70E-07
intracellular transport of virus	7.60E-07

Table 3.9: Top 20 GO terms downregulated in SETD2 CRISPR U2OS compared to wildtype after AZD1775 treatment

3.2.5.4 Downregulated KEGG pathways

Interestingly, the KEGG pathways enriched in the genes downregulated only in SETD2 CRISPR U2OS showed much more overlap with those enriched in both cell lines than the GO terms. ‘Cell cycle’ and ‘DNA replication’ were again among the most significantly affected pathways, although these were much more significantly enriched in the SETD2 CRISPR cell line alone (Table 3.10). The ‘cell cycle’ term contains genes involved in both the G1/S transition (MCM2, MCM6, MCM7, CDC45, RB, E2F2) and also genes involved in G2 and mitotic progression (CCNB2, PLK1) demonstrating the importance of WEE1 during multiple cell cycle phases.

Term	P-Value	Fold Enrichment
Alcoholism	4.30E-13	2.9
Cell cycle	9.20E-12	3.3
Systemic lupus erythematosus	1.40E-10	3
Viral carcinogenesis	3.60E-07	2.2
Hippo signaling pathway	1.50E-05	2.2
Adherens junction	5.60E-05	2.8
TGF-beta signaling pathway	6.00E-04	2.3
HTLV-I infection	1.10E-03	1.7
Lysine degradation	1.60E-03	2.6
RNA transport	2.10E-03	1.8
DNA replication	2.40E-03	3
Fanconi anemia pathway	5.90E-03	2.4
Ribosome biogenesis in eukaryotes	5.90E-03	2
Progesterone-mediated oocyte maturation	5.90E-03	2
Oocyte meiosis	6.20E-03	1.9
Fc gamma R-mediated phagocytosis	9.50E-03	2
Spliceosome	1.40E-02	1.7
Epstein-Barr virus infection	1.60E-02	1.6
Pyrimidine metabolism	1.60E-02	1.8
Axon guidance	1.70E-02	1.7

Table 3.10: Top 20 KEGG pathways downregulated in SETD2 CRISPR U2OS compared to wildtype after AZD1775 treatment

3.3 Discussion

3.3.1 Summary of chapter 3

- Loss of SETD2 affects transcription in untreated and WEE1 inhibited cells
- SETD2 deficient cells have decreased expression of E2F target genes
- The p53 response pathway is upregulated in SETD2 deficient cells, indicating increased DNA damage
- WEE1 inhibition leads to downregulation of genes involved in DNA replication in both wildtype and SETD2 deficient cells

3.3.2 Discussion of chapter 3

It is apparent from analysis of the RNA sequencing data that deletion of SETD2 has a strong impact on the cellular transcriptional profile in both untreated and WEE1 inhibited conditions. However, loss of SETD2 was also found to disrupt normal cell cycle progression, raising the possibility that some of the genes may not be directly impacted by the loss of SETD2. One possible solution to this would be to carry out RNA-Seq in synchronised cells, however this means that those genes expressed only in other stages of the cell cycle could not be investigated. Further optimisation of the RNA-Seq may include using a SETD2 complemented cell line, to identify those genes differentially regulated as a result of off-target CRISPR mutations.

Of particular interest amongst the differentially expressed genes is the observed downregulation of the E2F transcriptional network, which occurred after loss of SETD2 and also after inhibition of WEE1, suggesting that they are mutual targets of both. Many of the downregulated genes are essential for proper G1/S transition and DNA replication, including E2F1 and E2F2 themselves, the replication factors CDT1, CDC6, RRM2 and the MCM genes. These genes were therefore identified as likely candidates to be involved in the SETD2-WEE1 synthetic lethality, and were investigated further.

The dysregulated transcription of a number of genes related to collagen production observed is consistent with a published role for SETD2 in chondroblastomas, and may reveal a broader role for SETD2 in cytoskeletal regulation than previously thought.

WEE1 inhibition was found to affect transcription of many of the same pathways in both parental U2OS and U2OS SETD2 CRISPR, with significantly increased transcription of genes related to ribosomes and protein production. This may suggest a previously unidentified role for WEE1 and CDK activity in the regulation of translation, although this needs to be explored more.

Additionally, both cell lines showed significant dysregulation of genes related to cell cycle progression, with genes involved in DNA replication particularly affected. This is consistent with the published data showing replication stalling and S phase arrest in SETD2-deficient cells treated with the WEE1 inhibitor. Consistent with the lack of cell death observed in parental U2OS after WEE1 inhibition, there was no increase

in apoptotic gene transcription in parental cells, while it was seen in SETD2 CRISPR U2OS.

Upregulation of the p53 DNA damage response pathways was observed in both untreated and WEE1 inhibited SETD2 deficient cells, consistent with previously published data showing a role for SETD2 in the DNA damage response and increased genomic instability upon its loss. Improper transcription of replication factors can lead to DNA damage through induction of replication stress, and as these pathways were disrupted by both SETD2 loss and WEE1 inhibition, this possibility was further explored in chapter 4.

Chapter 4

Histone H3K36me3 facilitates efficient DNA replication through regulation of E2F transcription

4.1 Introduction

The RNA-sequencing described in chapter 3 revealed significant downregulation of the E2F transcriptional pathway upon loss of the histone methyltransferase SETD2. Impaired expression of E2F target genes has been shown to lead to replication stress, which can then result in DNA damage induction and genome instability. This chapter investigates the role of SETD2 and H3K36me3 in the regulation of E2F target gene expression, in both canonical G1/S phase, and also in replication stressed conditions.

4.2 Results

4.2.1 qRT-PCR analysis of E2F target genes in SETD2 deficient cells

The results from RNA sequencing described in chapter 3 showed that transcription of E2F target genes is impaired upon loss of H3K36me3. Transcription of E2F target genes is highly cell cycle regulated, so in order to confirm that these results were not simply an artefact of differential cell cycle distribution, U2OS parental and SETD2 CRISPR cells were synchronised in G1 by addition of the proteasome inhibitor lovastatin. RNA was extracted and levels of select E2F target genes measured by qRT-PCR. Consistent with the RNA-Seq findings, the transcription factors E2F1 and E2F2, along with their target genes CDT1, CCND1, MCM2, CDC6 and RRM2 were all found to be downregulated upon loss of SETD2 (Figure 4.1). These results indicate a potential role for SETD2 in regulation of the E2F transcription network.

To further investigate this, E2F transcript levels were measured by qRT-PCR after SETD2 depletion in T98G cells. T98G is a glioblastoma cell line that is thought to maintain a normal E2F regulatory network, and can be easily synchronised in G1 through removal of serum. Cells were transfected with either siNT or siSETD2 and synchronised in G1 by serum starvation. Consistent with what was observed in U2OS cells, E2F1, E2F2, CDT1, CCND1, MCM2, CDC6 and RRM2 were all found to be downregulated after SETD2 depletion (Figure 4.1). As decreased transcription does not always lead to decreased protein levels, Western blots were conducted to analyse the levels of E2F1, RRM2, CDC6 and MCM2 protein after SETD2 depletion. T98G cells were treated with siNT or siSETD2 and synchronised in G1 by removal of serum. Protein levels of all E2F target genes tested were found to be reduced upon

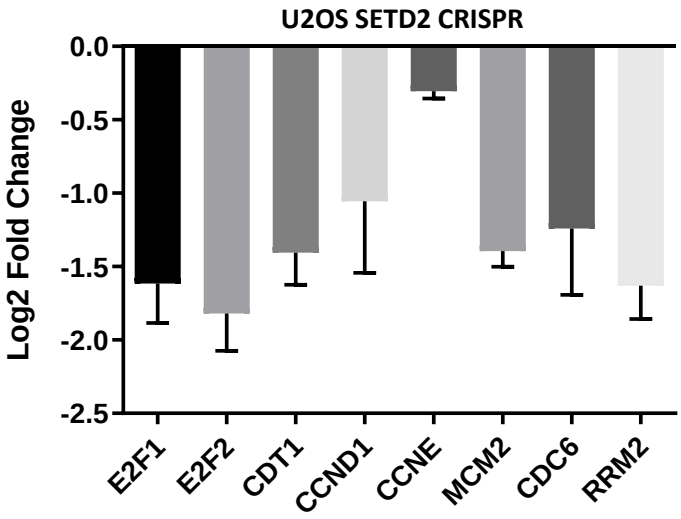
loss of SETD2, supporting a role for SETD2 in activating E2F transcription during G1 (Figure 4.1).

4.2.2 Complementation of SETD2 CRISPR U2OS

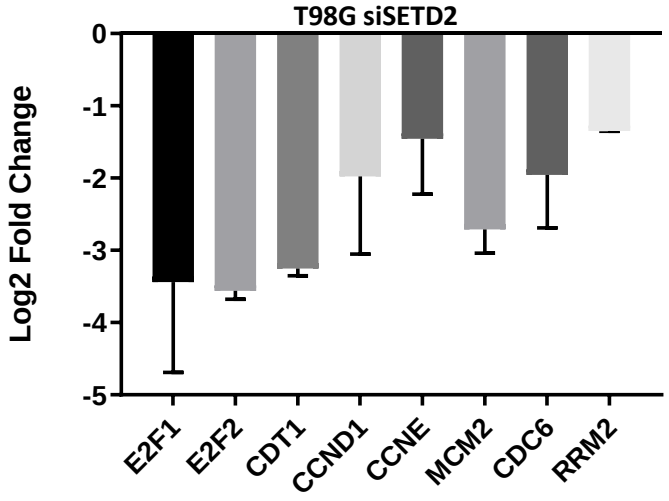
In order to confirm that loss of SETD2 is the cause of the reduced E2F transcription a SETD2 rescue experiment was performed. An N-terminal truncated (but functional) SETD2-GFP plasmid from the de Almeida lab (Carvalho et al., 2014) was expressed in SETD2 CRISPR U2OS cells, and levels of E2F transcription determined by qRT-PCR. Expression of the SETD2-GFP plasmid increased SETD2 mRNA levels by ~300 fold, but was unable to increase H3K36me3 to wildtype levels (Figure 4.2).

SETD2 is a large gene, and the SETD2-GFP insert is over 6400 base pairs in size. Due to this, it may be the case that the SETD2-GFP mRNA is poorly translated, leading to a limited increase in SETD2 protein levels. Despite this, cells transfected with the SETD2-GFP plasmid showed a small but significant increase in E2F1 mRNA, even in asynchronous conditions (Figure 4.2).

a



b



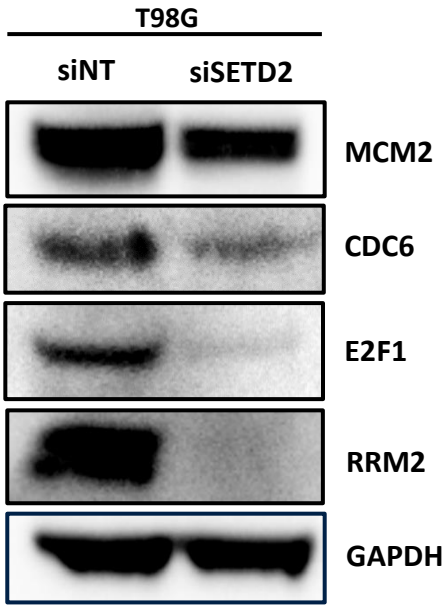
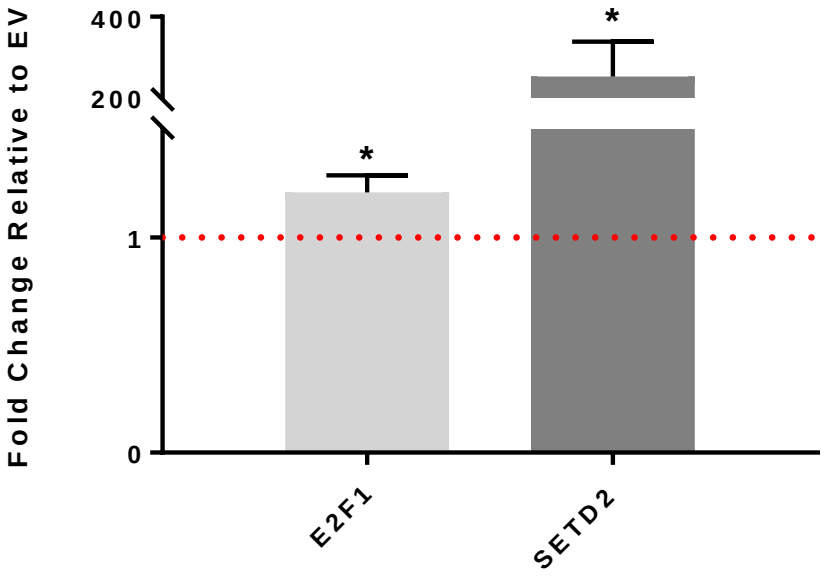


Figure 4.1: Validation of E2F target gene depletion in SETD2 deficient cells (a) Reduction of E2F target gene transcription confirmed in U2OS SETD2 CRISPR through qRT-PCR. Cells synchronised in G1 by addition of 40μM lovastatin. Expression relative to U2OS wildtype for SETD2. Data presented as mean ± SEM, n=3 independent experiments, $p<0.05$ **(b)** qRT-PCR in T98G cells treated with siSETD2. Cells synchronised in G1 by serum starvation. Expression relative to cells treated with siNT. Data presented as mean ± SEM, n=3 independent experiments, $p<0.05$ **(c)** Western blots of E2F target genes in T98G cells transfected with either siNT or siSETD2 and synchronised in G1 by serum starvation.

a



b

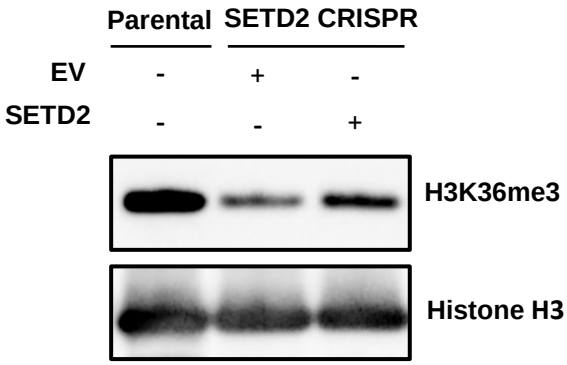


Figure 4.2: Complementation of SETD2 CRISPR U2OS with SETD2 plasmid (a) mRNA levels of indicated genes in SETD2 CRISPR U2OS cells transfected with SETD2 plasmid relative to empty vector control. Data presented as mean ± SEM, n=3 independent experiments, *p<0.05 **(b)** Western blot of H3K36me3 levels in parental and SETD2 CRISPR U2OS.

4.2.3 Readers of H3K36me3

Histones can be bound by a number of effector proteins that recognise specific lysine residues depending on their methylation state (Daniel et al., 2005). These 'readers' typically contain specific domains that bind to the lysine residue, including PHD, chromo, tudor, WD40 and PWWP. Reader proteins can have a variety of functions, such as chromatin remodelling, chromatin modification, or can themselves recruit other machinery to influence transcription or DNA repair. In order to determine whether the impaired E2F transcription seen in SETD2 deficient cells was modulated by a reader or occurred directly, U2OS cells were transfected with siRNA targeting several known H3K36me3 readers and E2F target gene expression measured by qRT-PCR.

Of the readers tested only HDAC2 knockdown was found to reduce E2F transcription in a manner similar to that of SETD2 loss (Figure 4.3). Consistent with this, HDAC2 knockdown but not MORF4L or ZMYND11 depletion, was found to sensitise cells to WEE1 inhibition (Figure 4.4). Additionally, published data shows that HDAC2 depletion leads to impaired G1/S progression and increased expression of p21 (Li et al., 2017), similar to what has been observed upon SETD2 loss. If SETD2 and HDAC2 modulate E2F target gene expression through the same pathway, depletion of both genes together should result in no further decrease in E2F target gene transcription. To determine whether this was the case, HDAC2 was depleted with siRNA in U2OS parental and SETD2 CRISPR cells, and qRT-PCR was performed to measure levels of E2F transcription. Surprisingly, depletion of both genes in combination further reduced expression of both E2F1 and RRM2 (Figure 4.5), suggesting that HDAC2 and SETD2 have independent roles in the regulation of E2F activity.

However, other proteins which have also been identified as readers of H3K36me3, including MRG15, were not tested here, and may potentially also be involved in the regulation of E2F transcription. Additionally, although all genes examined showed a robust depletion of mRNA levels after siRNA transfection, protein levels may not have been affected as strongly, and need to be investigated by Western blotting.

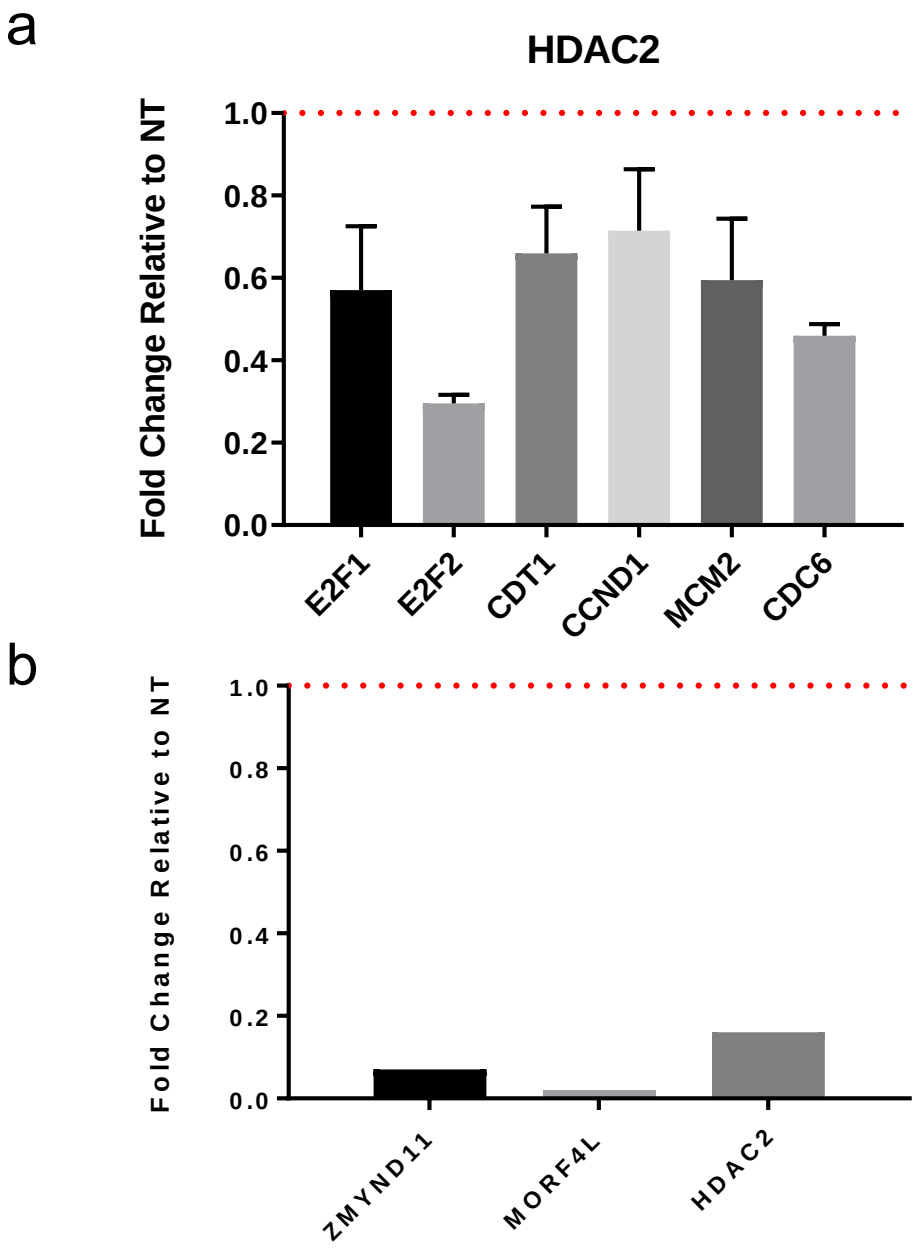


Figure 4.3: Depletion of HDAC2 leads to impaired E2F target gene expression (a) mRNA levels of indicated genes measured by qRT-PCR in T98G cells transfected with siHDAC2. Data presented as mean ± SEM, n=3 independent experiments, *p<0.05 **(b)** mRNA levels of indicated genes after depletion with siRNA.

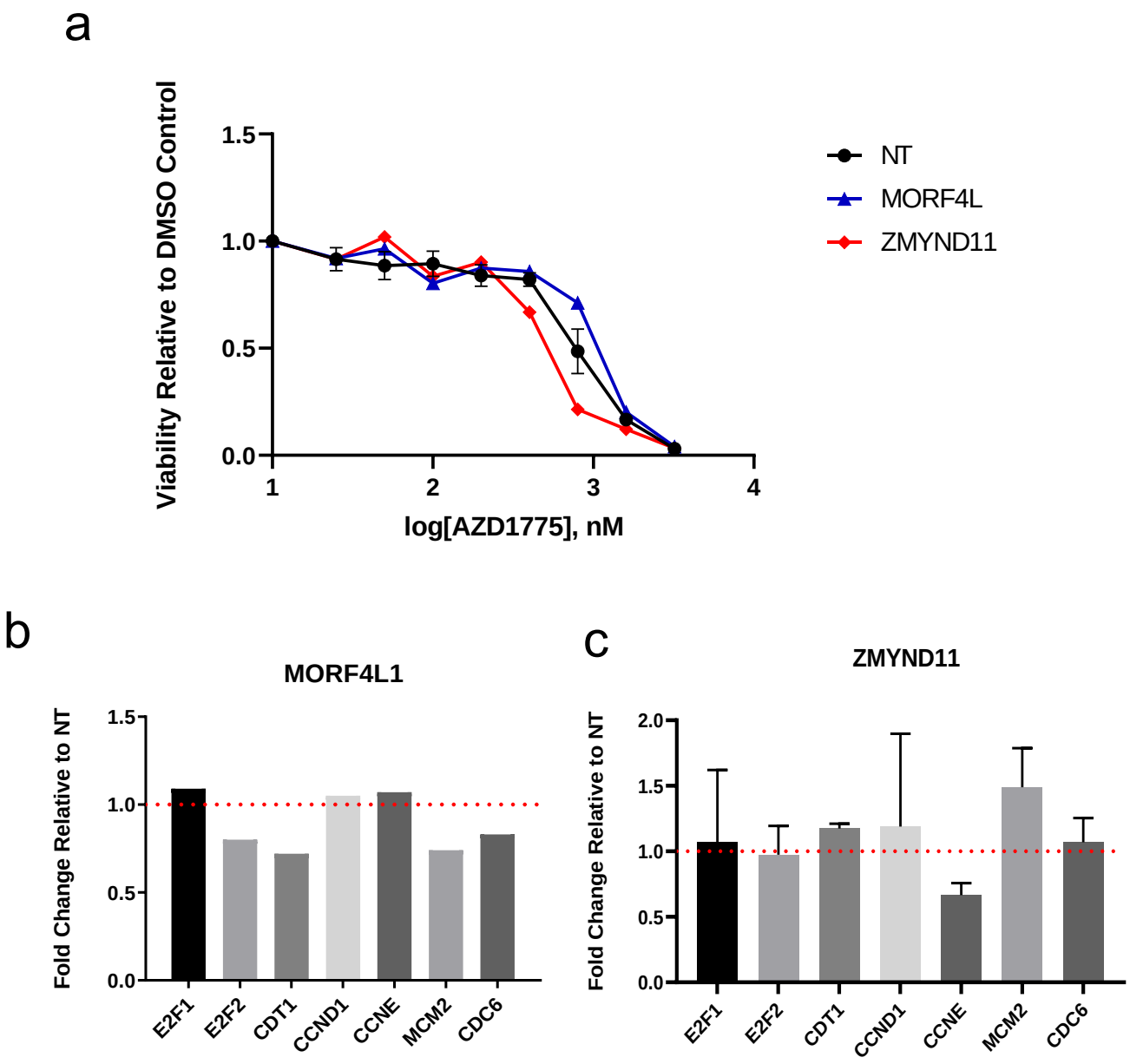


Figure 4.4: Depletion of H3K36me3 readers does not lead to impaired E2F target gene expression (a) Viability of T98G cells transfected with siRNA against the indicated genes after treatment with AZD1775 measured by resazurin assay. Data presented as mean ± SEM, n=2 independent experiments **(b)** mRNA levels of indicated genes measured by qRT-PCR in T98G cells transfected with siMORF4L1. **(c)** mRNA levels of indicated genes measured by qRT-PCR in T98G cells transfected with siZMYND11. Data presented as mean ± SEM, n=2 independent experiments.

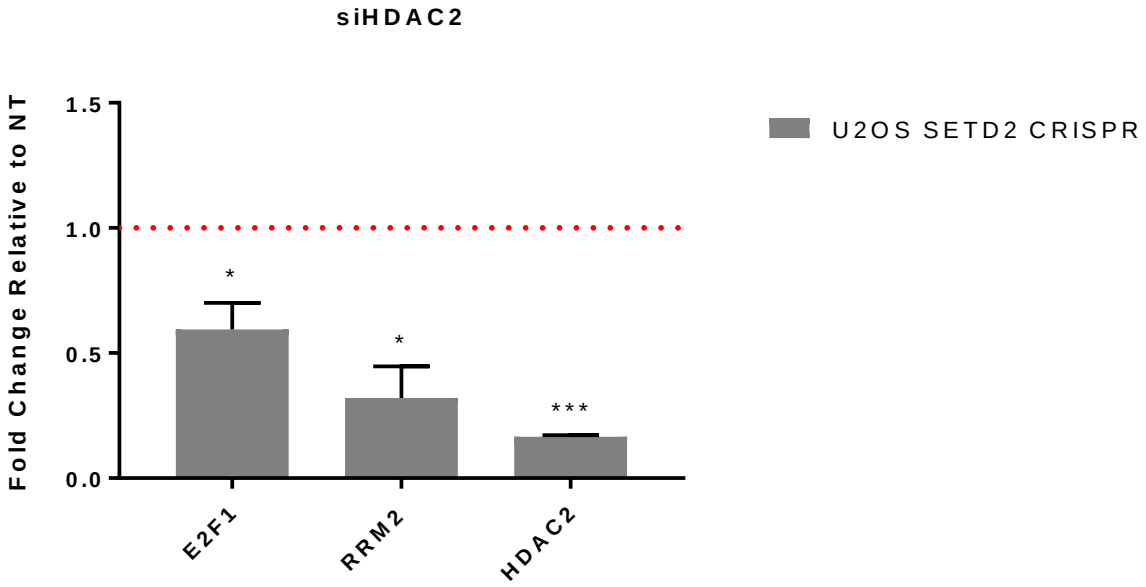


Figure 4.5: SETD2 and HDAC2 co-depletion is not epistatic. Fold change of E2F1 and RRM2 mRNA levels in U2OS SETD2 CRISPR cells transfected with siHDAC2 relative to siNT transfected cells. Data presented as mean ± SEM, n=3 independent experiments, *p<0.05, **p<0.01, ***p<0.001

4.2.4 Cell cycle analysis of SETD2 deficient cells

The transition from G1 to S phase is dependent on the E2F family of transcription factors (Bertoli et al., 2013b). Given the observed decrease in E2F target transcription in SETD2 deficient cells, it was hypothesised that impaired G1/S progression may be observed upon loss of SETD2. To test this, asynchronous parental and SETD2 CRISPR U2OS cells were collected and processed for cell cycle analysis by flow cytometry. A 15% increase in the G1 population was observed in SETD2 CRISPR U2OS cells compared to the isogenic parental cell line ($p=0.0027$) with a concurrent decrease in S phase cells (Figure 4.6), suggesting that the decreased E2F transcription in SETD2 deficient cells may result in increased G1 phase length.

To explore this further, the rate of progression into S phase was investigated with a G1 block and release experiment. T98G cells transfected with siNT or siSETD2 were deprived of serum to induce cell cycle arrest in G1, and released by addition of serum after 40 hours. Samples were taken before, and 24 hours after, addition of serum and analysed by flow cytometry. In the control cell line it was found that only 16% of the cells remained in G1 after 24 hours following release from G1 arrest. In contrast, in SETD2 knockdown cells over 30% of the cells were still in G1 (Figure 4.6), showing a significant delay in G1/S phase progression after loss of SETD2. Together these data support an important role for SETD2 in the G1/S transition, through regulation of E2F transcription.

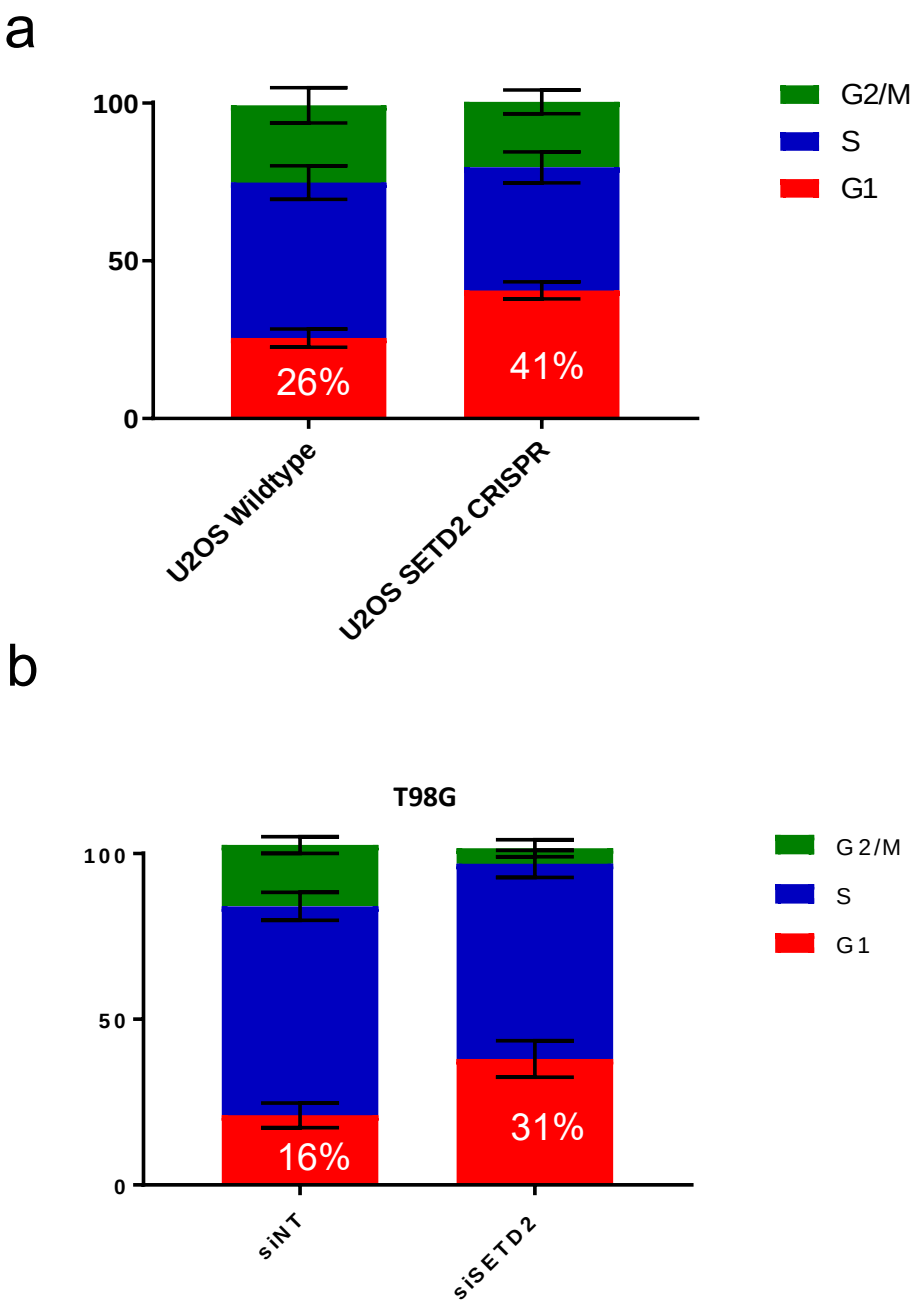


Figure 4.6: SETD2 deficient cells show impaired G1/S progression. (a) Cell cycle distribution of asynchronous U2OS wildtype and SETD2 CRISPR cells. **(b)** Cell cycle distribution 24 hours after release from serum starvation in T98G cells transfected with siNT or siSETD2. Data presented as mean ± SEM, n=3 independent experiments.

4.2.5 SETD2 deficient cells have increased endogenous damage

In addition to decreased E2F target transcription, RNA-Seq analysis of the SETD2 CRISPR U2OS cell line revealed a significant upregulation of p53 dependent transcription (Figure 4.7). Western blot analysis confirmed that loss of SETD2 resulted in a drastic increase in both p53 and p21 protein levels (Figure 4.7).

As p21 primarily acts as an inhibitor of the Cyclin E/CDK2 complex, which is required for S phase entry, it was next investigated whether the observed increase in p21 levels was important for the G1 delay observed after SETD2 loss. Asynchronous SETD2 CRISPR U2OS cells were transfected with siRNA targeting CDKN1A, and the subsequent cell cycle profile was examined by flow cytometry. siCDKN1A treated cells showed a mild reduction of G1 population and concurrent increase in S phase population (Figure 4.7), however depletion of p21 was insufficient to return SETD2 deficient cells to the wildtype cell cycle profile. It may be the case that even in the absence of p21, decreased levels of E2F transcription after loss of SETD2 result in impaired progression into S phase, and so complete rescue of the cell cycle defect is not possible through p21 depletion.

Upregulation of p53 and its target genes is typically indicative of the presence of DNA damage. To investigate whether this was the cause of the p53 upregulation, DNA damage markers were visualised by immunofluorescence microscopy in SETD2 wildtype and CRISPR deleted U2OS cells. Consistent with the upregulation of p53, SETD2 deficient cells were found to have significantly increased γH2AX and

53BP1 foci compared to wildtype (Figure 4.8), confirming that loss of SETD2 results in increased levels of endogenous DNA damage.

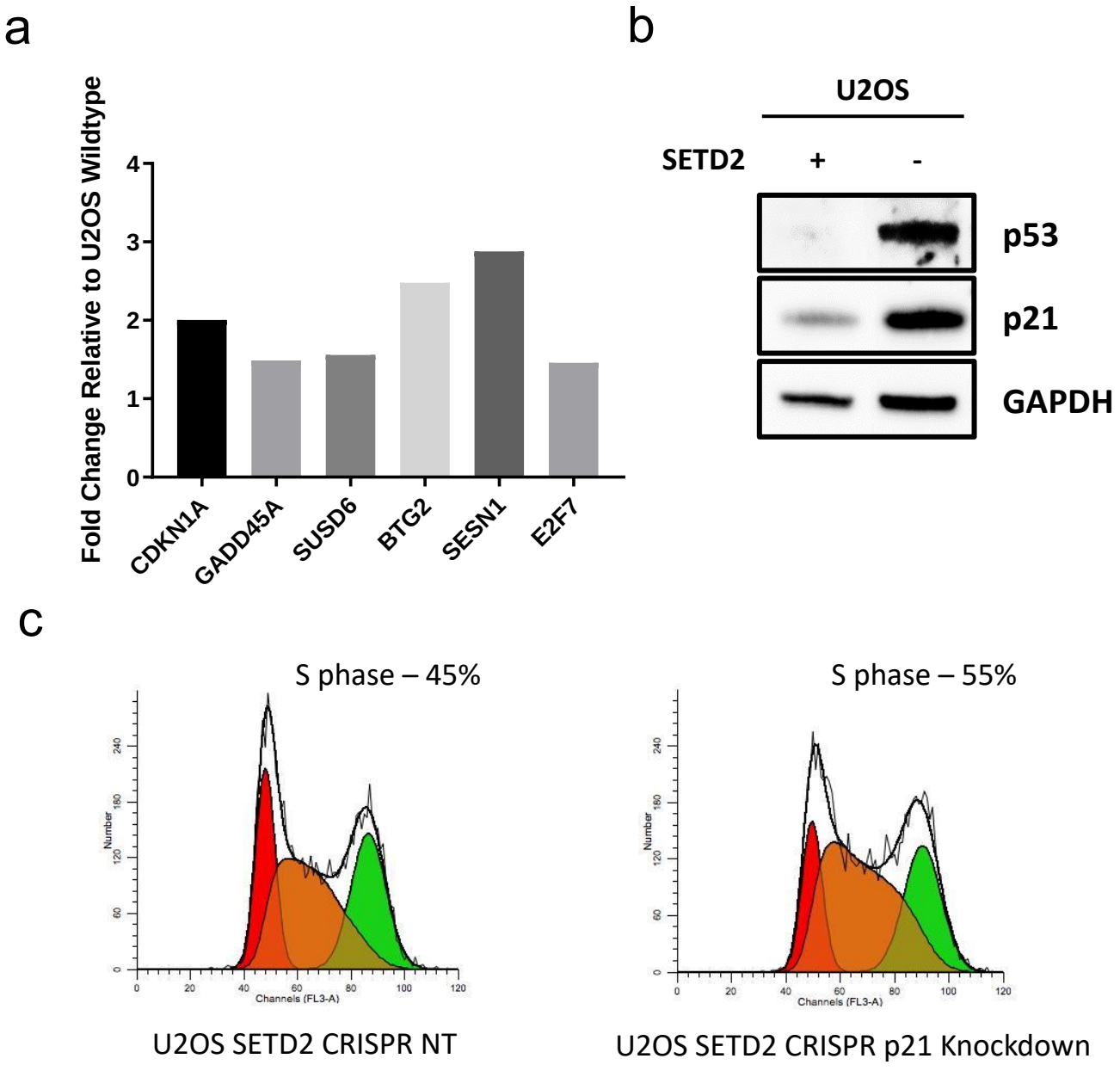


Figure 4.7: SETD2 deficient cells have increased p53 and p21 levels (a) mRNA levels of indicated genes in U2OS SETD2 CRISPR cells relative to wildtype measured by RNA-Seq. **(b)** Western blot of p53 and p21 protein in U2OS wildtype and SETD2 CRISPR. **(c)** Cell cycle profile of asynchronous U2OS SETD2 CRISPR cells transfected with siNT or siCDKN1A. The experiment described in figure 4.7b was performed by Kirsten Lopez

4.2.6 Replication stress induced DNA damage in SETD2 deficient cells

The next question to address was why loss of SETD2 results in increased levels of DNA damage. One possible source of endogenous DNA damage is replication stress. Any condition that compromises the faithful replication of the genome can be considered replication stress, including deregulation of origin firing, unscheduled replication, replication fork blockage, or insufficient nucleotide pools. One key consequence of replication stress is decreased stability of stalled replication forks, which therefore leads to increased DNA damage through increased levels of replication fork collapse (Gaillard et al., 2015).

SETD2 deficient cells have decreased levels of the ribonucleotide reductase subunit RRM2, which is required for the production of deoxyribonucleotides for replication. It was therefore considered that loss of SETD2 may result in replication stress through depletion of nucleotide pools due to a reduction of RRM2. To investigate whether this was the case, nucleotide pools were supplemented through the addition of exogenous nucleosides. T98G cells grown in the presence of exogenous nucleosides were found to have significantly reduced levels of γH2AX and 53BP1 foci, (Figure 4.9) implicating insufficient nucleotide pools as a source of DNA damage in SETD2 deficient cells.

As dNTP starvation results in replication stress through replication fork stalling, a DNA fibre assay was performed to determine whether fork speed was affected upon loss of SETD2. A significant reduction in fork velocity from an average of 0.4kb/min to 0.2kb/min was observed in SETD2 CRISPR U2OS compared to the isogenic parental U2OS cells. Additionally, supplementation with exogenous nucleosides was sufficient to rescue the decrease in replication fork speed (Figure 4.10).

In addition to decreased RRM2 levels, loss of SETD2 results in decreased expression of a number of other E2F target genes, including those involved in replication origin loading. It was therefore considered whether insufficient origin licensing may also be a source of replication stress upon loss of SETD2. Reduced levels of single stranded DNA can indicate a reduction in the number of replication forks, and so the single stranded DNA binding protein RPA was visualised in parental and SETD2 CRISPR U2OS cells. SETD2 deficient cells showed significantly fewer RPA foci, which may indicate reduced replication origin licensing during G1 (Figure 4.10). However, it has also been demonstrated that loss of SETD2 results in decreased recruitment of RPA to sites of DNA damage (Pfister et al., 2014), and so reduced RPA foci in these cells may result from impaired recruitment rather than reduced single stranded DNA.

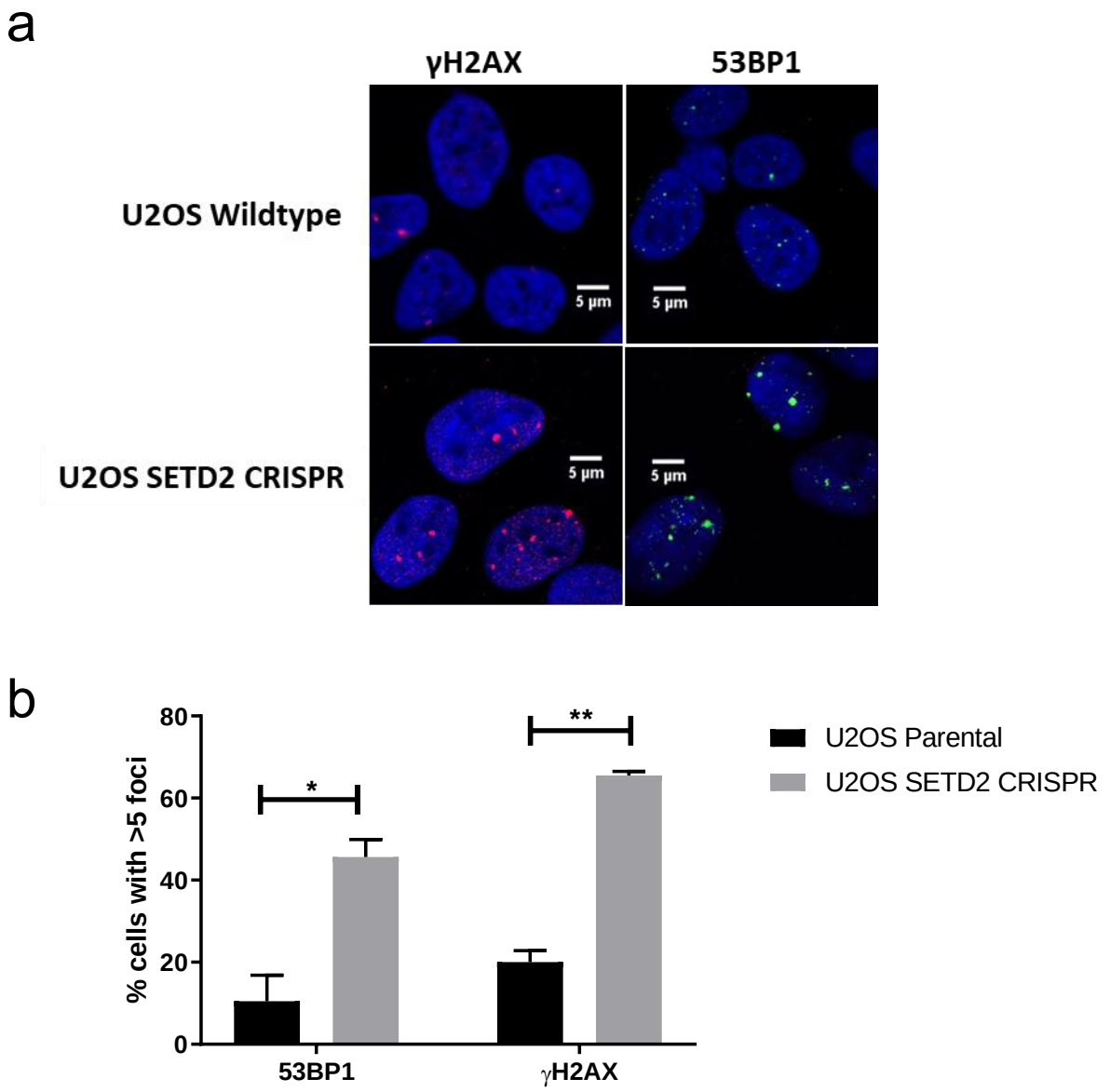


Figure 4.8: Increased endogenous damage in SETD2 deficient cells (a) Immunofluorescence visualisation of γH2AX and 53BP1 foci in U2OS wildtype and SETD2 CRISPR cells**. (b)** Quantification of (a). Data presented as mean ± SEM, n=3 independent experiments, *p<0.05, **p<0.01.

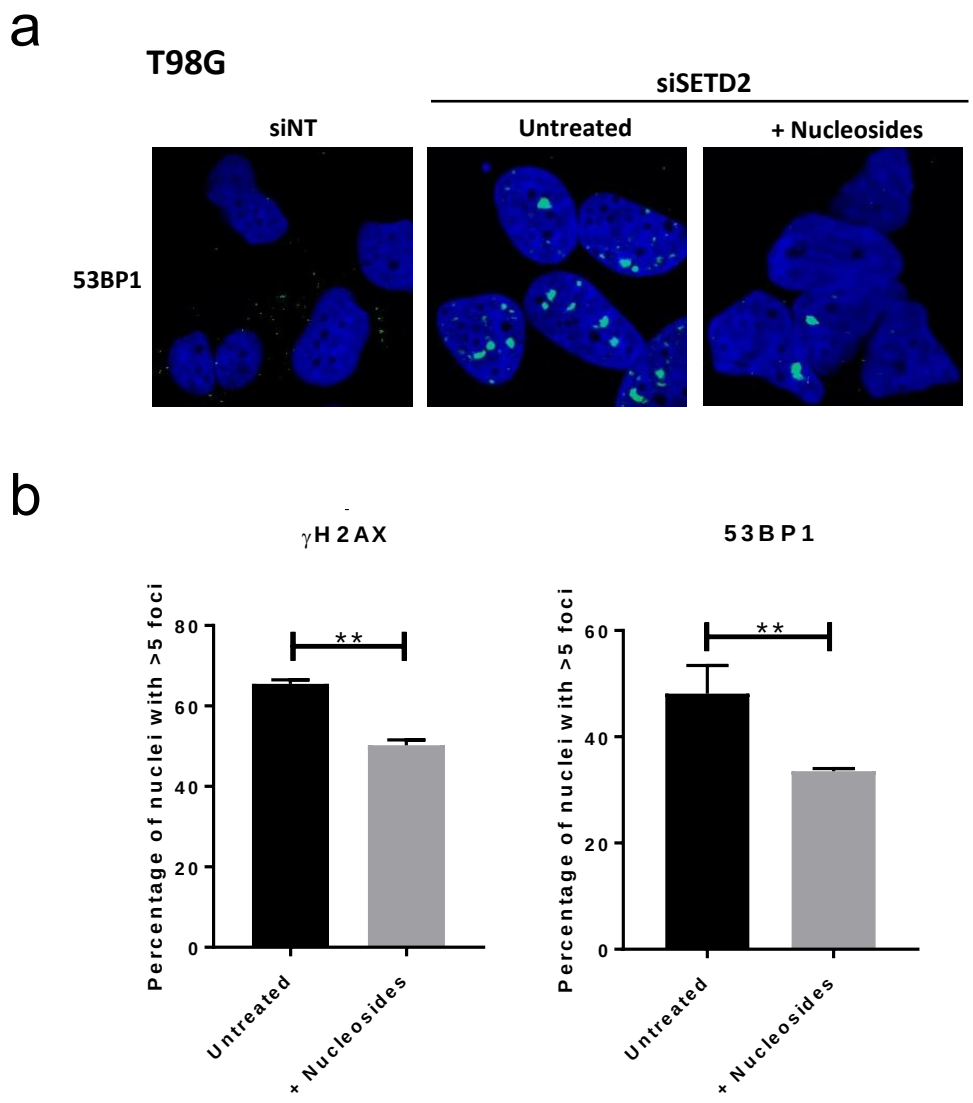


Figure 4.9: Exogenous nucleoside treatment partially rescues DNA damage in SETD2 deficient cells (a) Immunofluorescence visualisation of 53BP1 foci in siSETD2 transfected T98G cells grown in the presence or absence of Embryomax ES nucleosides. **(b)** Quantification of γH2AX and 53BP1 foci imaged in siSETD2 transfected T98G cells grown in the presence or absence of Embryomax ES nucleosides. Data presented as mean ± SEM, n=3 independent experiments, *p<0.05, **p<0.01.

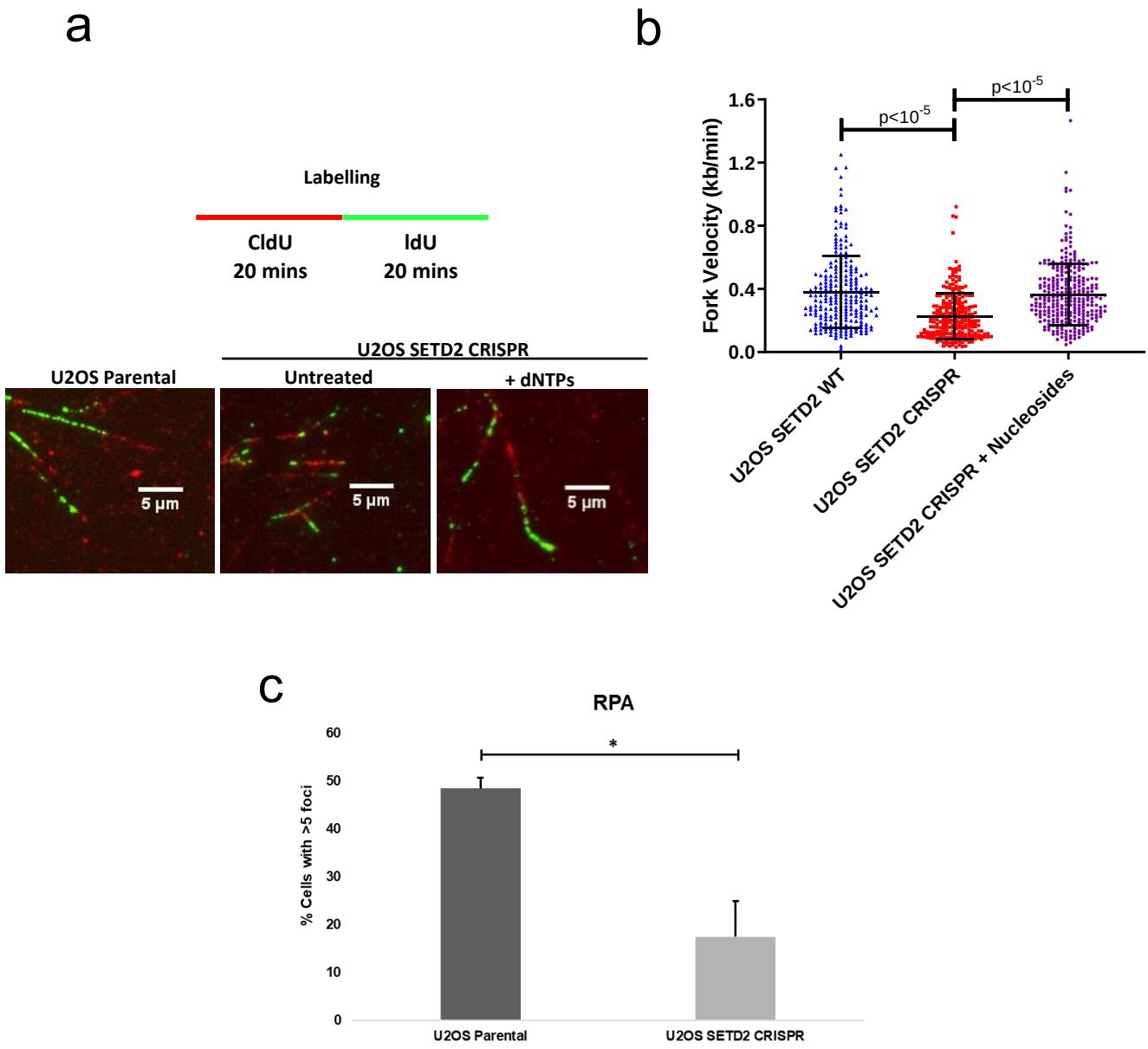


Figure 4.10: Decreased replication fork speed in SETD2 deficient cells (a) Representative images of DNA fibres in U2OS wildtype and SETD2 CRISPR cells with and without treatment with Embryomax ES nucleosides. **(b)** Fork velocity was analysed in over 200 ongoing replication forks in each condition. **(c)** Quantification of RPA foci imaged in U2OS parental and U2OPS SETD2 CRISPR cell lines. Data are presented as mean ± SEM. Data collected from 4 independent biological replicates.

4.2.7 Loss of SETD2 leads to increased G1 53BP1 bodies

It has previously been reported that under-replication of DNA leads to DNA damage that is repaired in the subsequent G1 phase, and can be visualised by the presence of 53BP1 bodies (Harrigan et al., 2011; Lukas et al., 2011). As decreased fork velocity was observed after depletion of SETD2, it was hypothesised that this may lead to under-replication, and subsequently to induction of G1 53BP1 bodies.

To test this, T98G cells were transfected with siSETD2, and arrested in G1 by removal of serum. A significant increase in the levels of G1 53BP1 bodies was observed in SETD2 depleted cells when compared to cells transfected with non-targeting siRNA (Figure 4.11), suggesting that depletion of SETD2 deficient cells may result in DNA under-replication.

Supplementation of SETD2 deficient cells with exogenous nucleosides was sufficient to restore normal fork speed, and so it was hypothesised that increased nucleotide pools may also rescue the induction of G1 53BP1 bodies by preventing under-replication. T98G cells were transfected with siSETD2, and arrested in G1 in the presence or absence of exogenous nucleosides. The addition of nucleosides was able to partially rescue the accumulation of G1 53BP1 foci in SETD2 deficient cells (Figure 4.11), supporting the idea that 53BP1 G1 bodies arise in SETD2 deficient cells though under-replication of DNA.

To investigate whether the low levels of replication licensing factors in SETD2 deficient cells may also contribute to the under-replication observed, cells were also transfected with siCDC6, and G1 53BP1 bodies visualised. It was found that depletion of CDC6 also results in significant accumulation of 53BP1 foci, which as expected cannot be rescued by nucleotide supplementation (Figure 4.11). The partial rescue by nucleoside supplementation in SETD2 deficient cells may indicate that under-replication arises as a consequence of both decreased RRM2 and therefore nucleotide pools, and also though insufficient origin licensing.

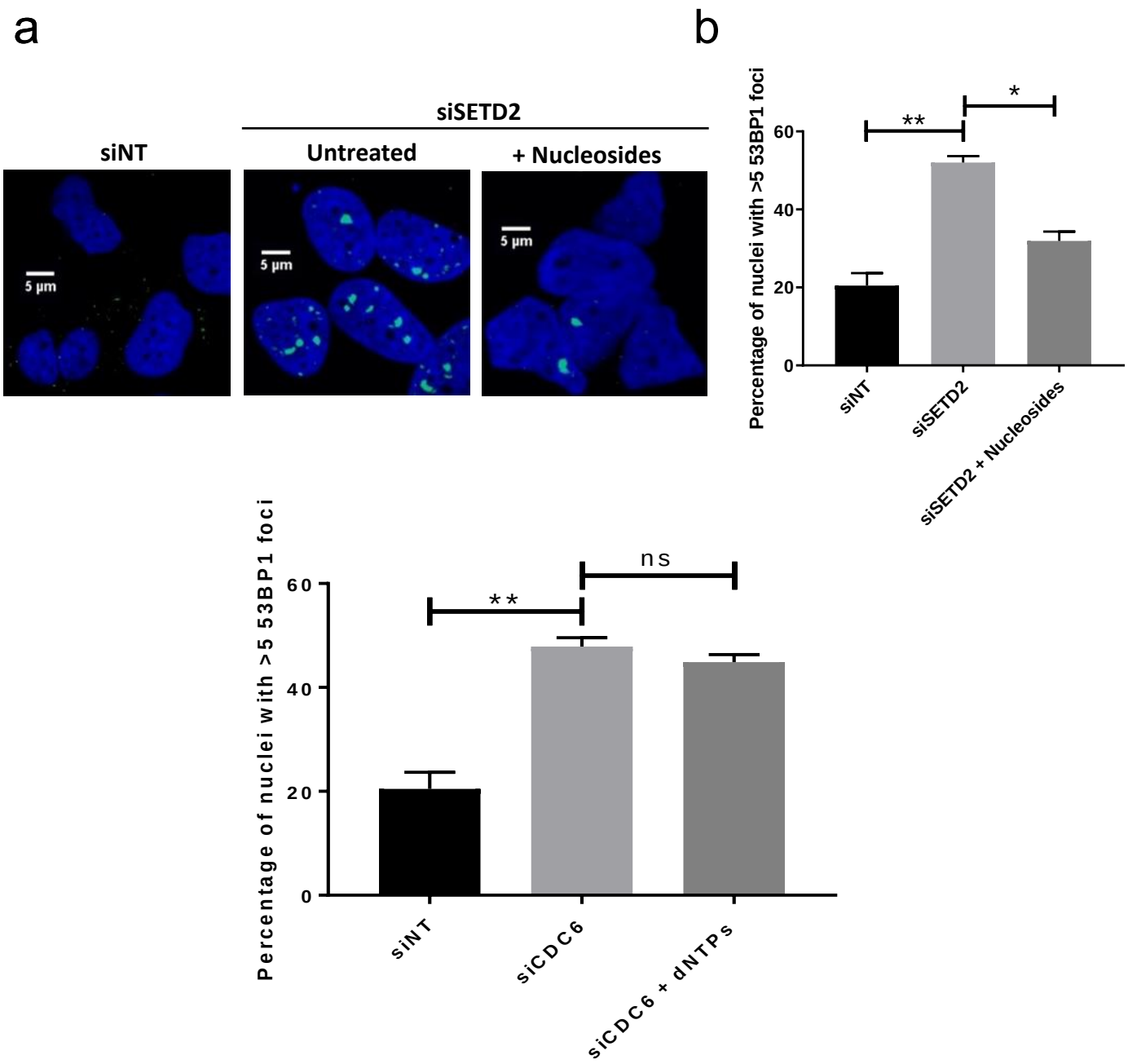


Figure 4.11: Increased G1 53BP1 bodies upon depletion of SETD2 (a) 53BP1 bodies imaged by immunofluorescence in G1 synchronised siSETD2 treated T98G cells plus and minus exogenous nucleosides. **(b)** Quantification of 53BP1 foci in (a). **(c)** Quantification of 53BP1 foci in siCDC6 transfected cells plus and minus exogenous nucleosides. Data presented as mean ± SEM, n=3 independent experiments, *p<0.05, **p<0.01.

4.2.8 Under-replicated DNA leads to mitotic damage in SETD2 deficient cells

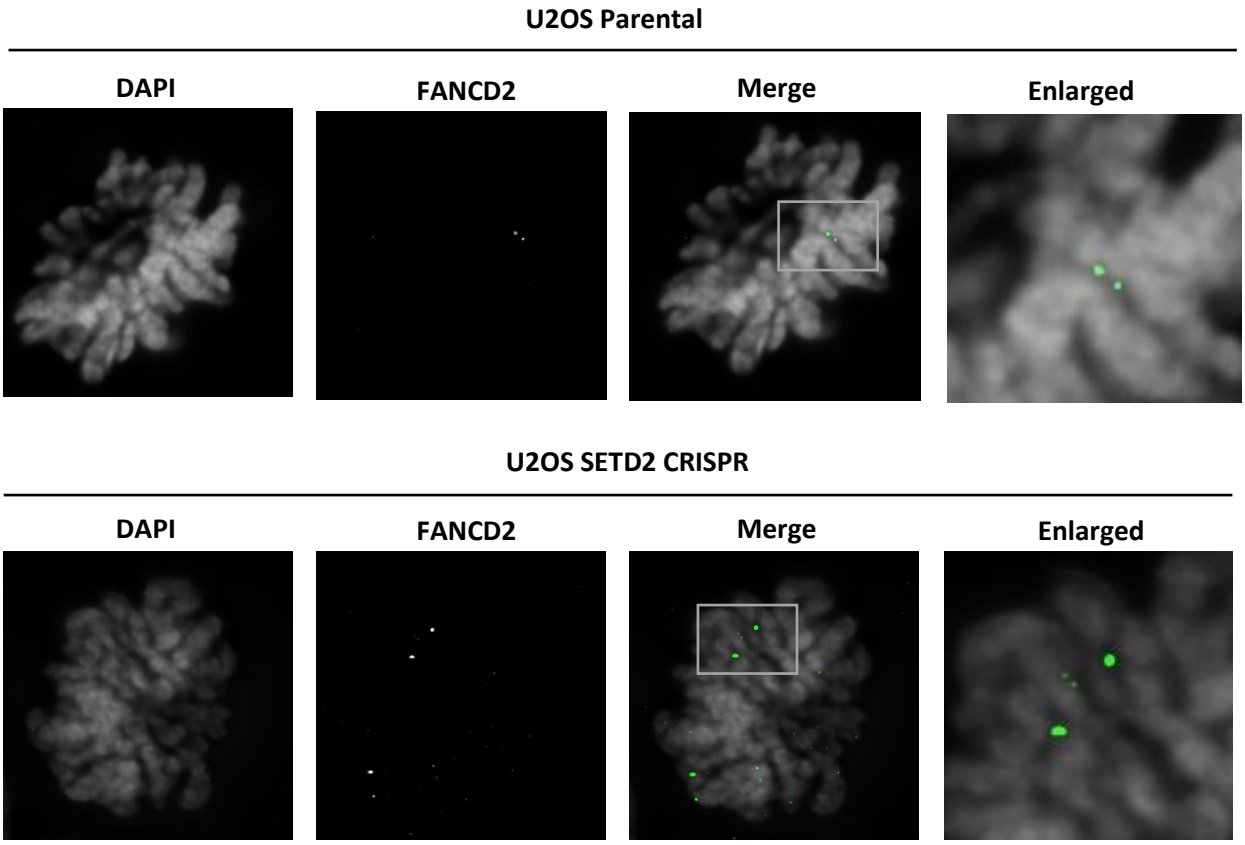
One of the major consequences arising from perturbation of replication is the presence of improperly replicated regions of DNA, which are unable to segregate correctly during mitosis. In replication stress conditions FANCD2 is recruited and forms nuclear foci at the replication fork. These foci persist into G2 phase and mitosis, and manifest as a pair of so-called ‘sister FANCD2 foci’ on sister chromatids. It is believed that the sister foci mark incompletely replicated regions, and has been used as an indicator of the level of replication stress present.

Consistent with the finding of elevated G1 nuclear body formation, it was observed that SETD2 deficient cells also showed increased numbers of paired FANCD2 foci in mitosis, compared to wildtype cells, further supporting that loss of SETD2 leads to induction of replication stress (Figure 4.12).

Upon chromosome segregation in anaphase, it has been shown that these incompletely replicated regions of DNA, bound by sister FANCD2 foci, may give rise the formation of ultrafine DNA bridges (UFBs) (Chan et al., 2007; Chan and Hickson, 2009; Chan et al., 2009). These bridges cannot be stained by traditional DNA dyes, but can be visualised by immunofluorescence staining for proteins such as PICH (PLK1-interacting checkpoint helicase) or RPA, which bind the bridges at double-stranded and single-stranded regions respectively.

As loss of SETD2 results in decreased replication fork velocity, it was hypothesised that the observed replication stress may result from under-replication. To investigate whether the decreased replication fork speed resulting from SETD2 loss also resulted in increased generation of FANCD2-associated DNA intertwinements, U2OS wildtype and SETD2 anaphase cells were stained for PICH and FANCD2, and imaged by immunofluorescence microscopy. FANCD2 positive UFBs were detected in both U2OS wildtype and SETD2 CRISPR cell lines, but a significantly greater number were observed in the SETD2 deficient population, indicating increased levels of under-replicated DNA after loss of SETD2 (Figure 4.13).

a



b

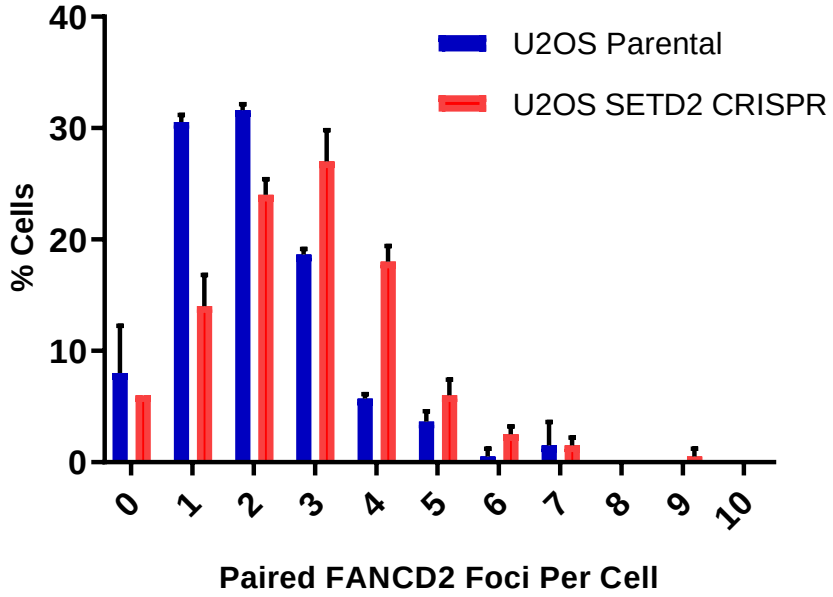


Figure 4.12: Loss of SETD2 leads to increased replication stress (a) Representative images of pre-anaphase cells showing FANCD2 sister foci **(b)** Quantification of FANCD2 foci in parental U2OS and U2OS SETD2 CRISPR cell lines. Data presented as mean ± SEM, n=3 independent biological replicates.

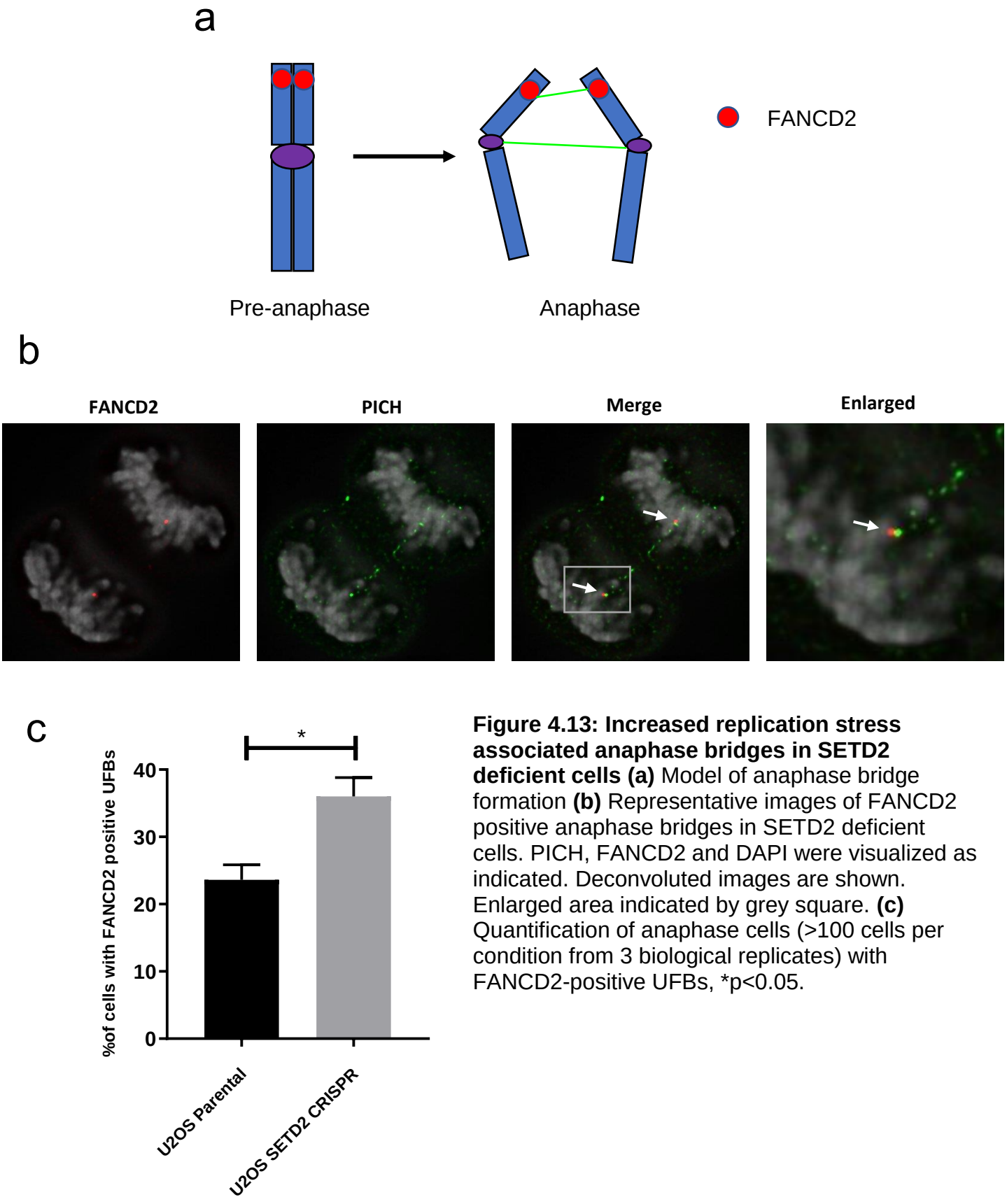


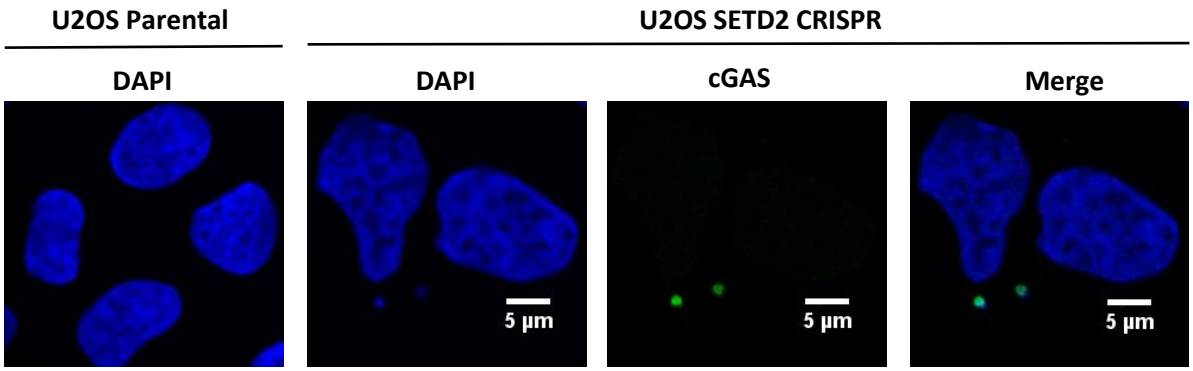
Figure 4.13: Increased replication stress associated anaphase bridges in SETD2 deficient cells (a) Model of anaphase bridge formation **(b)** Representative images of FANCD2 positive anaphase bridges in SETD2 deficient cells. PICH, FANCD2 and DAPI were visualized as indicated. Deconvoluted images are shown. Enlarged area indicated by grey square. **(c)** Quantification of anaphase cells (>100 cells per condition from 3 biological replicates) with FANCD2-positive UFBs, *p<0.05.

4.2.9 Increased micronuclei frequency in SETD2 deficient cells

Improper DNA replication can also result in mis-segregation of chromosomes during mitosis, leading to the formation of micronuclei (Xu et al., 2011). Micronuclei are defined as extra-nuclear bodies that contain damaged chromosome fragments or whole chromosomes, and serve as a reliable indicator of genomic instability (Luzhna et al., 2013).

Consistent with other data shown here, SETD2 CRISPR U2OS were observed to have significantly increased numbers of micronuclei compared to wildtype cells (Figure 4.14). Micronuclei have also been shown to activate the immune system through cGas driven activation of the STING pathway, resulting in increased expression of a number of cytokines and chemokines, and an increased anti-tumour immune response (Li and Chen, 2018). To investigate whether micronuclei arising as a result of SETD2 loss also activate this pathway, SETD2 CRISPR U2OS cells were stained with an antibody to cGas and visualised by immunofluorescence microscopy. It was observed that almost of half of the micronuclei present in SETD2-deficient cells stained positively for cGas (Figure 4.14), raising the possibility that cancers lacking SETD2 may potentially have an increased anti-tumour immune response.

a



b

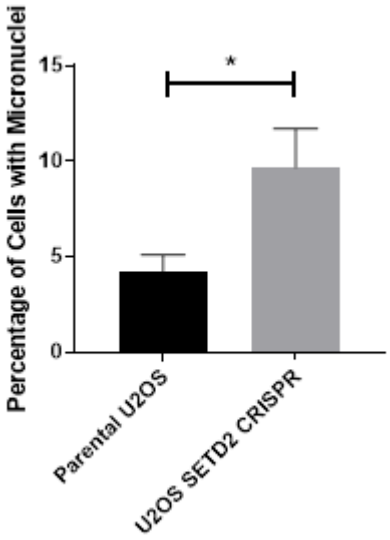


Figure 4.14: Loss of SETD2 leads to increased levels of micronuclei formation **(a)** Representative images of micronuclei in wildtype and SETD2 CRISPR U2OS cells. **(b)** Quantification of micronuclei in wildtype and SETD2 CRISPR U2OS. Data presented as mean ± SEM, n=3 independent biological replicates, *p<0.05.

4.2.10 Impaired replication stress response in SETD2-deficient cells

In addition to its role in canonical cell cycle progression, it has been shown that the E2F transcription profile is activated in response to replication stress, and plays an important role in the prevention of replication stress induced DNA damage (Bertoli et al., 2013a). E2F6, a repressive E2F that replaces activating E2Fs at target gene promoters upon S phase entry, is phosphorylated in an ATR-CHK1 dependent manner in response to replication stress. This results in E2F6 disassociation from promoters and facilitates the re-expression of E2F target genes, preventing DNA damage and subsequent cell death.

As E2F transcription is impaired and high levels of replication stress induced DNA damage are present in SETD2 deficient cells, it was hypothesised that H3K36me3 may also be required for effective induction of E2F target genes in response to replication stress. To test this, replication stress was induced in T98G cells treated with siNT or siSETD2 by treatment with hydroxyurea, and mRNA levels of several E2F target genes measured by qRT-PCR. While a strong upregulation was observed in control cells, SETD2 depleted cells showed significantly decreased levels of E2F target gene induction after replication stress, suggesting impaired E2F transcriptional activation in SETD2 deficient cells (Figure 4.15). These findings support a role for H3K36me3 in E2F transcription during both normal cell cycle progression, and in response to replication stress.

4.2.11 Replication stress induces SETD2 dependent upregulation of E2F target genes

Canonically H3K36me3 is highly enriched during G1, peaking at the G1/S transition in both yeast and humans. Upon S phase entry, the methyltransferase SETD2 is downregulated, while the demethylase KDM4A is upregulated, leading to a global decrease in H3K36me3 levels (Black et al., 2010; Li et al., 2013; Pai et al., 2014). This follows the same pattern as E2F target gene expression and is consistent with a role in E2F transcriptional regulation. As H3K36me3 is normally removed during S phase, it was hypothesised that H3K36 may be tri-methylated in response to replication stress to facilitate the re-expression of E2F target genes. To test this, the levels of H3K36me3 at several known E2F target genes were measured by ChIP in presence and absence of hydroxyurea. A significant increase in H3K36me3 levels was observed upon replication stress induction, which is consistent with the hypothesis that H3K36 trimethylation is induced upon replication stress, allowing re-expression of E2F target genes to help prevent DNA damage (Figure 4.16).

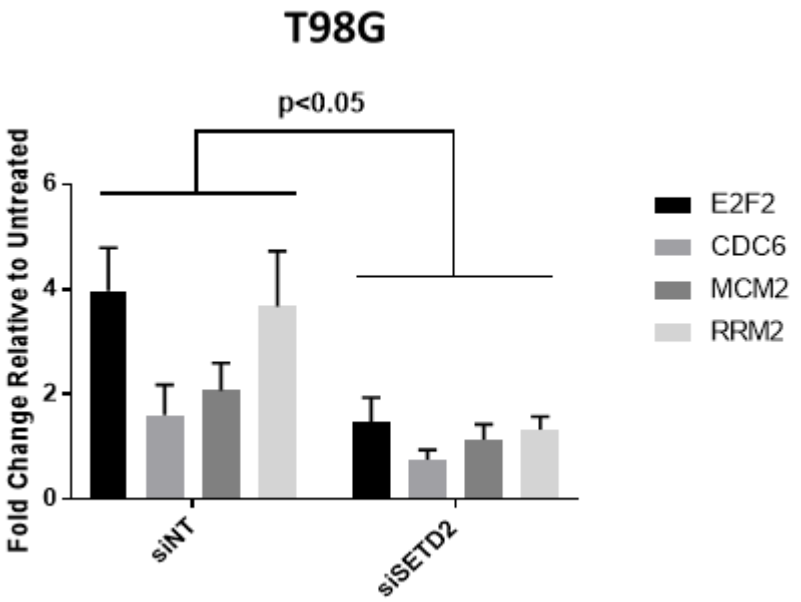


Figure 4.15: Replication stress induced E2F target gene expression is impaired after loss of SETD2. Fold change of E2F target gene expression measured by rt-PCR in T98G cells transfected with siNT or siSETD2 after treatment with 2 mM hydroxyurea for 4 hours. Data presented as mean ± SEM, n=3 independent experiments.

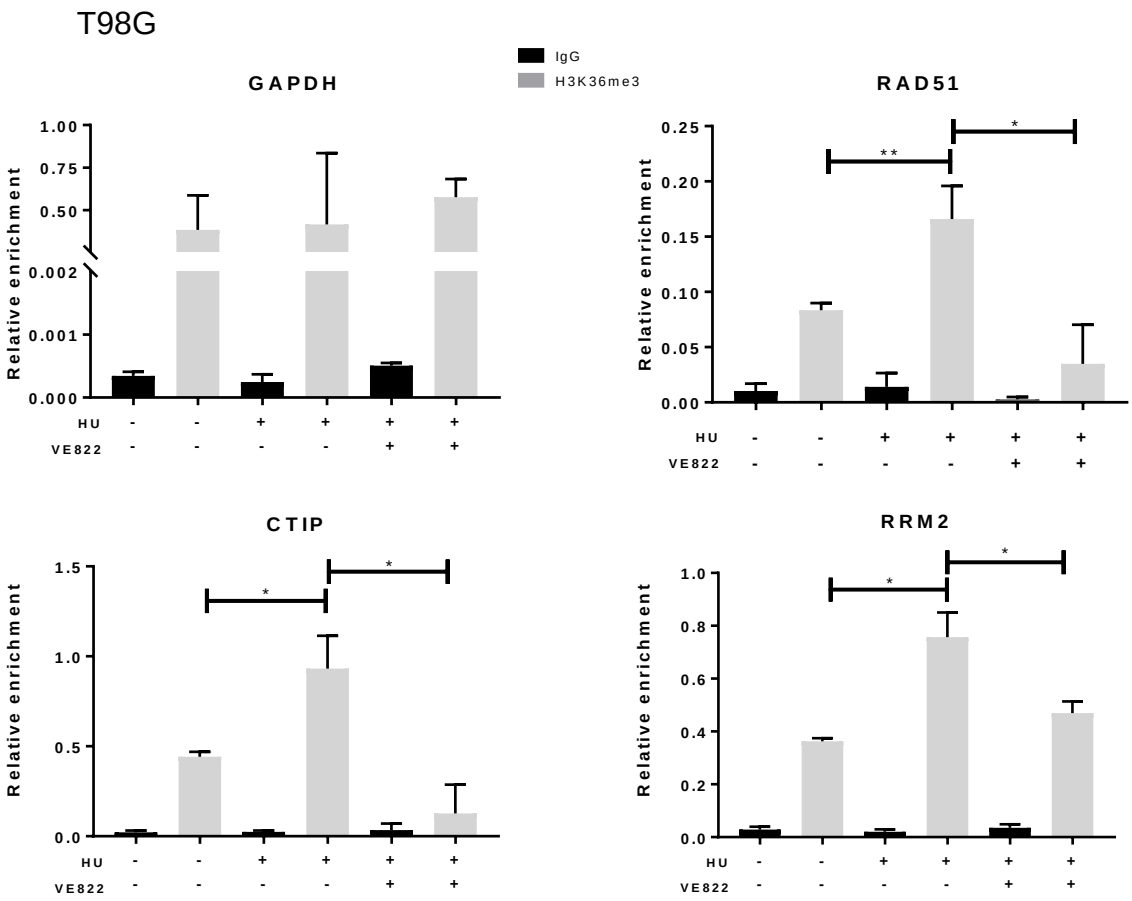


Figure 4.16: Replication stress induces H3K36me3 at E2F target gene promoters. T98G cells were treated with water, 2 mM hydroxyurea alone, or 2 mM hydroxyurea and the ATR inhibitor VE822 (2μM) for 4 hours. ChIP was performed with anti-H3K36me3 antibody and the binding to RRM2, Rad51, CtIP and GAPDH promoters was evaluated by qRT-PCR relative to input. Data presented as mean ± SEM, n=3 independent experiments, *p<0.05, **p<0.01.

4.2.12 KDM4A demethylation of H3K36me3 is not induced by replication stress

Next, the mechanism by which H3K36me3 is upregulated after replication stress was investigated. In somatic cells H3K36me3 is regulated by a single methyltransferase, SETD2, and primarily by a single demethylase. KDM4A, also known as JMJD2A, is a histone demethylase in the Jumonji domain family, and has demethylase activity for H3K4me3, H3K9me3, and H3K36me3. Consistent with the role of SETD2 as a tumour suppressor, overexpression of KDM4A has been found to lead to genome instability (Black et al., 2013), while a reduction in KDM4A levels promotes p53 and p21 pro-apoptotic activity (Kim et al., 2012a). Additionally, a role for KDM4A in the DNA damage response has been identified. KDM4A was found to be degraded in DNA damage conditions in an RNF8/RNF168 dependent manner (Mallette et al., 2012), facilitating recruitment of 53BP1.

It was therefore hypothesised that KDM4A may also be downregulated in response to replication stress, enabling upregulation of H3K36me3. However, no change in KDM4A levels was observed in response to HU (Figure 4.17), indicating that KDM4A is not downregulated after replication stress.

As KDM4A was not affected by replication stress, levels of SETD2 were investigated to determine if the H3K36me3 increase is due to upregulation of the methyltransferase. T98G cells were treated with hydroxyurea and SETD2 mRNA levels measured by qRT-PCR. Significantly increased SETD2 levels were observed following induction of replication stress, suggesting that replication stress may induce

upregulation of H3K36me3 by increasing levels of the methyltransferase SETD2. It is currently unclear whether this results in a global increase of SETD2 protein levels, and this needs to be investigated further.

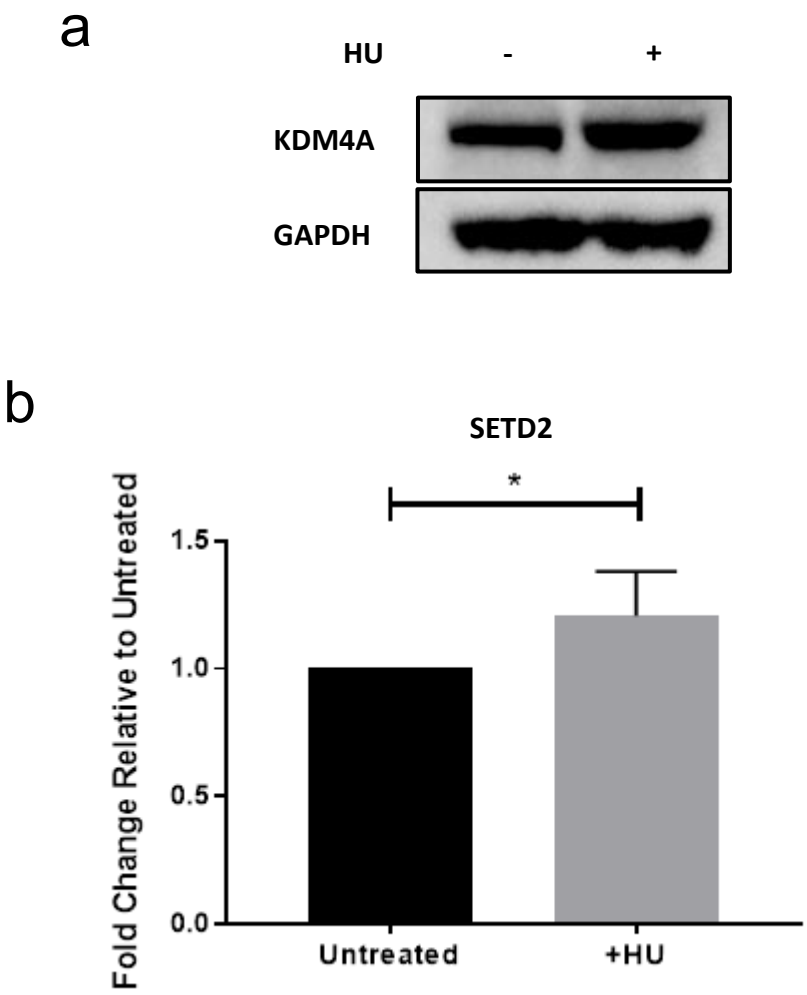


Figure 4.17: KDM4A protein levels are not affected by replication stress (a) Western blot for KDM4A protein levels in T98G cells treated with water or 2 mM HU for 4 hours. **(b)** mRNA levels of SETD2 in T98G cells treated with water or 2 mM HU measured by qRT-PCR. Data presented as mean ± SEM, n=3 independent experiments, *p<0.05.

4.2.13 Replication stress induced H3K36me3 is checkpoint dependent

Upregulation of E2F target genes has been shown to be induced by the replication checkpoint kinase CHK1, which is itself activated by ATR in the presence of stressed replication forks (Bertoli et al., 2013a; Saldivar et al., 2017). As H3K36me3 upregulation at E2F target genes is also induced by replication stress, and SETD2 is required for effective E2F target transcription, it was hypothesised that the ATR/CHK1 pathway may induce E2F target upregulation by inducing H3K36me3 at E2F target gene promoters.

To determine if this was the case, T98G cells were treated with hydroxyurea alone or in combination with the ATR inhibitor VE822, and the levels of H3K36me3 measured by ChIP at several known E2F target gene promoters. As seen previously, cells treated with hydroxyurea showed significantly increased levels of H3K36me3. In contrast, those cells treated with both HU and VE822 were unable to induce H3K36me3 upregulation at any of the E2F targets tested, indicating that H3K36me3 is induced at E2F target gene promoters by the replication stress checkpoint (Figure 4.16).

4.2.14 SETD2 has independent roles in DNA damage and replication stress responses

SETD2 has well established roles in the DNA damage response, particularly in double-strand break repair. Cells deficient in SETD2 have severely impaired ability to

recruit a number of factors required for homologous recombination, including RPA and RAD51 (Pfister et al., 2014). As a result, cells are forced to carry out micro-homology mediated end joining, leading to an increased rate of mutation and a subsequent loss of genomic stability. A number of genes involved in homologous recombination repair are also known E2F target genes, and E2F1 levels have been shown to increase upon induction of DNA damage (Lin et al., 2001). It was therefore investigated whether SETD2 acts through the same mechanism in both the replication stress response and the double-strand break repair pathway.

First it was tested whether E2F target gene expression was upregulated in response to DNA damage. T98G cells transfected with siNT or siSETD2 were exposed to 6Gy IR, and samples were harvested after indicated timepoints. It was found that at both 30 minutes and 4 hours after ionising radiation (IR) treatment there was no significant upregulation in the E2F target genes tested (Figure 4.18). This data indicates that the DNA damage response role for H3K36me3 is independent of its role in E2F regulation.

It has previously been demonstrated that SETD2-deficient cells are sensitive to inhibition of WEE1, which induces replication stress through uncontrolled CDK activation. This sensitivity is consistent with the idea that SETD2 deficient cells are unable to adequately activate the E2F transcription pathway upon replication stress.

To further investigate the relationship between the role of SETD2 in the replication stress response and DNA damage response cells were treated with the WEE

inhibitor AZD1775 together with ionising radiation. It was found that, in combination, WEE1 inhibition and IR synergise to give a loss of viability, which may indicate that SETD2 has functionally distinct roles in facilitating replication stress-induced E2F expression and HR repair (Figure 4.18), however the transcriptional role of SETD2 in DNA repair has yet to be investigated in detail.

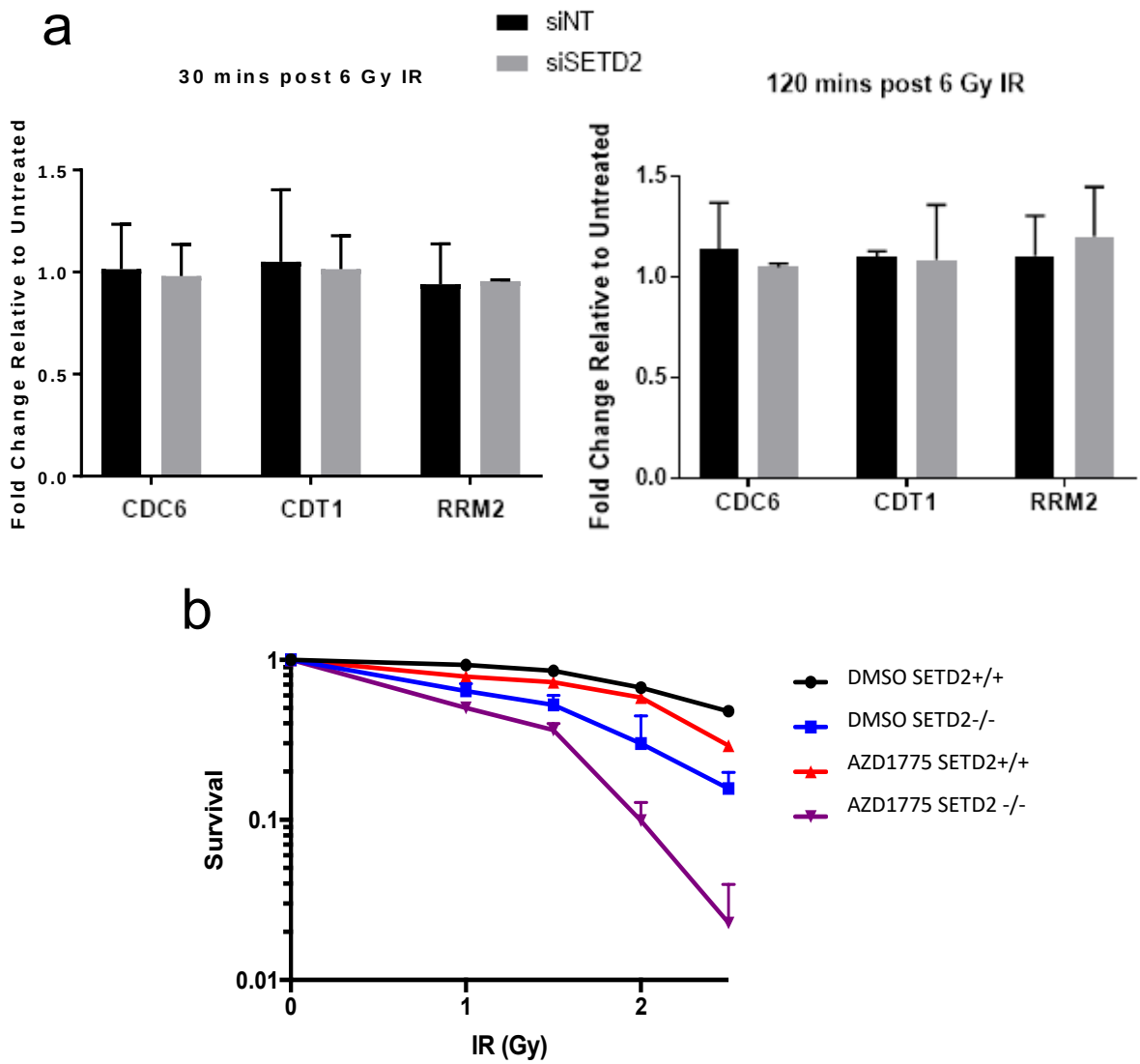


Figure 4.18: Independent roles for SETD2 in replication stress and DNA damage repair (a) Fold change of E2F target gene expression measured by rt-PCR in T98G cells transfected with siNT or siSETD2 and collected 30 or 120 minutes after 6 Gy IR. Data presented as mean ± SEM, n=4 independent biological replicates **(b)** U2OS Parental and SETD2 CRISPR cell lines were treated with DMSO or 150nM AZD1775 24 hours prior to irradiation and subjected to clonogenic survival assays. Data presented as mean ± SEM, n=2 independent experiments. The experiment described in figure 4.18b was performed by Dr Sovan Sarkar.

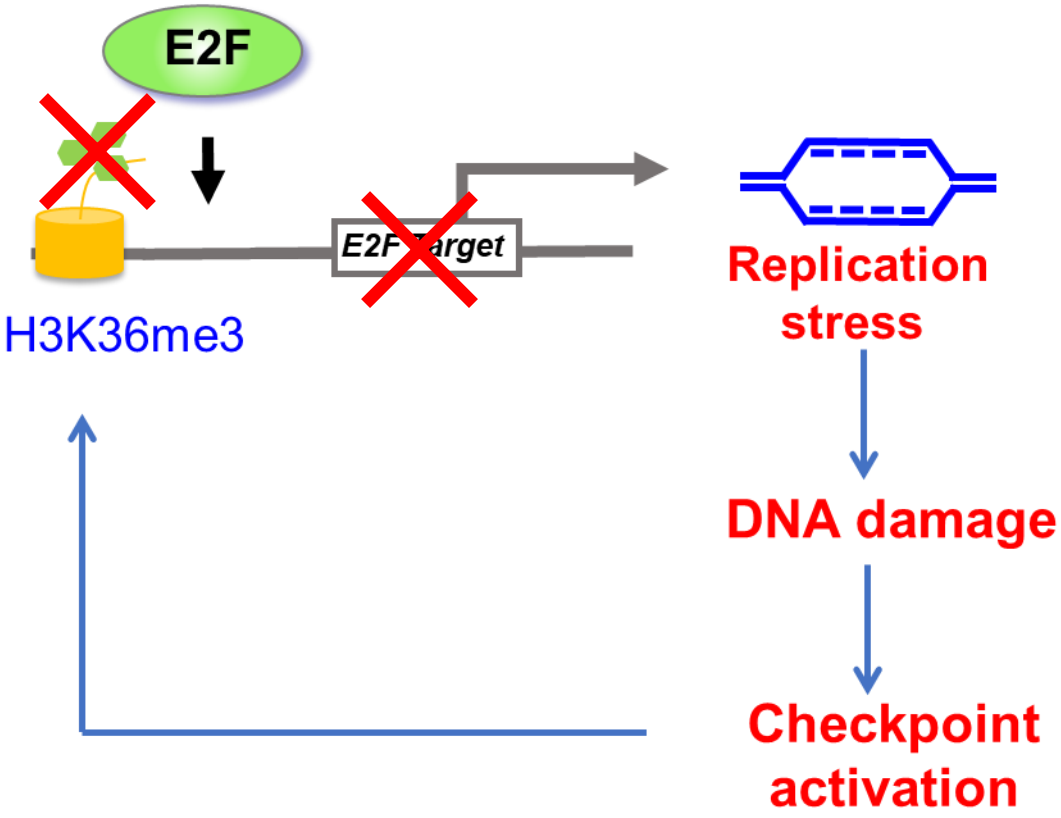


Figure 4.19: Model of the role H3K36 trimethylation in the replication stress checkpoint response. Loss of H3K36me3 leads to reduced E2F transcription, induction of replication stress, and impaired replication stress response.

4.3 Discussion

4.3.1 Summary of chapter 4

- Loss of SETD2 results in impaired cell cycle progression and increased replication stress
- Increased replication stress in SETD2 deficient cells leads to increased endogenous DNA damage
- A checkpoint dependent increase in H3K36me3 is required for efficient transcription of E2F target genes in replication stress conditions

4.3.2 Discussion of chapter 4

One consideration regarding the impaired G1/S progression observed is whether this occurs as a result of p53 induced G1 arrest in response to DNA damage. Regarding this, depletion of SETD2 in p53 mutant T98G cells also results in delayed G1/S progression and reduced E2F1 target gene expression, demonstrating that functional p53 is not required for this phenotype. Additionally, p21 depletion in SETD2-deficient cells produced only a mild increase in S phase population, further supporting the hypothesis that this is not the main cause of G1/S delay.

It has previously shown that H3K36me3 has a conserved role in DNA double strand break repair, where H3K36me3 is required for efficient recruitment of repair factors including CtIP and RPA. Interestingly, while DNA damage also triggers the upregulation of RRM2 through inhibition of cyclin F dependent degradation (D'Angiolella et al., 2012), there was no observed transcriptional upregulation upon

IR, even in SETD2 wildtype cells. This suggests that the SETD2 and H3K36me3 act in different pathways in response to DNA damage and replication stress.

Interestingly, the enrichment of H3K36me3 in response to replication stress occurs at the promoters of E2F1 target genes. H3K36 trimethylation has previously thought to be localised to the body of genes (Bannister et al., 2005) or constitutive heterochromatin (Chantalat et al., 2011b), although it has also been found at specific promoters (Ard and Allshire, 2016) and at DNA break sites in response to damage (Li and Wang, 2017). H3K36 trimethylation at promoter regions may be specifically recruited to facilitate transcriptional activation, in contrast to canonical gene body methylation which occurs co-transcriptionally. It is currently unclear whether the replication stress response increases the levels of H3K36me3 globally, or specifically at the promoters of E2F target genes. Global SETD2 and H3K36me3 levels decrease upon S phase entry, consistent with a role in promoting E2F1 target gene transcription, as these genes are also downregulated with replication initiation. Additionally, the H3K36me3 demethylase KDM4A peaks upon S phase entry, leading to a global decrease in H3K36me3 levels during S phase. Previous work has demonstrated SETD2-dependent, site-specific H3K36 trimethylation in response to double strand breaks in a LEDGF dependent manner (Li and Wang, 2017), showing that cells have the capacity to activate site-specific H3K36 methylation in response to a stimulus. One method to investigate this would be global ChIP-seq for H3K36me3 in the presence and absence of replication stress inducing agents.

Increased mitotic aberrations in SETD2-deficient cells have previously been shown (Park et al., 2016), where they were attributed to impaired SETD2-dependant microtubule methylation. While there may be an important role for SETD2 in cytoskeletal remodelling, the data here strongly indicates the mitotic defects and resulting damage observed are due to replication stress. The increased frequency of FANCD2 positive ultrafine bridges and 53BP1 foci in the subsequent G1 support the hypothesis that SETD2 depletion results in loss of genome stability through replication stress induced DNA damage. However, the data does not exclude the possibility of mitotic defects and genome instability in SETD2 deficient cells occurring through a combination of replication stress induced DNA damage and loss of microtubule integrity.

Chapter 5

Investigating synthetic lethalities with WEE1 inhibition

5.1 Introduction

AZD1775 is a selective, ATP competitive, small molecule inhibitor of the WEE1 kinase that was initially developed to target p53 deficient cancer cells (Mizuarai et al., 2009; Rajeshkumar et al., 2011). AZD1775 has been found to be well tolerated in Phase I clinical trials (Mendez et al., 2018; Takebe et al., 2018), and is currently in a number of Phase II trials both as a monotherapy and in combination with DNA damaging agents (Gray et al., 2017; Leijen et al., 2016; Oza et al., 2015; Spigel et al., 2016).

The initial hypothesis for the mechanism of AZD1775 was that cells would be driven through the cell cycle with p53 mutations impairing the G1/S checkpoint, and WEE1 inhibition blocking cell cycle arrest at the G2/M checkpoint, resulting in accumulation of DNA damage and cell death through mitotic catastrophe. However, not all p53 negative cell lines were found to be sensitive to WEE1 inhibition, suggesting that there are additional factors that determine sensitivity to WEE1 inhibition.

In addition to p53, a synthetic lethality between WEE1 inhibition and SETD2 has been identified, where depletion of both genes leads to a catastrophic decrease in nucleotide pools, and death through replication catastrophe (Pfister et al., 2015). Interestingly, it has previously been suggested that SETD2 and p53 function in the same pathway to activate the DNA damage checkpoint (Carvalho et al., 2014; Xie et al., 2008), raising the possibility that these synthetic lethalities may act through similar mechanisms. Consistent with this, a haploid genetic screen found that knockout of several G1/S regulatory genes induced resistance to AZD1775 (Heijink et al., 2015). Due to this, the mechanism of the synthetic lethality between p53 and WEE1 inhibition was investigated.

5.2 Results

5.2.1 Synthetic lethality between loss of p53 and WEE1

5.2.1.1 Combined loss of SETD2 and p53 does not further sensitise to WEE1 inhibition

To determine whether the SETD2 and p53 synthetic lethalities with WEE1 inhibition act through the same pathway both genes were co-depleted. If the mechanism of lethality is the same, depletion either p53 or SETD2 will be epistatic, and co-depletion will not result in further sensitisation to WEE1 inhibition. p53 negative H1299 cells were selected as they were used in the initial paper describing the synthetic lethality, and are highly sensitive to WEE1 inhibition (Figure 5.1). Knockdown of SETD2 in p53 negative H1299 cells showed no additional sensitisation to WEE1 inhibition (Figure 5.1), suggesting that the synthetic lethalities between WEE1 and p53 or SETD2 do indeed function through the same pathway.

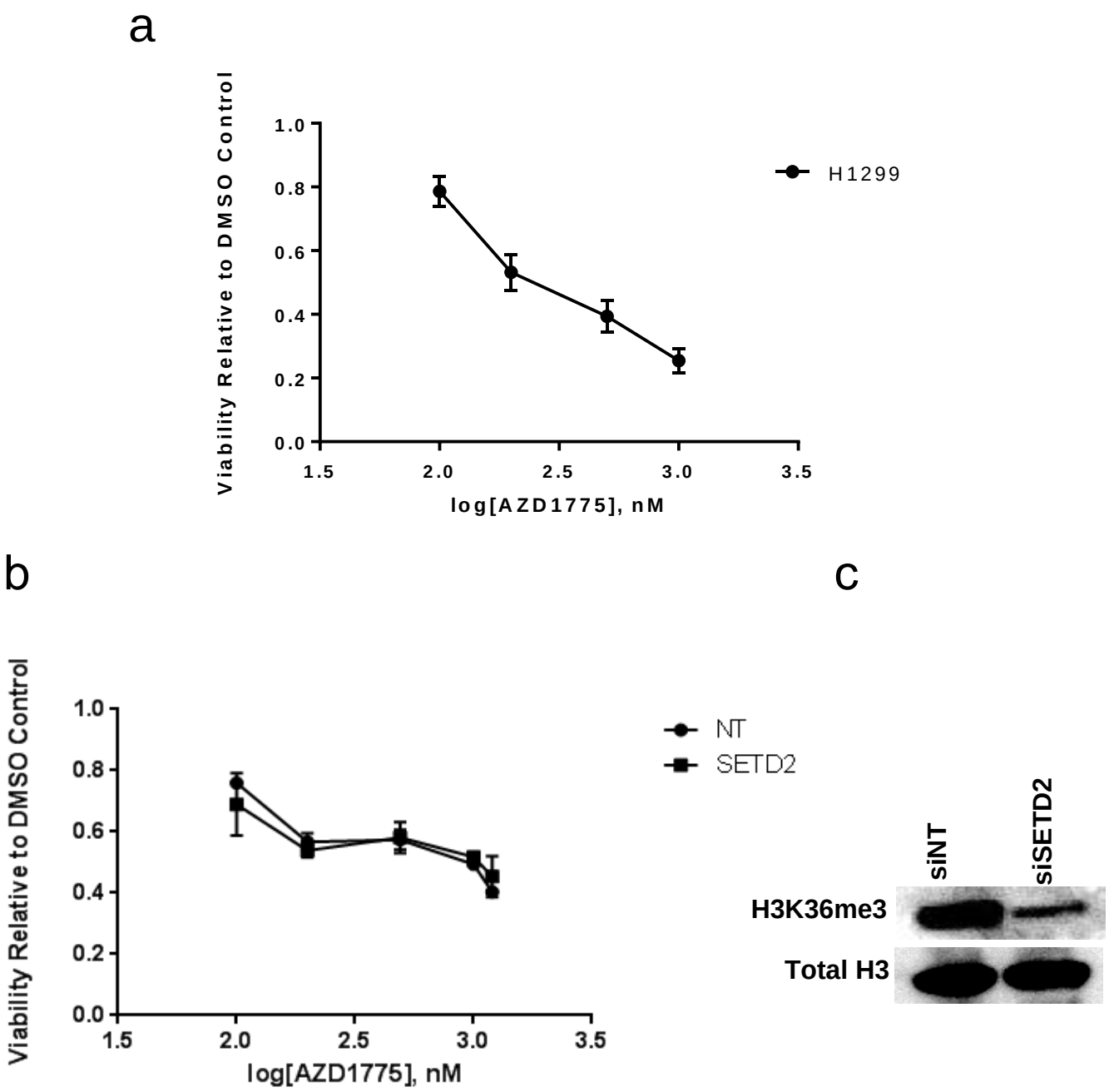


Figure 5.1: SETD2 depletion does not further sensitise H1299 cells to AZD1775 (a) Viability of H1299 cells after treatment with AZD1775 measured by resazurin assay. **(b)** Viability of H1299 cells transfected with siRNA against SETD2 after treatment with AZD1775 measured by resazurin assay. Data presented as mean ± SEM, n=2 independent experiments. **(c)** Western blot of H3K36me3 levels in H1299 cells transfected with siNT or siSETD2.

5.2.1.2 WEE1 inhibition induces S phase arrest in p53 negative cells

As WEE1 is canonically considered to regulate the G2/M transition through negative regulation of CDK1, it was expected that inhibition of WEE1 would drive cells into mitosis through increased CDK1 activity. However, WEE1 inhibition in SETD2 deficient cells results in S phase arrest due to impaired DNA replication. To determine whether p53 deficient cells also arrest in S phase after WEE1 inhibition H1299 cells were treated with AZD1775 and their cell cycle profile analysed by flow cytometry. Samples were taken prior too, and 48 hours after, addition of several concentrations of AZD1775, and analysed by flow cytometry. To investigate the presence of non-replicating S phase, cells were incubated with the nucleotide analogue BrdU for 30 minutes prior to collection. Incorporation of BrdU is indicative of actively replicating cells, and can be detected by flow cytometry. Those cells with a DNA content greater than 2N, but not incorporating BrdU are considered to be ‘non-replicating S phase’, and indicate replication stalling or blockage. Surprisingly it was found that, in addition to the predicted increase in mitotic population, an increased population of non-replicating S phase cells was observed after AZD1775 treatment in p53 negative cells (Figure 5.2), similar to what is seen in SETD2 deficient cells. This data suggests that p53 negative cells do not simply pass through the cell cycle and die through mitotic catastrophe, and that a large percentage arrest in S phase.

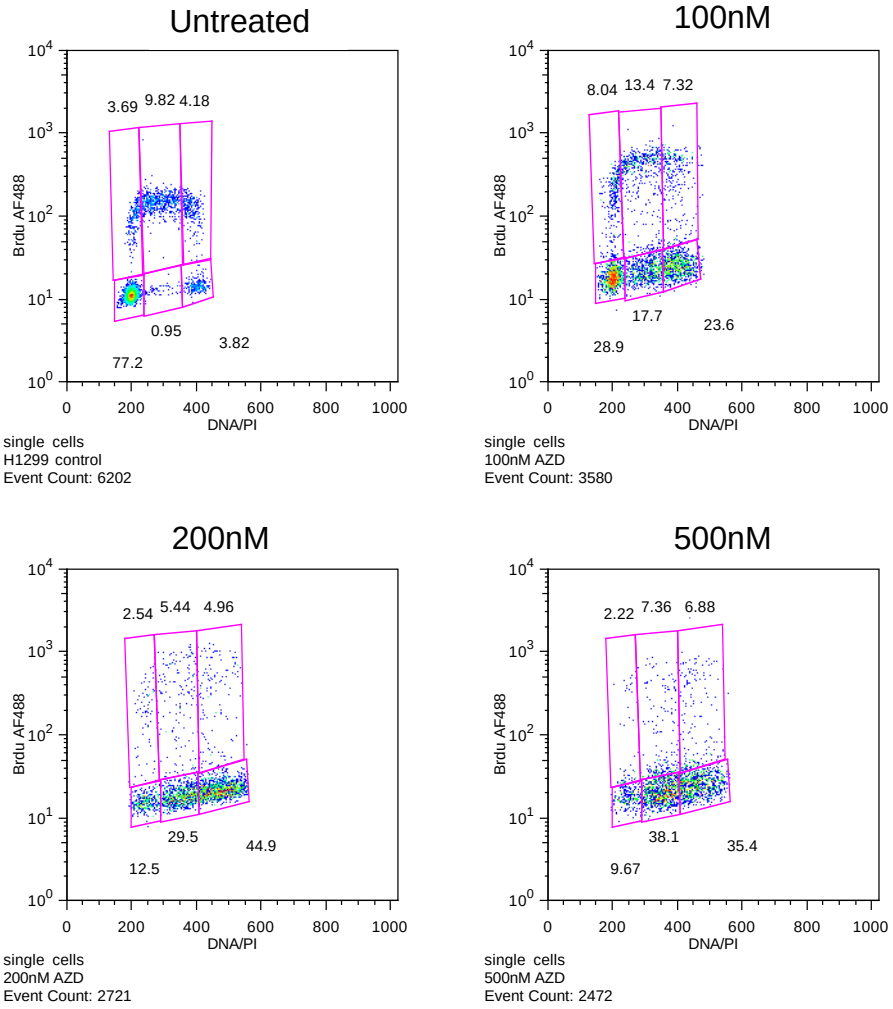


Figure 5.2: Cell cycle profile of H1299 cells. Cells were treated with indicated concentrations of AZD1775 measured by FACS analysis of BrdU incorporation.

5.2.1.3 RRM2-T33A expression partially rescues p53/WEE1 synthetic lethality

The synthetic lethality between WEE1 inhibition and SETD2 occurs through mutual depletion of RRM2, leading to nucleotide depletion and subsequently to S phase arrest. As S phase arrest also occurs in p53 deficient cells after WEE1 inhibition it was hypothesised that this may also occur as a result of insufficient nucleotide pools. To investigate this, a non-degradable RRM2 point mutant, RRM2-T33A, was expressed in H1299 cells. CDK dependent phosphorylation at T33 triggers ubiquitylation and subsequent degradation of RRM2. Inhibition of WEE1 increases the levels of CDK activity and results in increased phosphorylation and degradation of RRM2 (Pfister et al., 2015). Mutation of this phosphorylation site results in a variant of RRM2 that cannot be degraded, leading to increased nucleotide pools even in the presence of AZD1775. To investigate the role of nucleotide pools in the p53/WEE1 synthetic lethality, H1299 cells were transfected with RRM2-T33A and treated with a range of AZD1775 concentrations. Cells expressing RRM2-T33A showed in a mild decrease in sensitivity to AZD1775, suggesting a potential role for nucleotide pools in the p53/WEE1 synthetic lethality (Figure 5.3).

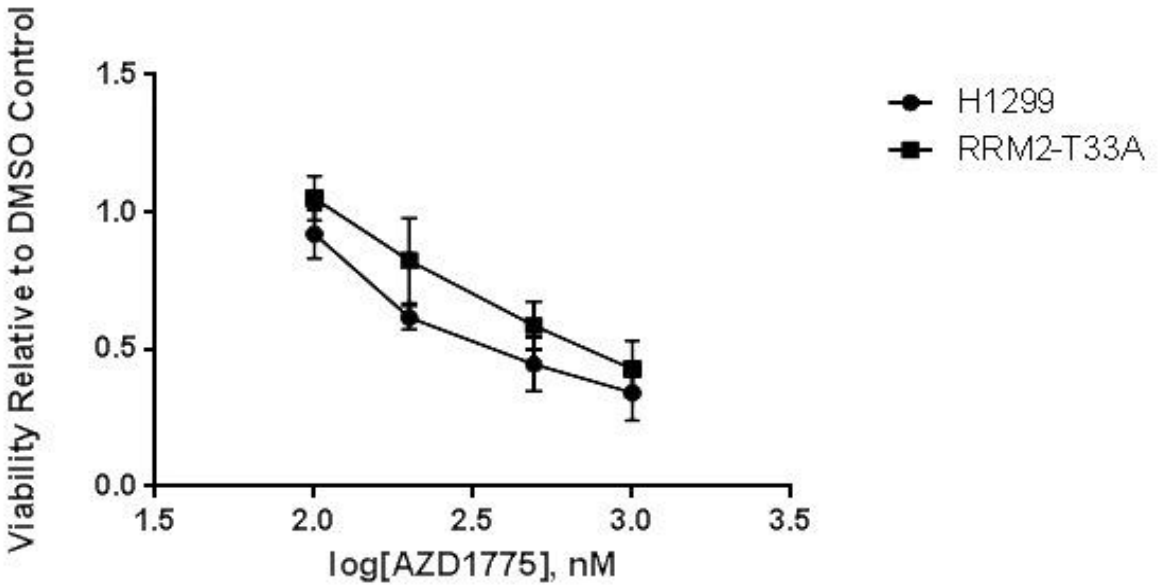


Figure 5.3: RRM2-T33A expression in p53 deficient cells. Viability of H1299 cells transfected with RRM2-T33A or control plasmid after treatment with AZD1775 measured by resazurin assay. Data presented as mean ± SEM, n=2 independent experiments.

5.2.1.4 MCF7 p53 CRISPR cells arrest in S phase after WEE1 inhibition

Although H1299 cells are highly sensitive to WEE1 inhibition, the lack of a paired p53 wildtype cell line makes it difficult to determine whether this sensitivity is dependent on the loss of p53, or if there are other determining factors involved. Due to this, a pair of isogenic MCF7 cell lines were also utilised. To investigate whether p53 deletion results in increased sensitivity to WEE1 inhibition, p53 wildtype and p53 CRISPR deleted MCF7 cell lines were treated with AZD1775 at a range of concentrations. The p53 CRISPR cell line was found to be more sensitive to WEE1 inhibition, with an IC50 of ~75nM, compared to ~150nM, for the p53 wildtype cells line (Figure 5.4). This data suggests that p53 deletion does indeed sensitise cells to WEE1 inhibition.

Next, it was investigated whether WEE1 inhibition in the MCF7 cell lines also resulted in S phase arrest. MCF7 p53 wildtype and p53 CRISPR cells were treated with AZD1775, and their cell cycle profiles analysed by flow cytometry. In the wildtype MCF7 cell line just under 50% of cells arrested in non-replicating S phase after 48 hours WEE1 inhibition, while in the p53 CRISPR cell line the non-replicating S phase population was over 60%, with a minimal increase in mitotic population (Figure 5.4). These data suggest that, rather than drive cells through the cell cycle and into mitosis, WEE1 inhibition in p53 deficient cells results in cell cycle arrest in S phase.

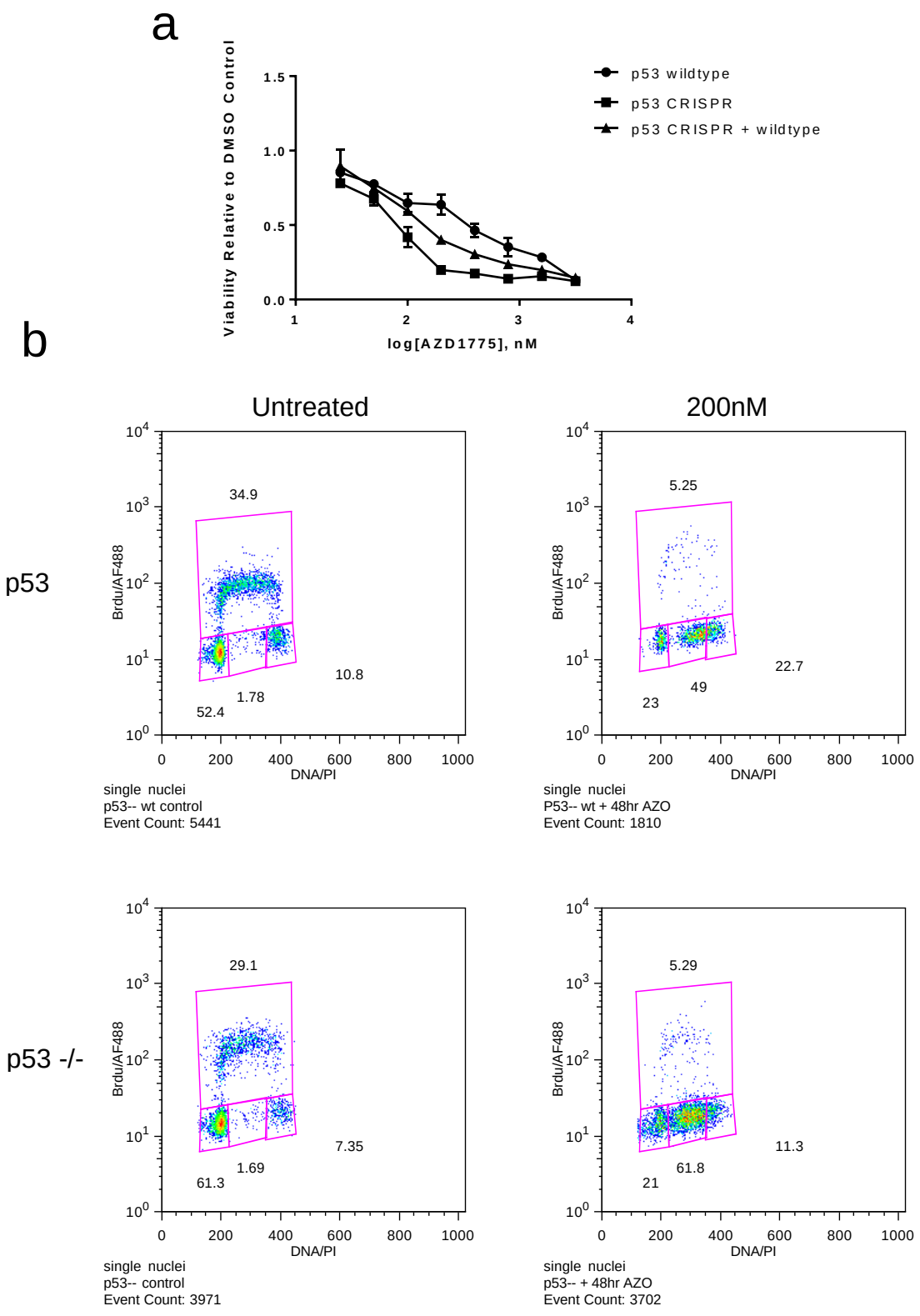


Figure 5.4: p53 CRISPR MCF7 cell sensitivity to AZD1775 (a) Viability assay of MCF7 wildtype and p53 CRISPR cells after treatment with indicated concentrations of AZD1775 for 48 hours. Data presented as mean ± SEM, n=4 independent biological replicates **(b)** FACS analysis of BrdU incorporation in MCF7 wildtype and p53 CRISPR cells treated with indicated concentrations of AZD1775.

5.2.1.5 WEE1 inhibition in p53 missense mutant cancers

Although AZD1775 was initially developed to target p53-negative cancers, deletions make up only a small percentage of the p53 mutations found in cancers (Olivier et al., 2010). Unlike many other tumour suppressors, the most common p53 mutations are missense, resulting in a single amino acid change, and can occur at several different positions. Missense mutations most frequently occur within the DNA binding region, with 6 'hotspot' mutations (R175, G245, R248, R249, R273, R282) making up 30% of all p53 missense mutations (Pavletich et al., 1993). A number of these mutations do not simply inactivate the tumour suppressor function of p53 but also confer additional tumourigenic activity, such as inactivation of p63, p73, or ATM (Lang et al., 2004; Olive et al., 2004; Song et al., 2007). As missense mutations make up a much larger proportion of p53 mutations than deletions, it was investigated whether AZD1775 could also be used to target this type of p53 mutation.

MCF7 p53 CRISPR cells complemented with either WT p53 or the R175H mutant were tested for their sensitivity to AZD1775. Interestingly, cells complemented with the R175H point mutant showed similar sensitivity to the p53 CRISPR MCF7 cells, while those complemented with WT p53 were markedly less sensitive (Figure 5.4), suggesting a possible susceptibility of p53 point mutants to WEE1 inhibition.

Next it was investigated whether cells with the p53 missense mutation also arrest in S phase after inhibition of WEE1. MCF7 p53 CRISPR cells complemented with R175H mutant were again treated with AZD1775 and their cell cycle profile analysed by flow cytometry. As with the p53-negative cells a large accumulation of cells in non-replicating S phase was observed after WEE1 inhibition, with no increase in the

mitotic population (Figure 5.5). Together these data suggest that cancers with p53 missense mutations may be targetable with AZD1775, greatly increasing the potential therapeutic usage of WEE1 inhibition.

5.2.1.6 WEE1 inhibition induces DNA damage in p53 deficient cells

p53 plays an important role in both the G1/S and G2/M cell cycle checkpoints, and acts to block cell cycle progression by inducing expression of a number of downstream targets, including the CDK inhibitor p21 (Agarwal et al., 1995). As p53 deficient cells are unable to efficiently enact a G1/S checkpoint, it was hypothesised that they may be more susceptible to inappropriate CDK activity resulting from WEE1 inhibition. This has previously been shown to induce replication stress (Beck et al., 2012), and subsequently result in DNA damage through replication fork stalling.

To investigate whether WEE1 inhibition induces DNA damage in p53 deficient cells MCF7 wildtype and p53 CRISPR cell lines were treated with 200nM AZD1775 for 48hours, after which γH2AX and 53BP1 foci were visualised by immunofluorescence microscopy. The MCF7 p53 CRISPR cell line showed a significant increase in the levels of both γH2AX and 53BP1 foci after WEE1 inhibition, while the wildtype cells showed no significant increase (Figure 5.6), indicating that loss of p53 renders cells more susceptible to DNA damage upon WEE1 inhibition.

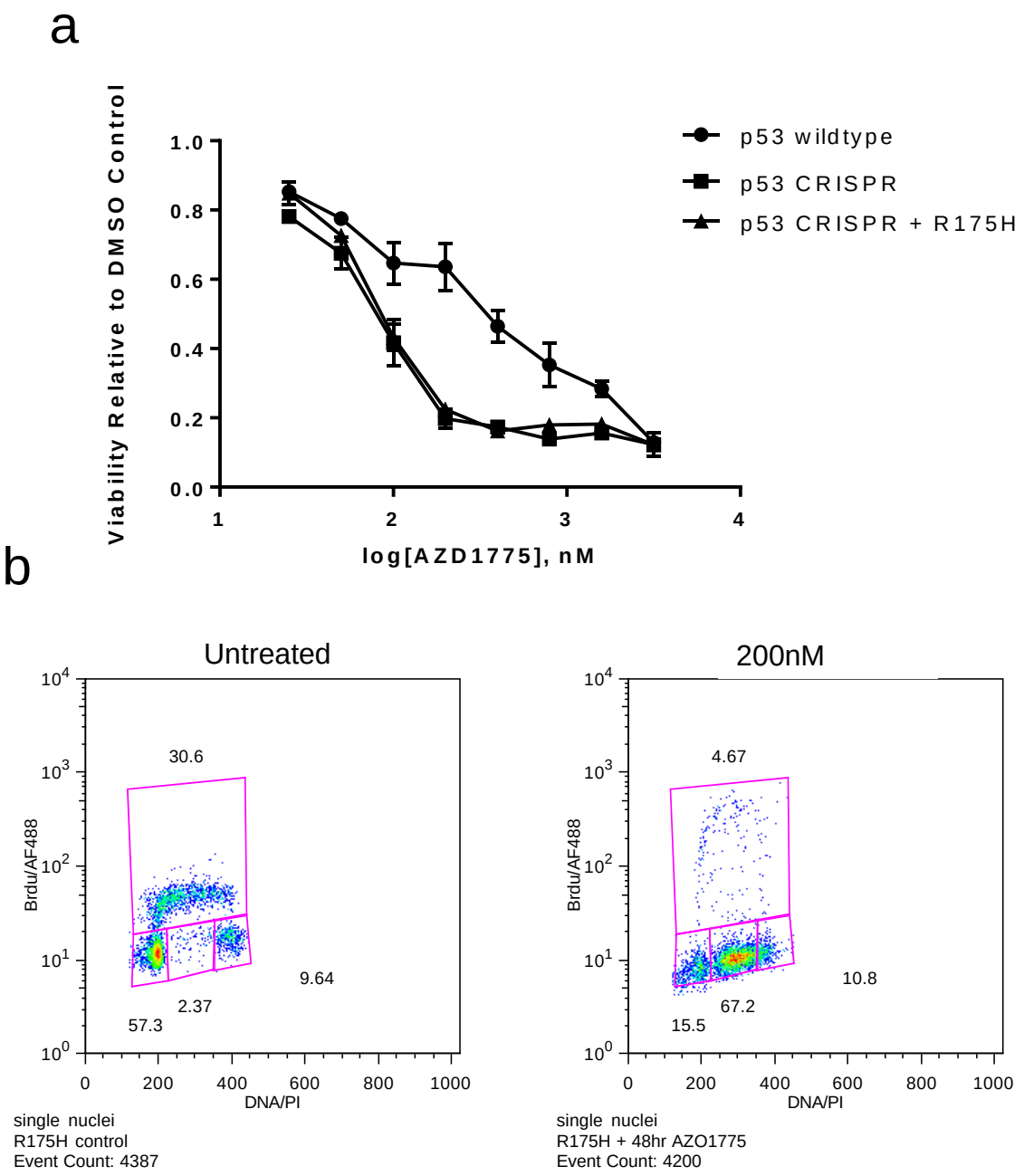


Figure 5.5: p53 point mutant MCF7 cell sensitivity to AZD1775 (a) Viability assay of MCF7 wildtype, p53 CRISPR and p53 CRISPR + R175H cells after treatment with indicated concentrations of AZD1775 for 48 hours. Data presented as mean ± SEM, n=4 independent biological replicates. **(b)** FACS analysis of BrdU incorporation in p53 CRISPR MCF7 cells expressing the p53 R175H point mutant after treatment with indicated concentrations of AZD1775.

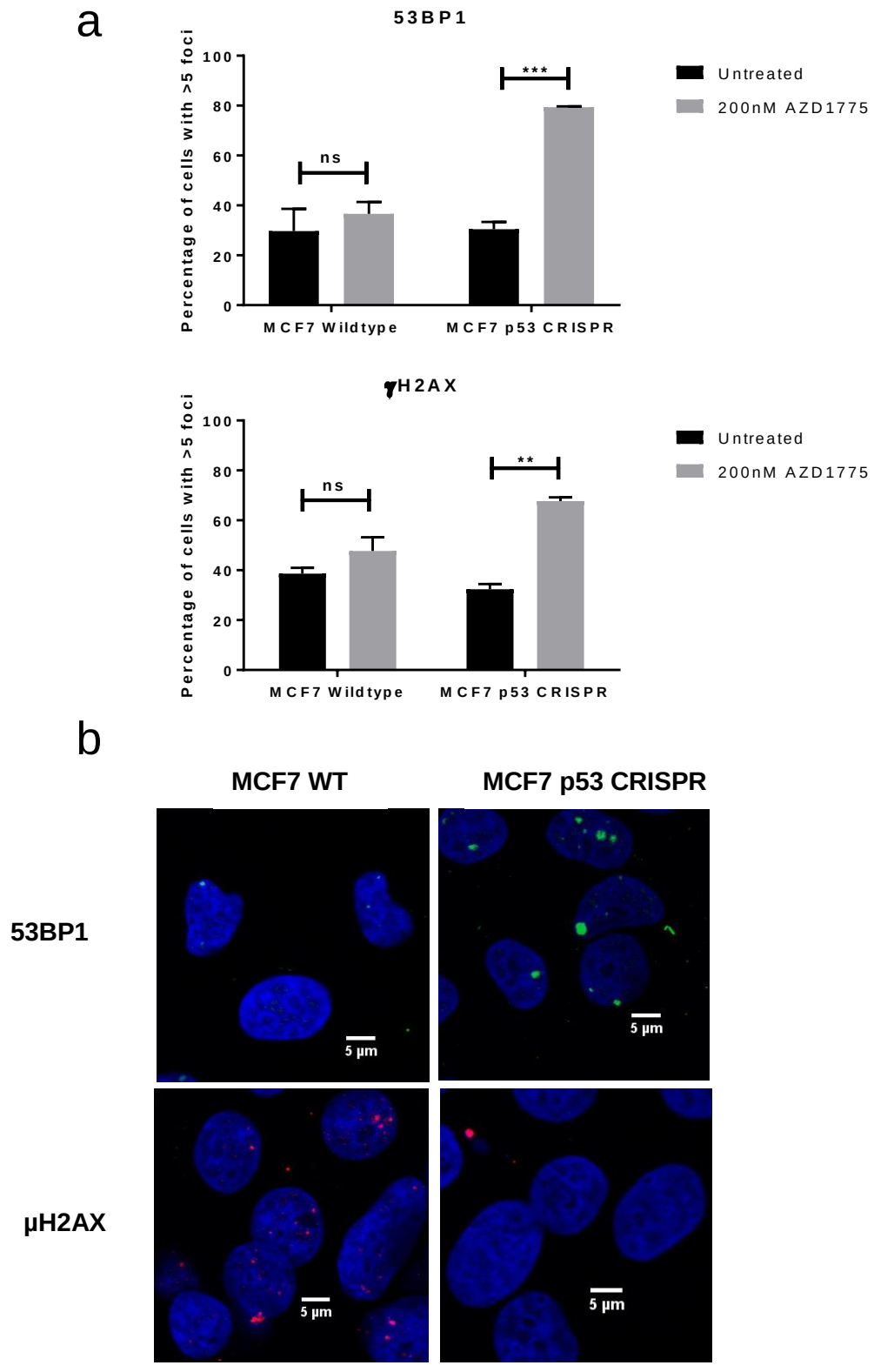


Figure 5.6: DNA damage markers visualised in p53 deficient cells treated with AZD1775 (a) Quantification of γH2AX and 53BP1foci imaged in MCF7 wildtype and p53 CRISPR cells treated with 200nM AZD1775 or DMSO control for 48 hours. Data presented as mean ± SEM, n=3 independent experiments, *p<0.05, **p<0.01, ***P<0.001. **(b)** Immunofluorescence visualisation of γH2AX and 53BP1 foci in MCF7 wildtype and p53 CRISPR cells.

5.2.1.7 Deletion of p53 does not sensitise non-cancerous cells to WEE1 inhibition

Although deletion of p53 in MCF7 cells results in a greater sensitivity to AZD1775, wildtype MCF7 cells are already highly sensitive to WEE1 inhibition, with an IC50 of around 150nM. To further investigate the synthetic lethality between p53 loss and WEE1 inhibition, RPE-1 wildtype and RPE-1 p53 CRISPR cell lines were utilised. RPE-1 is a human retinal pigment epithelial cell line that stably expresses human telomerase reverse transcriptase (hTERT), while maintaining a primary cell-like phenotype (Jiang et al., 1999). As RPE-1 cells lines are immortalised but not transformed, they are an ideal model to test the impact of p53 loss in an otherwise wildtype cell line.

Surprisingly, p53 deletion in RPE-1 cells did not result in increased sensitivity to AZD1775 (Figure 5.7), indicating that loss of p53 alone is not sufficient to sensitise cells to WEE1 inhibition. Consistent with this, p53 CRISPR RPE1 cells showed no increase the DNA damage marker 53BP1 compared to wildtype RPE1 cells after treatment with AZD1775 (Figure 5.7).

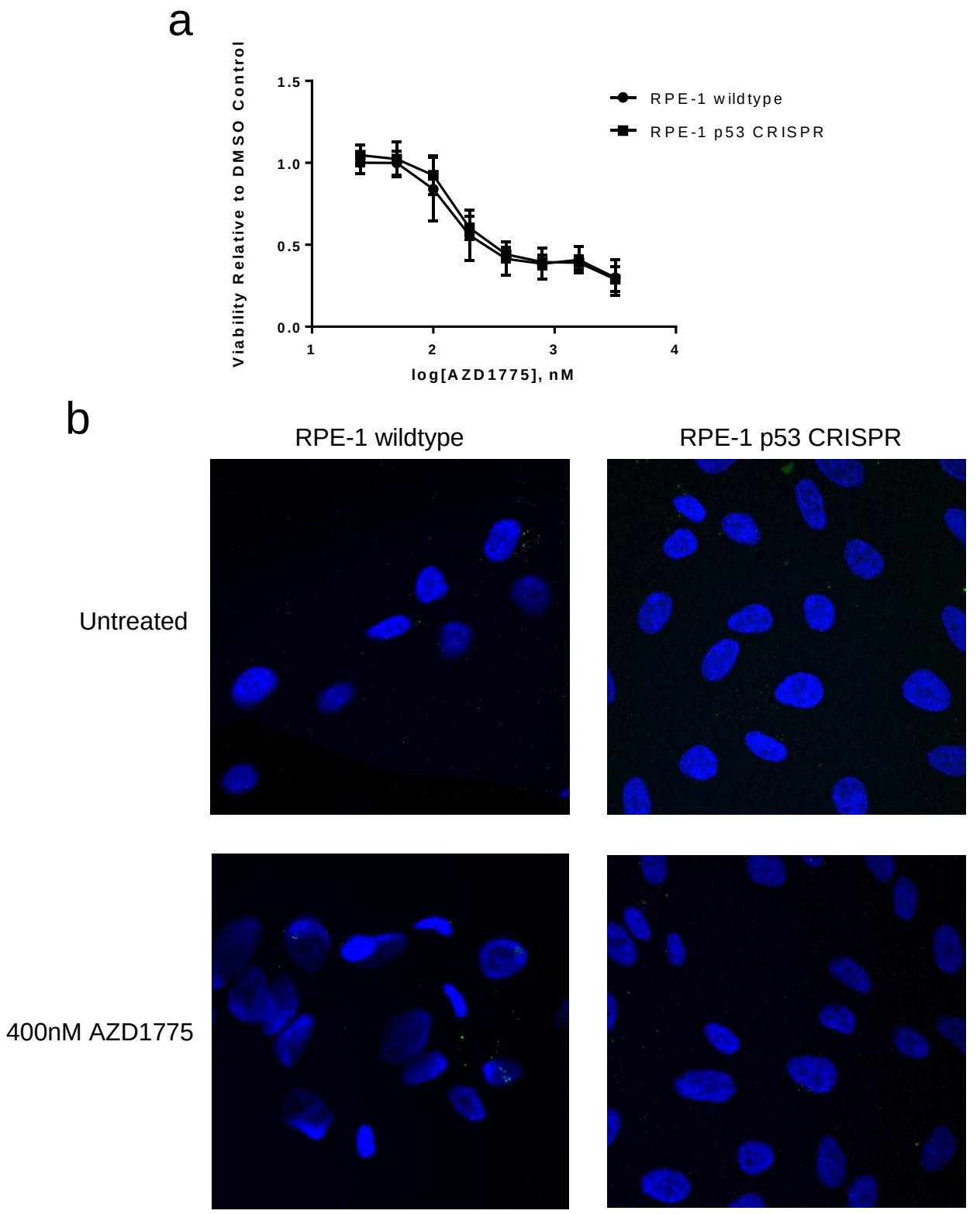


Figure 5.7: p53 depletion does not sensitise RPE-1 cells to AZD1775. **(a)** Viability assay of RPE-1 wildtype and p53 CRISPR cells after treatment with indicated concentrations of AZD1775 for 48 hours. Data presented as mean ± SEM, n=3 independent experiments. **(b)** 53BP1 foci imaged by immunofluorescence in AZD1775 treated RPE-1 wildtype and p53 CRISPR cells.

Together these data suggest that p53 depletion alone does not sensitise cells to WEE1 inhibition, and that additional mutations in combination with p53 loss result in sensitivity. Studies have shown that AZD1775 synergises with DNA damaging agents in p53-deficient cells (Hirai et al., 2009; Leijen et al., 2010; Meng et al., 2018; Rajeshkumar et al., 2011), which may indicate that high levels of DNA damage are required for sensitivity to WEE1 inhibition. MCF7 is a genomically unstable cell line that shows high levels of DNA damage even in the absence of DNA damaging agents, which may be sufficient to induce sensitivity to AZD1775. In contrast, RPE-1 cells have very low levels of endogenous DNA damage, and as such deletion of p53 alone appears to have very little impact on sensitivity to WEE1 inhibition.

One method to investigate this further would be to conduct a screen for genes whose knockdown or deletion sensitises p53 negative cells to WEE1 inhibition. It would be predicted if the synthetic lethality between p53 and WEE1 inhibition acts though the same mechanism as the SETD2/WEE1 synthetic lethality, loss of genes involved in DNA replication or the G1/S transition would sensitise p53 deficient cells to WEE1 inhibition.

5.2.2 Identification of novel synthetic lethalities with AZD1775

Although promising results have been seen with WEE1 inhibition in both p53 and SETD2 deficient cancers, identifying additional synthetic lethalities with WEE1 inhibition would be of biomedical value. WEE1 has well characterised roles in both the cell cycle and DNA repair (Matheson et al., 2016), pathways that are frequently disrupted in cancer (Jackson and Bartek, 2009; Otto and Sicinski, 2017; Williams and Stoeber, 2012). Owing to these important roles for WEE1, it was hypothesised that loss of other genes within these pathways may also be synthetic lethal with inhibition of WEE1.

5.2.2.1 A screen of cell cycle and DNA repair genes for synthetic lethality with AZD1775

To identify potential novel synthetic lethalities with WEE1 inhibition, an ON-Target *plus* SMART pool siRNA library obtained from Dharmacon was utilised. The library contains siRNAs targeting 169 cell cycle genes (G-103200), and 160 genes involved in DNA damage repair (G-106005), with 4 pooled siRNA sequences for each individual gene to ensure efficient knockdown. U2OS cells were transfected with each pool of siRNA, and subsequently incubated with the DMSO control or AZD1775 for 48 hours, after which cell viability was determined with a resazurin assay (Figure 5.7).

5.2.2.2 Screen identified 37 genes potentially synthetic lethal with WEE1 inhibition

Depletion of 17 genes in the cell cycle library and 22 genes in the DNA damage repair library showed a greater sensitivity to WEE1 inhibition than SETD2 depletion, which was used as a positive control (Table 5.1). Two genes, RPA3 and RAD17 appeared in both lists, giving a total of 37 unique hits.

To determine what pathways were enriched amongst the genes whose loss sensitised cells to AZD1775 treatment, gene ontology (GO) term enrichment was again utilised (Table 5.2). The DAVID Bioinformatics Resource (Huang da et al., 2009a, b) was used, with the siRNA libraries used as the background list of genes. Ten GO terms were found to be significantly enriched, with ‘DNA replication’ the most significant. This is consistent with the synthetic lethalities between SETD2 or p53 and WEE1, and suggests that a number of sources of replication stress can sensitise cells to WEE1 inhibition. Supporting this idea, depletion of any of the 3 isoforms of the single-stranded DNA binding protein RPA (RPA1, RPA2, RPA3) was found to sensitise cells to WEE1 inhibition, as was the replication checkpoint protein CHK1 (Table 5.1).

One of the other enriched GO terms was ‘Negative regulation of cell cycle’, which included the cyclin-dependent kinase inhibitors CDKN1B (p27) and CDKN2D (p19), which act to block the G1/S phase transition. This may suggest that premature G1/S transition could sensitise cells to WEE1 inhibition, although more work needs to be done to validate the mechanism of these hits.

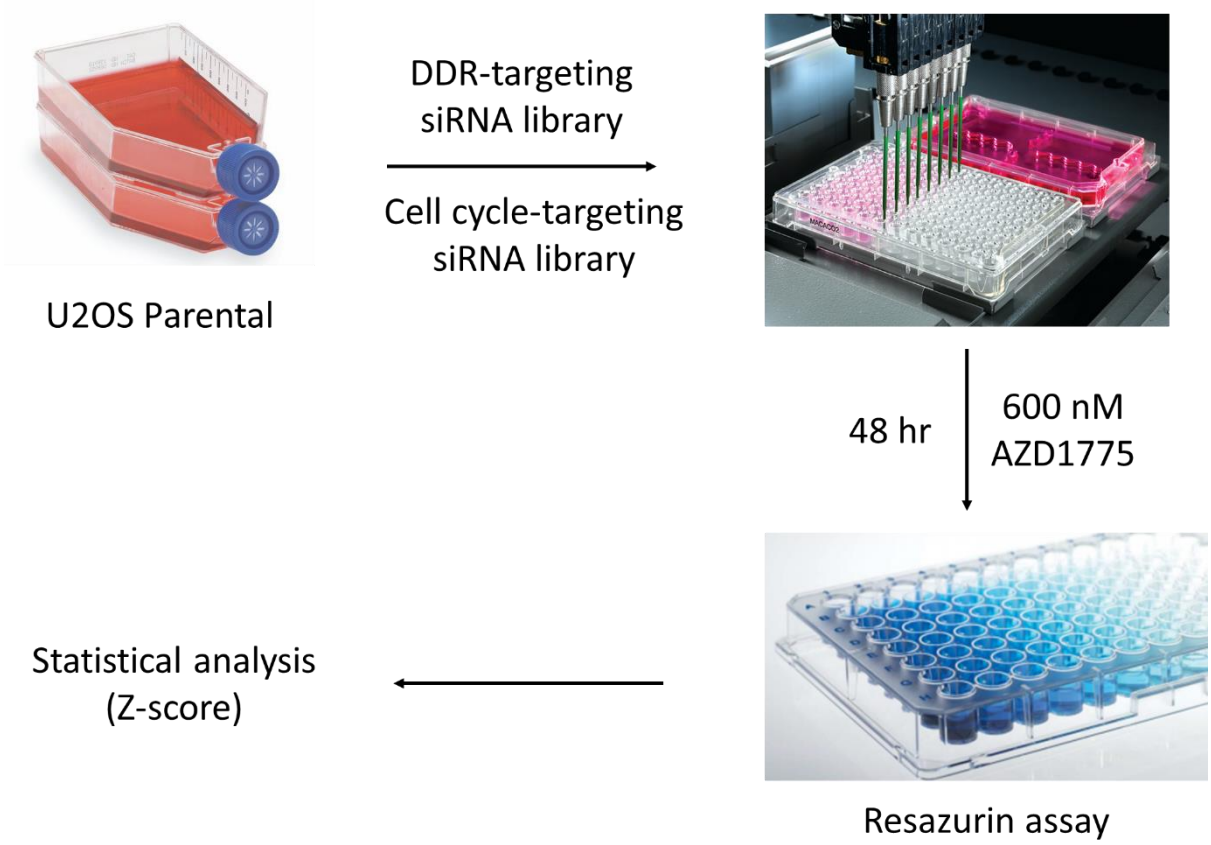


Figure 5.8: Schematic overview detailing key steps in the siRNA screen protocol.

Cell Cycle	DDR
RAD9	TCEA1
GML	RTEL1
FANCG	RPA1
CDC34	TRIP13
RAD1	RPS27L
RAD17	DNA2L
TIPIN	RAD17
CDKN1B	TOP2A
E2F5	XAB2
RPA3	UVRAG
MCM6	PRPF19
ANAPC2	FRAP1
CCNF	RAD23B
CHEK1	DCLRE1C
CDKN2D	CETN2
GMNN	POLK
WEE1	RPA2
	MIZF
	RBBP8
	RPA3
	CHAF1A
	USP1

Table 5.1: List of genes from the Cell Cycle and DNA Damage Response siRNA libraries whose knockdown was found to sensitise U2OS cells to AZD1775 treatment.

GO Term	Fold Enrichment	P value
Cell cycle DNA replication	3.17	1.07E-02
Regulation of cellular response to heat	3.52	2.63E-02
Error-free translesion synthesis	3.96	3.98E-02
Negative regulation of cell cycle	1.49	3.42E-02
DNA integrity checkpoint	1.66	3.63E-02
Cellular response to DNA damage stimulus	1.27	3.06E-02
Spliceosomal conformational changes to generate catalytic conformation	7.92	2.65E-02
Generation of catalytic spliceosome for first transesterification step	7.92	2.65E-02
Detection of stimulus	4.53	1.15E-02
Ribonucleoprotein complex subunit organization	5.94	1.40E-02

Table 5.2: GO terms enriched in the subset of genes whose knockdown resulted in sensitisation to AZD1775.

5.2.2.3 Novel synthetic lethalities between tumour suppressors and AZD1775

As synthetic lethalities had been identified between WEE1 inhibition and the tumour suppressors p53 and SETD2, it was considered whether WEE1 inhibiton could be utilised to target mutations in additional tumour suppressor genes. The tumour suppressors investigated were identified as part of a computational analysis of over 9000 tumour exomes from The Cancer Genome Atlas Project (Bailey et al., 2018). As not all tumour suppressors from the study could be included, genes were selected based on functional similarity to SETD2, including roles histone modification, cell cycle progression and DNA repair (Table 5.3). Additionally, ATR and SETD2 were included as positive controls for sensitivity to WEE1 inhibition (Pfister et al., 2015), with PLK1 acting a control for successful siRNA transfection (Liu and Erikson, 2003; Liu et al., 2006).

U2OS cells were transfected with a custom ON-Target *plus* SMART pool siRNA library was obtained from Dharmacon, and 48 hours after transfection cells were treated with 200 or 600nM AZD1775. 48 hours after addition of the drug, viability was measured using the rezasurin assay. Four biological repeats were conducted for each siRNA. Sensitivity to WEE1 inhibition was determined as described previously, where cell viability was first normalised to a non-transfected control, and Z scores were then calculated relative to the non-targeting siRNA. The tumour suppressors

were subsequently ranked by change in viability relative to the untreated siRNA knockdown (Table 5.3).

a

AJUBA
ATF7IP
ATR
BRCA1
BTG2
CDK12
CDKN1B
CDKN2D
CHD3
FOXQ1
GPS2
HDAC3
HUWE1
KDM5C
KMT2B
KMT2D
LATS1
LATS2
MGA
MSH6
NIPBL
PDS5B
PLK1
RFC1
SCAF4
SETD2
SIN3A
TCEB1
TXNIP
ZFHX3
ZMYM3

b

200nM	
1	ZMYM3
1	ATR
3	SCAF4
4	ZFHX3
5	MSH6
5	KDM5C
7	TXNIP
8	SIN3A
9	KMT2D
10	SETD2
11	ATF7IP
12	HDAC3
13	LATS1
14	MGA
15	CHD3
16	CDKN1B
16	AJUBA
18	BRCA1
19	BTG2
20	FOXQ1
21	PDS5B
21	KMT2B
23	LATS2
24	GPS2
24	HUWE1
26	RFC1
27	NIPBL
28	TCEB1
29	CDK12
30	CDKN2D
31	PLK1

c

600nM	
1	ATR
2	SIN3A
3	SETD2
4	ZMYM3
4	KDM5C
6	SCAF4
7	TXNIP
8	CDKN1B
9	MGA
10	ZFHX3
11	BTG2
11	KMT2D
11	HDAC3
14	ATF7IP
15	PDS5B
15	GPS2
17	MSH6
17	BRCA1
19	LATS1
19	TCEB1
21	KMT2B
21	CHD3
23	CDKN2D
24	LATS2
24	AJUBA
24	RFC1
27	CDK12
28	NIPBL
28	PLK1
30	HUWE1
31	FOXQ1

Table 5.3: Sensitivity of tumour suppressors screened to AZD1775 (a) Table of tumour suppressors investigated for sensitivity to WEE1 inhibition. **(b)** Heatmap table of tumour suppressor sensitivity to 200nM AZD1775.**(c)** Ranking of tumour suppressor sensitivity to 600nM AZD1775. Genes more sensitive than SETD2 are outlined.

5.2.2.4 Initial screen results identified 9 tumour suppressors sensitive to WEE1 inhibition

Only 2 siRNAs, ATR and SIN3A, were found to be more sensitive than SETD2 at the higher concentration of 600nM, while 9 were more sensitive at the lower 200nM concentration. As expected, PLK1 was the lowest ranked siRNA, as its depletion resulted in complete cell death independent of WEE1 inhibition. The most sensitive siRNAs were consistent across the two concentrations, and so the most sensitive 9 genes were selected for validation.

5.2.2.5 Depletion of KMT2D, KDM5C or MGA sensitises cells to WEE1 inhibition

To eliminate any false positive hits from the initial screen, the 9 most sensitive genes were again depleted with siRNA and treated with AZD1775 at a range of concentrations. Cell viability was then determined using the resazurin assay as described previously. Interestingly, only 3 of the initial 9 genes (KMT2D, KDM5C and MGA) were confirmed to be significantly more sensitive to WEE1 inhibition than the NT control (Figure 5.9 and appendix), suggesting the initial screen may need to be refined to reduce the number of false positive results.

In the previously identified synthetic lethalities WEE1 inhibition results in accumulation of cells in non-replicating S phase. To determine whether this was also the case in the newly identified synthetic lethalities, cells were treated with AZD1775 and their subsequent cell cycle distribution measured by flow cytometry. As seen

with both SETD2 and p53, WEE1 inhibition resulted in a significant accumulation of S phase cells in cells deficient in KMT2D, KDM5C or MGA (Figure 5.10).

To determine whether this increased S phase population was due to the presence of a non-replicating S phase population, cells were incubated with BrdU prior to collection, and both DNA content and BrdU incorporation were measured by flow cytometry. Consistent with the previously identified synthetic lethalities, over 40% of cells were found to be arrested in non-replicating S phase after 48 hours treatment with WEE1 inhibition (Figure 5.11). This may indicate a similar mechanism of lethality to that observed in SETD2 and p53 negative cells, although more work needs to be done to confirm if this is the case.

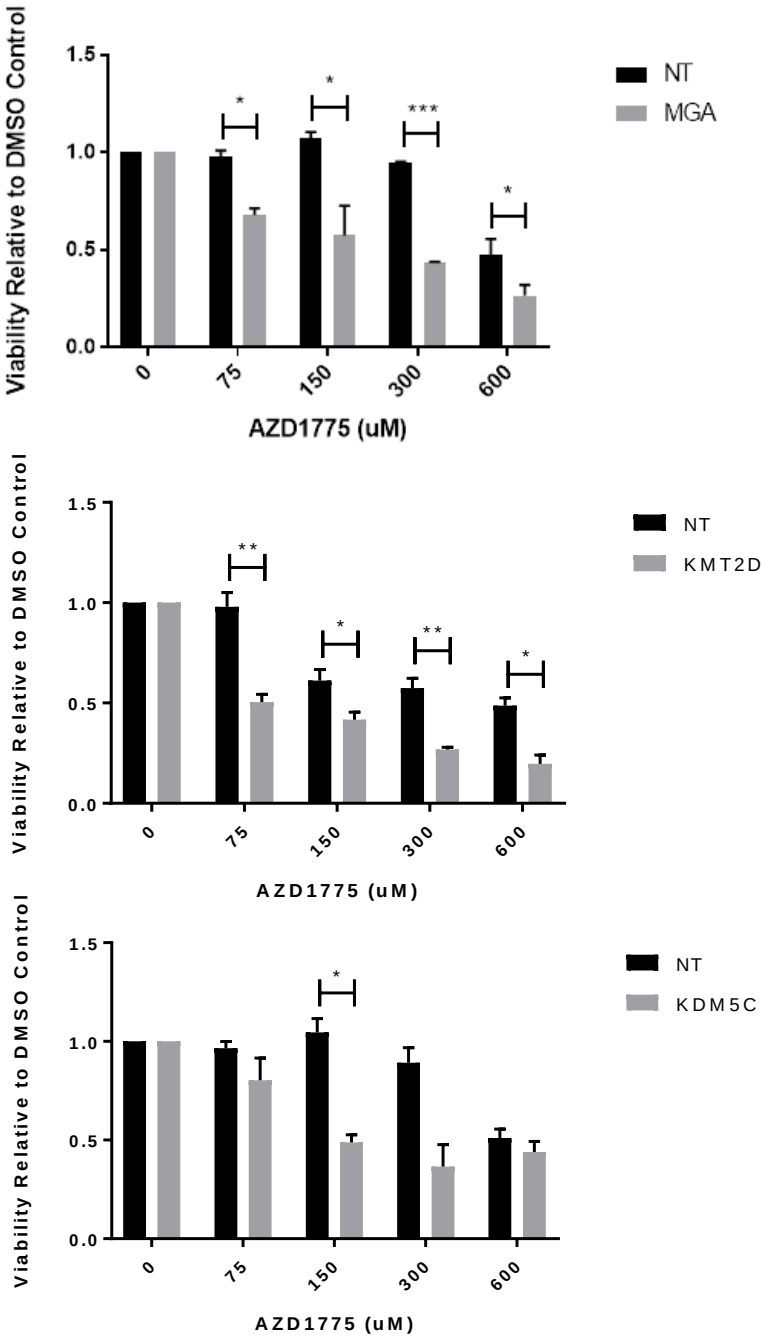


Figure 5.9: Viability assay of U2OS cells after treatment with indicated concentrations of AZD1775 for 48 hours relative to DMSO control. Data presented as mean ± SEM, n=3 independent experiments, *p<0.05, **p<0.01, ***P<0.001. Experiment performed by Thomas Foord under supervision from Lee Armfield.

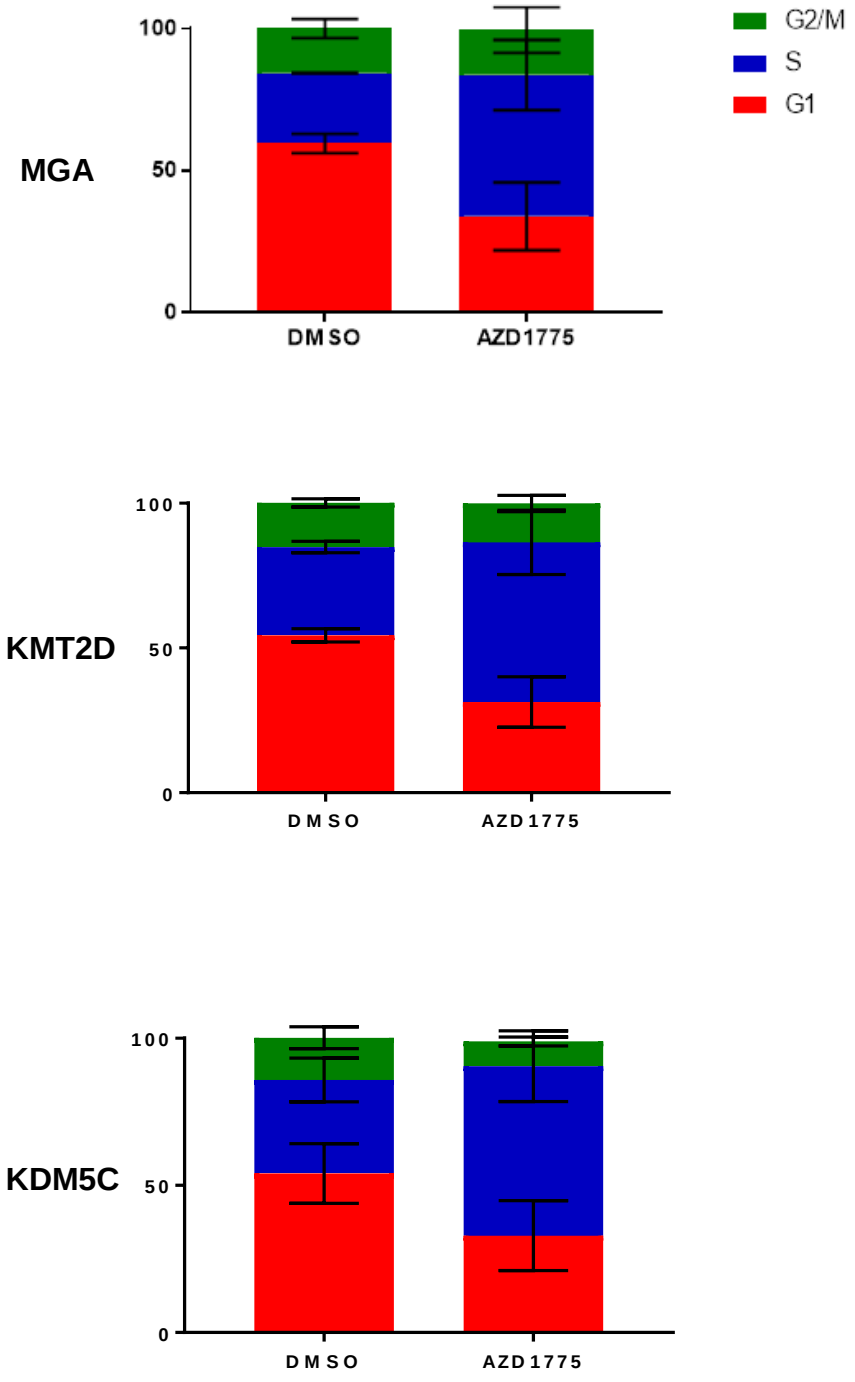


Figure 5.10: Cell cycle distribution of U2OS cells treated with DMSO or 300nM AZD1775. Cells were treated for 48hrs and cell cycle profile measured by flow cytometry. Data presented as mean ± SEM, n=3 independent experiments. Experiment performed by Thomas Foord under supervision from Lee Armfield.

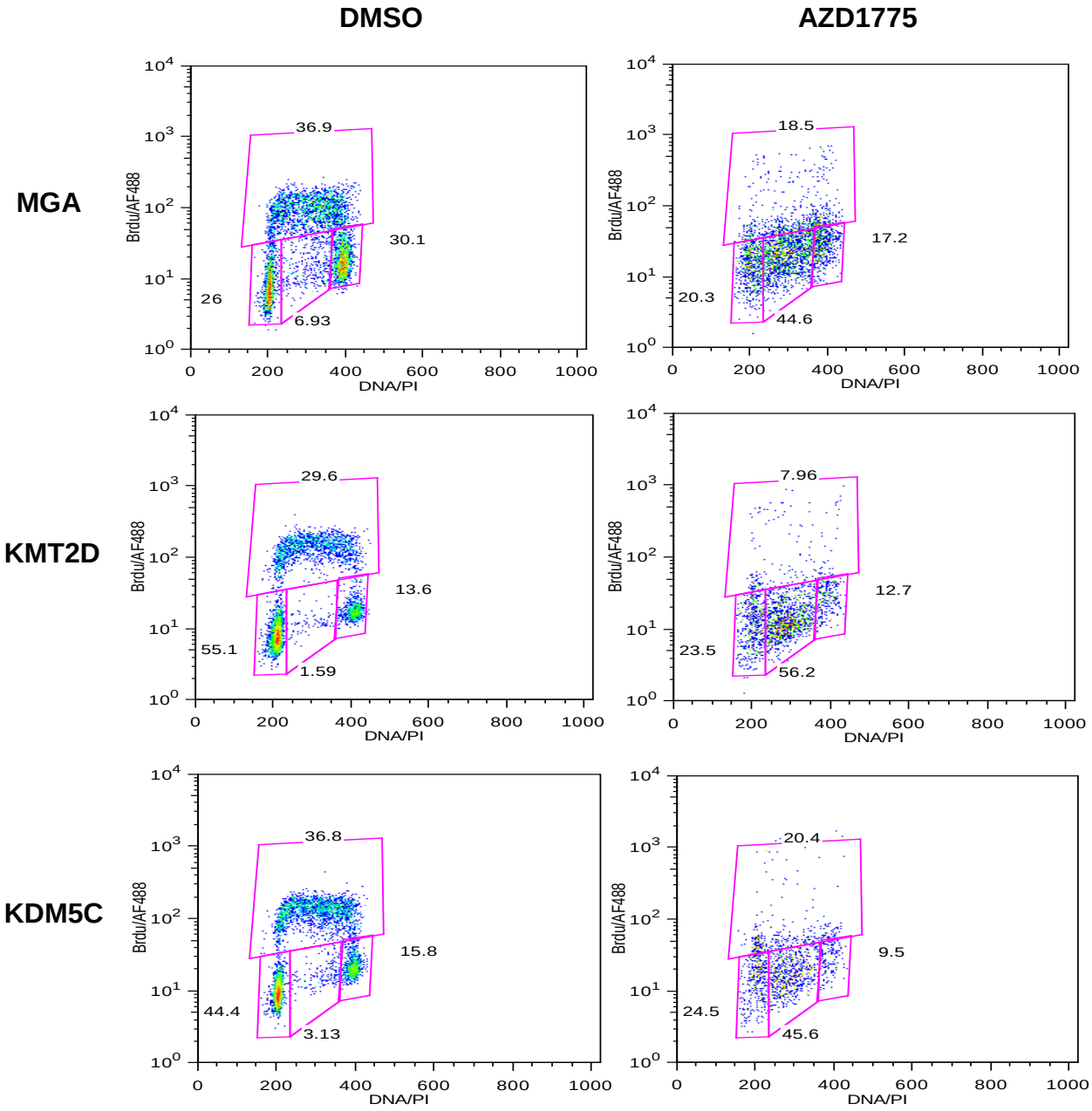


Figure 5.11: BrdU incorporation in U2OS cells treated with DMSO or AZD1775. Cell cycle distribution of U2OS cells treated with DMSO or 300nM AZD1775 for 48hrs measured by FACS analysis of BrdU incorporation.

5.3 Discussion

5.3.1 Summary of chapter 5

- The synthetic lethality between p53 and WEE1 acts through S phase arrest
- Loss of other genes involved in cell cycle progression or the DNA damage response can sensitise cells to WEE1 inhibition
- Three tumour suppressors identified as potential novel synthetic lethalities with WEE1 inhibition
- Disruption of H3K4 methylation may sensitise cells to WEE1 inhibition

5.3.2 Discussion of chapter 5

The data described in this chapter demonstrates a number of potential novel synthetic lethalities with WEE1 inhibition. The synthetic lethality between loss of p53 and WEE1 inhibition has previously been thought to act through forced mitotic entry, leading to cell death through mitotic catastrophe. However, this does not appear to be the case, as accumulation of cells in non-replicating S phase was observed after treatment with AZD1775, suggesting a similar mechanism to the SETD2/WEE1 synthetic lethality.

The screen of genes involved in the cell cycle and DNA damage response also found a significant enrichment of genes involved in DNA replication amongst those which sensitised cells to WEE1 inhibition. However, the mechanism of these potential novel synthetic lethalities have not yet been investigated. To determine

whether the mechanism is similar to that of the SETD2/WEE1 synthetic lethality the cell cycle profile could be measured after AZD1775 treatment. Accumulation of cells in non-replicating S phase would suggest a similar mechanism. Additionally, the role of nucleotide pools in the novel synthetic lethalities could be investigated by expression of the non-degradable RRM2-T33A variant, or treatment with exogenous nucleosides, and the effect on cell viability measured.

Interestingly, of the three genes identified as synthetic lethal with WEE1 inhibition in the screen of tumour suppressors, KDM5C and KMT2D both function to regulate H3K4 methylation (Froimchuk et al., 2017; Outchkourov et al., 2013). It has previously been demonstrated that H3K36me3 is spatially reciprocal with a number of other histone marks (Huff et al., 2010). Although it is not currently clear whether there is a relationship between H3K4 methylation and H3K36me3, it is possible that disruption of H3K4 methylation may also lead to dysregulation of H3K36 methylation. It would be possible to investigate this by measuring the levels of H3K36me3 after depletion of KDM5C or KMT2D.

It is also possible that depletion of KDM5C and KMT2D leads to AZD1775 sensitivity in a manner independent of H3K36me3. KMT2D has been shown to methylate at replication forks in response to replication stress (Ray Chaudhuri et al., 2016), facilitating recruitment of MRE11. It may also be the case that the impaired replication stress response resulting from depletion of KMT2D leads to accumulation of DNA damage and subsequent replication catastrophe. KDM5C depletion has been shown to result in impaired DNA replication origin firing (Rondinelli et al.,

2015), suggesting that the synthetic lethality between KDM5C and WEE1 may also act through replication stress induction. Consistent with these roles in preventing replication stress and DNA damage, both KDM5C and KMT2D are amongst the most highly mutated genes in cancers (Lawrence et al., 2014), and as such are attractive targets for therapy.

Chapter 6

General Discussion

This study has investigated the role of H3K36me3 and SETD2 in the regulation of RRM2, described a novel role for SETD2 in the both the G1/S transition and the replication stress response, and investigated novel synthetic lethalities with WEE1 inhibition. It was previously shown that SETD2 is required for efficient transcription of the ribonucleotide reductase subunit RRM2, and the mechanism by which this occurs was investigated by RNA sequencing, as described in chapter 3.

It was found that SETD2 is required to facilitate normal transcription of E2F target genes, and as shown in chapter 4, loss of SETD2 results in G1/S delay, slower replication fork progression, replication stress induction and genome instability. A novel role for H3K36me3 in the replication stress response was also identified. Checkpoint dependent upregulation of H3K36me3 at E2F target gene promoters facilitates replication stress induced transcription of E2F target genes. This work is consistent with previously published work in fission yeast, where H3K36me3 facilitates efficient DNA replication through induction of MBF target genes. Interestingly, while the MBF and E2F genes are functionally analogous, they have no conserved sequence homology. Despite this, the role of H3K36me3 in both DNA replication and response to replication stress appears to be highly evolutionarily conserved.

Chapter 5 investigated the synthetic lethality between WEE1 inhibition and loss of p53, and showed mechanistic similarities to the SETD2/WEE1 synthetic lethality. Novel synthetic lethalities with WEE1 were also investigated, with genes involved in cell cycle regulation or the DNA damage response, and with a set of tumour suppressors similar in functionality to SETD2.

6.1 The role of H3K36me3 in regulation of E2F transcription

While it is clear that SETD2 is required for efficient transcription of E2F target genes, the exact mechanism by which SETD2 facilitates E2F transcription is currently unclear. In yeast, Set2 is required for efficient binding of the MBF transcription factor complex to target gene promoters, and SETD2 may act in a similar way in mammalian cells. Alternatively, SETD2 mediated methylation of the E2F transcription factors may be required for their activation. It has previously been shown that E2F1 is methylated by SET9, leading to increased transcription of a subset of target genes (Xie et al., 2011), and so it is possible that SETD2 may also act in this way. Consistent with this idea, SETD2 activates transcription of a subset of STAT1 target genes through directly methylation of STAT1. SETD2 is then recruited to STAT1 target gene promoters, where it methylates H3K36, leading to transcriptional activation (Chen et al., 2017).

6.2 H3K36 trimethylation in response to replication stress

Additionally, the mechanism by which H3K36 is trimethylated in response to replication stress is also not fully understood. H3K36me3 is canonically deposited in co-transcriptionally in the gene body, through the interaction between SETD2 and

the C-terminal domain of RNA polymerase II (Kizer et al., 2005; Schaft et al., 2003). In contrast to this, replication stress induced H3K36me3 was found at the gene promoter region. This may indicate that H3K36me3 is recruited under replication stressed conditions by a different mechanism, possibly independent of RNA polymerase II, which needs to be investigated further. Deposition of H3K36me3 at the promoter region has been described previously (Ard and Allshire, 2016; Gautam et al., 2018; Lee et al., 2017), where it was found to be required for efficient gene expression, potentially indicating that H3K36 trimethylation at promoter regions may be specifically recruited to facilitate transcriptional activation.

SETD2 and H3K36me3 levels decrease upon S phase entry, consistent with their role in E2F target gene transcription. While it is clear that activation of the ATR-dependent replication stress checkpoint is required for the observed increase in H3K36 trimethylation, it is unclear how, and the downstream mechanisms have yet to be elucidated. Global KDM4A protein levels are unchanged in response to replication stress, however that does not rule out the possibility of other mechanisms of KDM4A regulation. KDM4A can form both homo and heterodimers (with KDM4B and C) which may impact its demethylation activity (Shin and Janknecht, 2007).

It is also possible that SETD2 is upregulated in response to replication stress. mRNA levels of SETD2 were elevated after treatment with hydroxyurea, although it is currently unclear if protein levels or activity are similarly increased. It is also possible that SETD2 is not regulated globally after replication stress, and instead is recruited only to specific promoters. Site specific SETD2-dependent methylation of H3K36 has been observed in response to DNA damage (Li and Wang, 2017), which suggests the possibility that replication stress may trigger H3K36 trimethylation through recruitment of SETD2 to E2F target genes. Consistent with this idea, methylation at

the GAPDH promoter was not found to be upregulated after replication stress induction, unlike the E2F target genes tested.

6.3 The synthetic lethality between loss p53 and WEE1 inhibition

Loss of p53 appears to sensitise cells to WEE1 inhibition by a similar mechanism to that observed in the SETD2/WEE1 synthetic lethality, with cells accumulating in non-replicating S phase. However, loss of p53 in otherwise unperturbed RPE-1 cells did not give any additional sensitisation to WEE1 inhibition, indicating that p53 loss alone is not sufficient to indicate susceptibility to WEE1 inhibition. This may be due to the low levels of endogenous DNA damage present in RPE-1 cells, and lack of disruption to other DNA damage response pathways. In contrast, cancers cells typically have high levels of endogenous DNA damage, and so may be naturally more susceptible to WEE1 inhibition.

Previous work on the p53/WEE1 synthetic lethality has primarily focussed on p53 null cancers, which make up only a small percentage of p53 mutations present in cancers. The gain of function R175H point mutation was also found to sensitise cells to WEE1 inhibition, suggesting a broader set of p53 mutants may also be targetable, although this need to be researched further.

6.4 Novel tumour suppressor synthetic lethalities with WEE1 inhibition

Two of the three genes identified as potential novel synthetic lethalities with WEE1 inhibition function to methylate or demethylate H3K4. As with H3K36me3, H3K4 methylation has been found to be important for normal cell cycle progression, and

disruption of this may lead to WEE1 inhibitor sensitivity. H3K4 methylation also has roles in regulation of origin firing and recruitment of replication stress response proteins, and disruption of these functions may also lead to WEE1 inhibitor sensitivity.

Alternatively, it may indicate a relationship between H3K4 methylation and H3K36me3. Substantial cross-regulation of histone modifications has been observed (Latham and Dent, 2007), and so it may be possible that disruption of the H3K4 methylation state indirectly sensitises cells to WEE1 inhibition through loss of H3K36me3.

6.5 Future work

The work described here explains the role of H3K36me3 in the mammalian G1/S transition and DNA replication, and demonstrates a novel mechanism through which H3K36me3 maintains genome stability and helps to prevent replication stress-induced DNA damage. This dual role for H3K36me3 provides insight into the sensitivity of H3K36me3 deficient cells to WEE1 inhibition, and may be useful in identifying other synthetic lethalities. This work also indicates that our understanding of the epigenetic contribution to both cell cycle progression and checkpoints is still incomplete, and other histone modifications may have as yet undiscovered functions in these pathways.

Bibliography

Agarwal, M.L., Agarwal, A., Taylor, W.R., and Stark, G.R. (1995). p53 controls both the G2/M and the G1 cell cycle checkpoints and mediates reversible growth arrest in human fibroblasts. Proceedings of the National Academy of Sciences of the United States of America *92*, 8493-8497.

Al Sarakbi, W., Sasi, W., Jiang, W.G., Roberts, T., Newbold, R.F., and Mokbel, K. (2009). The mRNA expression of SETD2 in human breast cancer: correlation with clinico-pathological parameters. BMC Cancer *9*, 290.

Angrand, P.O., Apiou, F., Stewart, A.F., Dutrillaux, B., Losson, R., and Chambon, P. (2001). NSD3, a new SET domain-containing gene, maps to 8p12 and is amplified in human breast cancer cell lines. Genomics *74*, 79-88.

Aoto, T., Saitoh, N., Sakamoto, Y., Watanabe, S., and Nakao, M. (2008). Polycomb group protein-associated chromatin is reproduced in post-mitotic G1 phase and is required for S phase progression. J Biol Chem *283*, 18905-18915.

Ard, R., and Allshire, R.C. (2016). Transcription-coupled changes to chromatin underpin gene silencing by transcriptional interference. Nucleic Acids Res *44*, 10619-10630.

Audia, J.E., and Campbell, R.M. (2016). Histone Modifications and Cancer. Cold Spring Harb Perspect Biol *8*, a019521.

Aymard, F., Bugler, B., Schmidt, C.K., Guillou, E., Caron, P., Briois, S., Iacovoni, J.S., Daburon, V., Miller, K.M., Jackson, S.P.*, et al.* (2014). Transcriptionally active chromatin recruits homologous recombination at DNA double-strand breaks. Nat Struct Mol Biol *21*, 366-374.

Bailey, M.H., Tokheim, C., Porta-Pardo, E., Sengupta, S., Bertrand, D., Weerasinghe, A., Colaprico, A., Wendl, M.C., Kim, J., Reardon, B.*, et al.* (2018). Comprehensive Characterization of Cancer Driver Genes and Mutations. Cell *173*, 371-385 e318.

Bannister, A.J., and Kouzarides, T. (2011). Regulation of chromatin by histone modifications. Cell Res *21*, 381-395.

Bannister, A.J., Schneider, R., Myers, F.A., Thorne, A.W., Crane-Robinson, C., and Kouzarides, T. (2005). Spatial distribution of di- and tri-methyl lysine 36 of histone H3 at active genes. J Biol Chem *280*, 17732-17736.

Bannister, A.J., Zegerman, P., Partridge, J.F., Miska, E.A., Thomas, J.O., Allshire, R.C., and Kouzarides, T. (2001). Selective recognition of methylated lysine 9 on histone H3 by the HP1 chromo domain. Nature *410*, 120-124.

Barry, E.R., Krueger, W., Jakuba, C.M., Veilleux, E., Ambrosi, D.J., Nelson, C.E., and Rasmussen, T.P. (2009). ES cell cycle progression and differentiation require the action of the histone methyltransferase Dot1L. Stem Cells *27*, 1538-1547.

Beck, H., Nähse-Kumpf, V., Larsen, M.S.Y., O'Hanlon, K.A., Patzke, S., Holmberg, C., Mejlvang, J., Groth, A., Nielsen, O., Syljuåsen, R.G.*, et al.* (2012). Cyclin-Dependent Kinase Suppression by WEE1 Kinase Protects the Genome through Control of Replication Initiation and Nucleotide Consumption. Molecular and Cellular Biology *32*, 4226-4236.

Behjati, S., Tarpey, P.S., Presneau, N., Scheipl, S., Pillay, N., Van Loo, P., Wedge, D.C., Cooke, S.L., Gundem, G., Davies, H.*, et al.* (2013). Distinct H3F3A and H3F3B driver mutations define chondroblastoma and giant cell tumor of bone. Nat Genet *45*, 1479-1482.

Beijersbergen, R.L., Kerkhoven, R.M., Zhu, L., Carlee, L., Voorhoeve, P.M., and Bernards, R. (1994). E2F-4, a new member of the E2F gene family, has oncogenic activity and associates with p107 in vivo. Genes Dev *8*, 2680-2690.

Beilharz, T.H., Harrison, P.F., Miles, D.M., See, M.M., Le, U.M., Kalanon, M., Curtis, M.J., Hasan, Q., Saksouk, J., Margaritis, T.*, et al.* (2017). Coordination of Cell Cycle Progression and Mitotic Spindle Assembly Involves Histone H3 Lysine 4 Methylation by Set1/COMPASS. Genetics *205*, 185-199.

Bell, S.P., and Stillman, B. (1992). ATP-dependent recognition of eukaryotic origins of DNA replication by a multiprotein complex. Nature *357*, 128-134.

Berry, W.L., and Janknecht, R. (2013). KDM4/JMJD2 histone demethylases: epigenetic regulators in cancer cells. Cancer Res *73*, 2936-2942.

Bertoli, C., Klier, S., McGowan, C., Wittenberg, C., and de Bruin, R.A. (2013a). Chk1 inhibits E2F6 repressor function in response to replication stress to maintain cell-cycle transcription. Curr Biol *23*, 1629-1637.

Bertoli, C., Skotheim, J.M., and de Bruin, R.A.M. (2013b). Control of cell cycle transcription during G1 and S phases. Nat Rev Mol Cell Biol *14*, 518-528.

Bhaskara, S., Chyla, B.J., Amann, J.M., Knutson, S.K., Cortez, D., Sun, Z.W., and Hiebert, S.W. (2008). Deletion of histone deacetylase 3 reveals critical roles in S phase progression and DNA damage control. Mol Cell *30*, 61-72.

Bjerke, L., Mackay, A., Nandhabalan, M., Burford, A., Jury, A., Popov, S., Bax, D.A., Carvalho, D., Taylor, K.R., Vinci, M.*, et al.* (2013). Histone H3.3. mutations drive pediatric glioblastoma through upregulation of MYCN. Cancer Discov *3*, 512-519.

Black, J.C., Allen, A., Van Rechem, C., Forbes, E., Longworth, M., Tschop, K., Rinehart, C., Quiton, J., Walsh, R., Smallwood, A.*, et al.* (2010). Conserved antagonism between JMJD2A/KDM4A and HP1gamma during cell cycle progression. Mol Cell *40*, 736-748.

Black, J.C., Manning, A.L., Van Rechem, C., Kim, J., Ladd, B., Cho, J., Pineda, C.M., Murphy, N., Daniels, D.L., Montagna, C.*, et al.* (2013). KDM4A lysine demethylase induces site-specific copy gain and rereplication of regions amplified in tumors. Cell *154*, 541-555.

Botuyan, M.V., Lee, J., Ward, I.M., Kim, J.E., Thompson, J.R., Chen, J., and Mer, G. (2006). Structural basis for the methylation state-specific recognition of histone H4-K20 by 53BP1 and Crb2 in DNA repair. Cell *127*, 1361-1373.

Bracken, A.P., Ciro, M., Cocito, A., and Helin, K. (2004). E2F target genes: unraveling the biology. Trends Biochem Sci *29*, 409-417.

Brehm, A., Miska, E.A., McCance, D.J., Reid, J.L., Bannister, A.J., and Kouzarides, T. (1998). Retinoblastoma protein recruits histone deacetylase to repress transcription. Nature *391*, 597-601.

Carvalho, S., Raposo, A.C., Martins, F.B., Grosso, A.R., Sridhara, S.C., Rino, J., Carmo-Fonseca, M., and de Almeida, S.F. (2013). Histone methyltransferase SETD2 coordinates FACT recruitment with nucleosome dynamics during transcription. Nucleic Acids Res *41*, 2881-2893.

Carvalho, S., Vitor, A.C., Sridhara, S.C., Martins, F.B., Raposo, A.C., Desterro, J.M., Ferreira, J., and de Almeida, S.F. (2014). SETD2 is required for DNA double-strand break repair and activation of the p53-mediated checkpoint. Elife *3*, e02482.

Chan, K.-L., North, P.S., and Hickson, I.D. (2007). BLM is required for faithful chromosome segregation and its localization defines a class of ultrafine anaphase bridges. The EMBO journal *26*, 3397-3409.

Chan, K.L., and Hickson, I.D. (2009). On the origins of ultra-fine anaphase bridges. Cell Cycle *8*, 3065-3066.

Chan, K.L., Palmai-Pallag, T., Ying, S., and Hickson, I.D. (2009). Replication stress induces sister-chromatid bridging at fragile site loci in mitosis. Nature Cell Biology *11*, 753.

Chan, K.M., Fang, D., Gan, H., Hashizume, R., Yu, C., Schroeder, M., Gupta, N., Mueller, S., James, C.D., Jenkins, R.*, et al.* (2013). The histone H3.3K27M mutation in pediatric glioma reprograms H3K27 methylation and gene expression. Genes Dev *27*, 985-990.

Chang, Q., Chandrashekhar, M., Ketela, T., Fedyshyn, Y., Moffat, J., and Hedley, D. (2016). Cytokinetic effects of Wee1 disruption in pancreatic cancer. Cell Cycle *15*, 593-604.

Chantalat, S., Depaux, A., Héry, P., Barral, S., Thuret, J.-Y., Dimitrov, S., and Gérard, M. (2011a). Histone H3 trimethylation at lysine 36 is associated with constitutive and facultative heterochromatin. Genome Res *21*, 1426-1437.

Chantalat, S., Depaux, A., Hery, P., Barral, S., Thuret, J.Y., Dimitrov, S., and Gerard, M. (2011b). Histone H3 trimethylation at lysine 36 is associated with constitutive and facultative heterochromatin. Genome research *21*, 1426-1437.

Charier, G., Couprie, J., Alpha-Bazin, B., Meyer, V., Quemeneur, E., Guerois, R., Callebaut, I., Gilquin, B., and Zinn-Justin, S. (2004). The Tudor tandem of 53BP1: a new structural motif involved in DNA and RG-rich peptide binding. Structure *12*, 1551-1562.

Chen, K., Liu, J., Liu, S., Xia, M., Zhang, X., Han, D., Jiang, Y., Wang, C., and Cao, X. (2017). Methyltransferase SETD2-Mediated Methylation of STAT1 Is Critical for Interferon Antiviral Activity. Cell *170*, 492-506 e414.

Cho, H.S., Toyokawa, G., Daigo, Y., Hayami, S., Masuda, K., Ikawa, N., Yamane, Y., Maejima, K., Tsunoda, T., Field, H.I.*, et al.* (2012). The JmjC domain-containing histone demethylase KDM3A is a positive regulator of the G1/S transition in cancer cells via transcriptional regulation of the HOXA1 gene. Int J Cancer *131*, E179-189.

Cimprich, K.A., and Cortez, D. (2008). ATR: an essential regulator of genome integrity. Nat Rev Mol Cell Biol *9*, 616-627.

D'Angiolella, V., Donato, V., Forrester, F.M., Jeong, Y.T., Pellacani, C., Kudo, Y., Saraf, A., Florens, L., Washburn, M.P., and Pagano, M. (2012). Cyclin F-mediated degradation of ribonucleotide reductase M2 controls genome integrity and DNA repair. Cell *149*, 1023-1034.

Dahmann, C., Diffley, J.F., and Nasmyth, K.A. (1995). S-phase-promoting cyclin-dependent kinases prevent re-replication by inhibiting the transition of replication origins to a pre-replicative state. Curr Biol *5*, 1257-1269.

Daniel, J.A., Pray-Grant, M.G., and Grant, P.A. (2005). Effector Proteins for Methylated Histones: An Expanding Family. Cell Cycle *4*, 919-926.

Dasgupta, T., Antony, J., Braithwaite, A.W., and Horsfield, J.A. (2016). HDAC8 Inhibition Blocks SMC3 Deacetylation and Delays Cell Cycle Progression without Affecting Cohesin-dependent Transcription in MCF7 Cancer Cells. J Biol Chem *291*, 12761-12770.

Deegan, T.D., Yeeles, J.T., and Diffley, J.F. (2016). Phosphopeptide binding by Sld3 links Dbf4-dependent kinase to MCM replicative helicase activation. EMBO J *35*, 961-973.

Den Haese, G.J., Walworth, N., Carr, A.M., and Gould, K.L. (1995). The Wee1 protein kinase regulates T14 phosphorylation of fission yeast Cdc2. Mol Biol Cell *6*, 371-385.

Dhalluin, C., Carlson, J.E., Zeng, L., He, C., Aggarwal, A.K., and Zhou, M.M. (1999). Structure and ligand of a histone acetyltransferase bromodomain. Nature *399*, 491-496.

Dhayalan, A., Rajavelu, A., Rathert, P., Tamas, R., Jurkowska, R.Z., Ragozin, S., and Jeltsch, A. (2010). The Dnmt3a PWWP domain reads histone 3 lysine 36 trimethylation and guides DNA methylation. J Biol Chem *285*, 26114-26120.

Diagouraga, B., Clement, J.A.J., Duret, L., Kadlec, J., de Massy, B., and Baudat, F. (2018). PRDM9 Methyltransferase Activity Is Essential for Meiotic DNA Double-Strand Break Formation at Its Binding Sites. Mol Cell *69*, 853-865 e856.

Do, K., Doroshow, J.H., and Kummar, S. (2013). Wee1 kinase as a target for cancer therapy. Cell Cycle *12*, 3159-3164.

Dominguez-Kelly, R., Martin, Y., Koundrioukoff, S., Tanenbaum, M.E., Smits, V.A., Medema, R.H., Debatisse, M., and Freire, R. (2011). Wee1 controls genomic stability during replication by regulating the Mus81-Eme1 endonuclease. J Cell Biol *194*, 567-579.

Duan, L., Rai, G., Roggero, C., Zhang, Q.J., Wei, Q., Ma, S.H., Zhou, Y., Santoyo, J., Martinez, E.D., Xiao, G.*, et al.* (2015). KDM4/JMJD2 Histone Demethylase Inhibitors Block Prostate Tumor Growth by Suppressing the Expression of AR and BMYB-Regulated Genes. Chem Biol *22*, 1185-1196.

Duns, G., van den Berg, E., van Duivenbode, I., Osinga, J., Hollema, H., Hofstra, R.M., and Kok, K. (2010). Histone methyltransferase gene SETD2 is a novel tumor suppressor gene in clear cell renal cell carcinoma. Cancer Res *70*, 4287-4291.

Dutta, C., Patel, P.K., Rosebrock, A., Oliva, A., Leatherwood, J., and Rhind, N. (2008). The DNA replication checkpoint directly regulates MBF-dependent G1/S transcription. Mol Cell Biol *28*, 5977-5985.

Edmunds, J.W., Mahadevan, L.C., and Clayton, A.L. (2008). Dynamic histone H3 methylation during gene induction: HYPB/Setd2 mediates all H3K36 trimethylation. EMBO J *27*, 406-420.

Egea, P.F., Stroud, R.M., and Walter, P. (2005). Targeting proteins to membranes: structure of the signal recognition particle. Curr Opin Struct Biol *15*, 213-220.

Eram, M.S., Bustos, S.P., Lima-Fernandes, E., Siarheyeva, A., Senisterra, G., Hajian, T., Chau, I., Duan, S., Wu, H., Dombrovski, L*., et al.* (2014). Trimethylation of histone H3 lysine 36 by human methyltransferase PRDM9 protein. J Biol Chem *289*, 12177-12188.

Evrin, C., Clarke, P., Zech, J., Lurz, R., Sun, J., Uhle, S., Li, H., Stillman, B., and Speck, C. (2009). A double-hexameric MCM2-7 complex is loaded onto origin DNA during licensing of eukaryotic DNA replication. Proc Natl Acad Sci U S A *106*, 20240-20245.

Fang, D., Gan, H., Lee, J.H., Han, J., Wang, Z., Riester, S.M., Jin, L., Chen, J., Zhou, H., Wang, J*., et al.* (2016). The histone H3.3K36M mutation reprograms the epigenome of chondroblastomas. Science *352*, 1344-1348.

Feng, Q., Wang, H., Ng, H.H., Erdjument-Bromage, H., Tempst, P., Struhl, K., and Zhang, Y. (2002). Methylation of H3-lysine 79 is mediated by a new family of HMTases without a SET domain. Curr Biol *12*, 1052-1058.

Ferlay, J., Colombet, M., Soerjomataram, I., Mathers, C., Parkin, D.M., Pineros, M., Znaor, A., and Bray, F. (2019). Estimating the global cancer incidence and mortality in 2018: GLOBOCAN sources and methods. Int J Cancer *144*, 1941-1953.

Fischer, M. (2017). Census and evaluation of p53 target genes. Oncogene *36*, 3943-3956.

Fnu, S., Williamson, E.A., De Haro, L.P., Brenneman, M., Wray, J., Shaheen, M., Radhakrishnan, K., Lee, S.H., Nickoloff, J.A., and Hromas, R. (2011). Methylation of histone H3 lysine 36 enhances DNA repair by nonhomologous end-joining. Proc Natl Acad Sci U S A *108*, 540-545.

Fontebasso, A.M., Schwartzentruber, J., Khuong-Quang, D.A., Liu, X.Y., Sturm, D., Korshunov, A., Jones, D.T., Witt, H., Kool, M., Albrecht, S*., et al.* (2013). Mutations in SETD2 and genes affecting histone H3K36 methylation target hemispheric high-grade gliomas. Acta Neuropathol *125*, 659-669.

Froimchuk, E., Jang, Y., and Ge, K. (2017). Histone H3 lysine 4 methyltransferase KMT2D. Gene *627*, 337-342.

Fu, H., Maunakea, A.K., Martin, M.M., Huang, L., Zhang, Y., Ryan, M., Kim, R., Lin, C.M., Zhao, K., and Aladjem, M.I. (2013). Methylation of histone H3 on lysine 79 associates with a group of replication origins and helps limit DNA replication once per cell cycle. PLoS Genet *9*, e1003542.

Fujisawa, T., and Filippakopoulos, P. (2017). Functions of bromodomain-containing proteins and their roles in homeostasis and cancer. Nat Rev Mol Cell Biol *18*, 246-262.

Gaillard, H., Garcia-Muse, T., and Aguilera, A. (2015). Replication stress and cancer. Nature reviews. Cancer *15*, 276-289.

Gan, W., Guan, Z., Liu, J., Gui, T., Shen, K., Manley, J.L., and Li, X. (2011). R-loop-mediated genomic instability is caused by impairment of replication fork progression. Genes Dev *25*, 2041-2056.

Gao, Y.G., Yang, H., Zhao, J., Jiang, Y.J., and Hu, H.Y. (2014). Autoinhibitory structure of the WW domain of HYPB/SETD2 regulates its interaction with the proline-rich region of huntingtin. Structure *22*, 378-386.

Gaubatz, S., Lindeman, G.J., Ishida, S., Jakoi, L., Nevins, J.R., Livingston, D.M., and Rempel, R.E. (2000). E2F4 and E2F5 play an essential role in pocket protein-mediated G1 control. Mol Cell *6*, 729-735.

Gautam, D., Johnson, B.A., Mac, M., and Moody, C.A. (2018). SETD2-dependent H3K36me3 plays a critical role in epigenetic regulation of the HPV31 life cycle. PLoS Pathog *14*, e1007367.

Gerlinger, M., Rowan, A.J., Horswell, S., Math, M., Larkin, J., Endesfelder, D., Gronroos, E., Martinez, P., Matthews, N., Stewart, A.*, et al.* (2012). Intratumor heterogeneity and branched evolution revealed by multiregion sequencing. N Engl J Med *366*, 883-892.

Giangrande, P.H., Zhu, W., Schlisio, S., Sun, X., Mori, S., Gaubatz, S., and Nevins, J.R. (2004). A role for E2F6 in distinguishing G1/S- and G2/M-specific transcription. Genes Dev *18*, 2941-2951.

Giono, L.E., and Manfredi, J.J. (2006). The p53 tumor suppressor participates in multiple cell cycle checkpoints. J Cell Physiol *209*, 13-20.

Gray, J.E., Tanvetyanon, T., Creelan, B.C., Antonia, S.J., Haura, E.B., Williams, C.C., Yaseen, R., Schell, M.J., Godin, R., Rix, U.*, et al.* (2017). Phase II trial of AZD1775 in combination with carboplatin and paclitaxel in stage IV squamous cell lung cancer (sqNSCLC): Preliminary results. Journal of Clinical Oncology *35*, e20672-e20672.

Hacker, K.E., Fahey, C.C., Shinsky, S.A., Chiang, Y.J., DiFiore, J.V., Jha, D.K., Vo, A.H., Shavit, J.A., Davis, I.J., Strahl, B.D.*, et al.* (2016). Structure/Function Analysis of Recurrent Mutations in SETD2 Protein Reveals a Critical and Conserved Role for a SET Domain Residue in Maintaining Protein Stability and Histone H3 Lys-36 Trimethylation. J Biol Chem *291*, 21283-21295.

Hakimi, A.A., Ostrovnaya, I., Reva, B., Schultz, N., Chen, Y.B., Gonen, M., Liu, H., Takeda, S., Voss, M.H., Tickoo, S.K.*, et al.* (2013). Adverse outcomes in clear cell renal cell carcinoma with mutations of 3p21 epigenetic regulators BAP1 and SETD2: a report by MSKCC and the KIRC TCGA research network. Clin Cancer Res *19*, 3259-3267.

Harper, J.W., and Elledge, S.J. (2007). The DNA damage response: ten years after. Mol Cell *28*, 739-745.

Harrigan, J.A., Belotserkovskaya, R., Coates, J., Dimitrova, D.S., Polo, S.E., Bradshaw, C.R., Fraser, P., and Jackson, S.P. (2011). Replication stress induces 53BP1-containing OPT domains in G1 cells. J Cell Biol *193*, 97-108.

Hateboer, G., Kerkhoven, R.M., Shvarts, A., Bernards, R., and Beijersbergen, R.L. (1996). Degradation of E2F by the ubiquitin-proteasome pathway: regulation by retinoblastoma family proteins and adenovirus transforming proteins. Genes Dev *10*, 2960-2970.

Hauer, M.H., and Gasser, S.M. (2017). Chromatin and nucleosome dynamics in DNA damage and repair. Genes Dev *31*, 2204-2221.

Heijink, A.M., Blomen, V.A., Bisteau, X., Degener, F., Matsushita, F.Y., Kaldis, P., Foijer, F., and van Vugt, M.A. (2015). A haploid genetic screen identifies the G1/S regulatory machinery as a determinant of Wee1 inhibitor sensitivity. Proc Natl Acad Sci U S A *112*, 15160-15165.

Heit, R., Rattner, J.B., Chan, G.K., and Hendzel, M.J. (2009). G2 histone methylation is required for the proper segregation of chromosomes. J Cell Sci *122*, 2957-2968.

Helin, K., Harlow, E., and Fattaey, A. (1993). Inhibition of E2F-1 transactivation by direct binding of the retinoblastoma protein. Mol Cell Biol *13*, 6501-6508.

Hills, S.A., and Diffley, J.F. (2014). DNA replication and oncogene-induced replicative stress. Curr Biol *24*, R435-444.

Hirai, H., Iwasawa, Y., Okada, M., Arai, T., Nishibata, T., Kobayashi, M., Kimura, T., Kaneko, N., Ohtani, J., Yamanaka, K.*, et al.* (2009). Small-molecule inhibition of Wee1 kinase by MK-1775 selectively sensitizes p53-deficient tumor cells to DNA-damaging agents. Molecular Cancer Therapeutics *8*, 2992-3000.

Hofmann, F., Martelli, F., Livingston, D.M., and Wang, Z. (1996). The retinoblastoma gene product protects E2F-1 from degradation by the ubiquitin-proteasome pathway. Genes Dev *10*, 2949-2959.

Huang da, W., Sherman, B.T., and Lempicki, R.A. (2009a). Bioinformatics enrichment tools: paths toward the comprehensive functional analysis of large gene lists. Nucleic Acids Res *37*, 1-13.

Huang da, W., Sherman, B.T., and Lempicki, R.A. (2009b). Systematic and integrative analysis of large gene lists using DAVID bioinformatics resources. Nat Protoc *4*, 44-57.

Huang, Y., Fang, J., Bedford, M.T., Zhang, Y., and Xu, R.M. (2006). Recognition of histone H3 lysine-4 methylation by the double tudor domain of JMJD2A. Science *312*, 748-751.

Huertas, P., and Aguilera, A. (2003). Cotranscriptionally formed DNA:RNA hybrids mediate transcription elongation impairment and transcription-associated recombination. Mol Cell *12*, 711-721.

Huff, J.T., Plocik, A.M., Guthrie, C., and Yamamoto, K.R. (2010). Reciprocal intronic and exonic histone modification regions in humans. Nat Struct Mol Biol *17*, 1495-1499.

Ibarra, A., Schwob, E., and Mendez, J. (2008). Excess MCM proteins protect human cells from replicative stress by licensing backup origins of replication. Proc Natl Acad Sci U S A *105*, 8956-8961.

Ilves, I., Petojevic, T., Pesavento, J.J., and Botchan, M.R. (2010). Activation of the MCM2-7 helicase by association with Cdc45 and GINS proteins. Mol Cell *37*, 247-258.

Jackson, S.P., and Bartek, J. (2009). The DNA-damage response in human biology and disease. Nature *461*, 1071-1078.

Jazayeri, A., Falck, J., Lukas, C., Bartek, J., Smith, G.C., Lukas, J., and Jackson, S.P. (2006). ATM- and cell cycle-dependent regulation of ATR in response to DNA double-strand breaks. Nat Cell Biol *8*, 37-45.

Jeggo, P.A., Downs, J.A., and Gasser, S.M. (2017). Chromatin modifiers and remodellers in DNA repair and signalling. Philos Trans R Soc Lond B Biol Sci *372*.

Jiang, X.R., Jimenez, G., Chang, E., Frolkis, M., Kusler, B., Sage, M., Beeche, M., Bodnar, A.G., Wahl, G.M., Tlsty, T.D.*, et al.* (1999). Telomerase expression in human somatic cells does not induce changes associated with a transformed phenotype. Nat Genet *21*, 111-114.

Johnson, D.G., and Walker, C.L. (1999). Cyclins and cell cycle checkpoints. Annu Rev Pharmacol Toxicol *39*, 295-312.

Jones, B., Su, H., Bhat, A., Lei, H., Bajko, J., Hevi, S., Baltus, G.A., Kadam, S., Zhai, H., Valdez, R.*, et al.* (2008). The histone H3K79 methyltransferase Dot1L is essential for mammalian development and heterochromatin structure. PLoS Genet *4*, e1000190.

Kanu, N., Gronroos, E., Martinez, P., Burrell, R.A., Yi Goh, X., Bartkova, J., Maya-Mendoza, A., Mistrik, M., Rowan, A.J., Patel, H.*, et al.* (2015). SETD2 loss-of-function promotes renal cancer branched evolution through replication stress and impaired DNA repair. Oncogene *34*, 5699-5708.

Karnani, N., and Dutta, A. (2011). The effect of the intra-S-phase checkpoint on origins of replication in human cells. Genes Dev *25*, 621-633.

Kastan, M.B., and Bartek, J. (2004). Cell-cycle checkpoints and cancer. Nature *432*, 316-323.

Kim, D.W., Kim, K.B., Kim, J.Y., and Seo, S.B. (2011). Characterization of a novel histone H3K36 methyltransferase setd3 in zebrafish. Biosci Biotechnol Biochem *75*, 289-294.

Kim, J., Daniel, J., Espejo, A., Lake, A., Krishna, M., Xia, L., Zhang, Y., and Bedford, M.T. (2006). Tudor, MBT and chromo domains gauge the degree of lysine methylation. EMBO Rep *7*, 397-403.

Kim, T.D., Shin, S., Berry, W.L., Oh, S., and Janknecht, R. (2012a). The JMJD2A demethylase regulates apoptosis and proliferation in colon cancer cells. J Cell Biochem *113*, 1368-1376.

Kim, W., Kim, R., Park, G., Park, J.W., and Kim, J.E. (2012b). Deficiency of H3K79 histone methyltransferase Dot1-like protein (DOT1L) inhibits cell proliferation. J Biol Chem *287*, 5588-5599.

Kizer, K.O., Phatnani, H.P., Shibata, Y., Hall, H., Greenleaf, A.L., and Strahl, B.D. (2005). A novel domain in Set2 mediates RNA polymerase II interaction and couples histone H3 K36 methylation with transcript elongation. Mol Cell Biol *25*, 3305-3316.

Kobayashi, H., Golsteyn, R., Poon, R., Stewart, E., Gannon, J., Minshull, J., Smith, R., and Hunt, T. (1991). Cyclins and their partners during Xenopus oocyte maturation. Cold Spring Harb Symp Quant Biol *56*, 437-447.

Kohler, C., Koalick, D., Fabricius, A., Parplys, A.C., Borgmann, K., Pospiech, H., and Grosse, F. (2016). Cdc45 is limiting for replication initiation in humans. Cell Cycle *15*, 974-985.

Kornberg, R.D. (1974). Chromatin structure: a repeating unit of histones and DNA. Science *184*, 868-871.

Kornberg, R.D., and Thomas, J.O. (1974). Chromatin structure; oligomers of the histones. Science *184*, 865-868.

Kotake, Y., Cao, R., Viatour, P., Sage, J., Zhang, Y., and Xiong, Y. (2007). pRB family proteins are required for H3K27 trimethylation and Polycomb repression complexes binding to and silencing p16INK4alpha tumor suppressor gene. Genes Dev *21*, 49-54.

Krek, W., Xu, G., and Livingston, D.M. (1995). Cyclin A-kinase regulation of E2F-1 DNA binding function underlies suppression of an S phase checkpoint. Cell *83*, 1149-1158.

Krohn, M., Skjolberg, H.C., Soltani, H., Grallert, B., and Boye, E. (2008). The G1-S checkpoint in fission yeast is not a general DNA damage checkpoint. J Cell Sci *121*, 4047-4054.

Kuo, A.J., Cheung, P., Chen, K., Zee, B.M., Kioi, M., Lauring, J., Xi, Y., Park, B.H., Shi, X., Garcia, B.A*., et al.* (2011). NSD2 links dimethylation of histone H3 at lysine 36 to oncogenic programming. Mol Cell *44*, 609-620.

Lachner, M., O'Carroll, D., Rea, S., Mechtler, K., and Jenuwein, T. (2001). Methylation of histone H3 lysine 9 creates a binding site for HP1 proteins. Nature *410*, 116-120.

Laiho, M., and Latonen, L. (2003). Cell cycle control, DNA damage checkpoints and cancer. Ann Med *35*, 391-397.

Lang, G.A., Iwakuma, T., Suh, Y.A., Liu, G., Rao, V.A., Parant, J.M., Valentin-Vega, Y.A., Terzian, T., Caldwell, L.C., Strong, L.C*., et al.* (2004). Gain of function of a p53 hot spot mutation in a mouse model of Li-Fraumeni syndrome. Cell *119*, 861-872.

Latham, J.A., and Dent, S.Y. (2007). Cross-regulation of histone modifications. Nat Struct Mol Biol *14*, 1017-1024.

Lawrence, M.S., Stojanov, P., Mermel, C.H., Robinson, J.T., Garraway, L.A., Golub, T.R., Meyerson, M., Gabriel, S.B., Lander, E.S., and Getz, G. (2014). Discovery and saturation analysis of cancer genes across 21 tumour types. Nature *505*, 495-501.

Lazzaro, F., Novarina, D., Amara, F., Watt, D.L., Stone, J.E., Costanzo, V., Burgers, P.M., Kunkel, T.A., Plevani, P., and Muzi-Falconi, M. (2012). RNase H and postreplication repair protect cells from ribonucleotides incorporated in DNA. Mol Cell *45*, 99-110.

Lee, K., Park, O.S., and Seo, P.J. (2017). Arabidopsis ATXR2 deposits H3K36me3 at the promoters of LBD genes to facilitate cellular dedifferentiation. Sci Signal *10*.

Lee, S.H., Oshige, M., Durant, S.T., Rasila, K.K., Williamson, E.A., Ramsey, H., Kwan, L., Nickoloff, J.A., and Hromas, R. (2005). The SET domain protein Metnase mediates foreign DNA integration and links integration to nonhomologous end-joining repair. Proc Natl Acad Sci U S A *102*, 18075-18080.

Leijen, S., Beijnen, J.H., and Schellens, J.H. (2010). Abrogation of the G2 checkpoint by inhibition of Wee-1 kinase results in sensitization of p53-deficient tumor cells to DNA-damaging agents. Curr Clin Pharmacol *5*, 186-191.

Leijen, S., van Geel, R.M., Sonke, G.S., de Jong, D., Rosenberg, E.H., Marchetti, S., Pluim, D., van Werkhoven, E., Rose, S., Lee, M.A*., et al.* (2016). Phase II Study of WEE1 Inhibitor AZD1775 Plus Carboplatin in Patients With TP53-Mutated Ovarian Cancer Refractory or Resistant to First-Line Therapy Within 3 Months. J Clin Oncol *34*, 4354-4361.

Lewis, P.W., Muller, M.M., Koletsky, M.S., Cordero, F., Lin, S., Banaszynski, L.A., Garcia, B.A., Muir, T.W., Becher, O.J., and Allis, C.D. (2013). Inhibition of PRC2 activity by a gain-of-function H3 mutation found in pediatric glioblastoma. Science *340*, 857-861.

Li, F., Mao, G., Tong, D., Huang, J., Gu, L., Yang, W., and Li, G.M. (2013). The histone mark H3K36me3 regulates human DNA mismatch repair through its interaction with MutSalpha. Cell *153*, 590-600.

Li, J., Ding, Y., and Li, A. (2016a). Identification of COL1A1 and COL1A2 as candidate prognostic factors in gastric cancer. World J Surg Oncol *14*, 297-297.

Li, J., Kluiver, J., Osinga, J., Westers, H., van Werkhoven, M.B., Seelen, M.A., Sijmons, R.H., van den Berg, A., and Kok, K. (2016b). Functional Studies on Primary Tubular Epithelial Cells Indicate a Tumor Suppressor Role of SETD2 in Clear Cell Renal Cell Carcinoma. Neoplasia *18*, 339-346.

Li, J., Moazed, D., and Gygi, S.P. (2002). Association of the histone methyltransferase Set2 with RNA polymerase II plays a role in transcription elongation. J Biol Chem *277*, 49383-49388.

Li, J., Ran, C., Li, E., Gordon, F., Comstock, G., Siddiqui, H., Cleghorn, W., Chen, H.Z., Kornacker, K., Liu, C.G.*, et al.* (2008). Synergistic function of E2F7 and E2F8 is essential for cell survival and embryonic development. Dev Cell *14*, 62-75.

Li, L., and Wang, Y. (2017). Cross-talk between the H3K36me3 and H4K16ac histone epigenetic marks in DNA double-strand break repair. J Biol Chem *292*, 11951-11959.

Li, M., Phatnani, H.P., Guan, Z., Sage, H., Greenleaf, A.L., and Zhou, P. (2005). Solution structure of the Set2-Rpb1 interacting domain of human Set2 and its interaction with the hyperphosphorylated C-terminal domain of Rpb1. Proc Natl Acad Sci U S A *102*, 17636-17641.

Li, M., and Zhang, P. (2009). The function of APC/CCdh1 in cell cycle and beyond. Cell Div *4*, 2.

Li, S., Wang, F., Qu, Y., Chen, X., Gao, M., Yang, J., Zhang, D., Zhang, N., Li, W., and Liu, H. (2017). HDAC2 regulates cell proliferation, cell cycle progression and cell apoptosis in esophageal squamous cell carcinoma EC9706 cells. Oncol Lett *13*, 403-409.

Li, T., and Chen, Z.J. (2018). The cGAS-cGAMP-STING pathway connects DNA damage to inflammation, senescence, and cancer. The Journal of experimental medicine *215*, 1287-1299.

Li, Y., Peng, L., and Seto, E. (2015). Histone Deacetylase 10 Regulates the Cell Cycle G2/M Phase Transition via a Novel Let-7-HMGA2-Cyclin A2 Pathway. Mol Cell Biol *35*, 3547-3565.

Lim, K.K., Nguyen, T.T.T., Li, A.Y., Yeo, Y.P., and Chen, E.S. (2018). Histone H3 lysine 36 methyltransferase mobilizes NER factors to regulate tolerance against alkylation damage in fission yeast. Nucleic Acids Res *46*, 5061-5074.

Lin, W.C., Lin, F.T., and Nevins, J.R. (2001). Selective induction of E2F1 in response to DNA damage, mediated by ATM-dependent phosphorylation. Genes & development *15*, 1833-1844.

Liu, P., Slater, D.M., Lenburg, M., Nevis, K., Cook, J.G., and Vaziri, C. (2009). Replication licensing promotes cyclin D1 expression and G1 progression in untransformed human cells. Cell Cycle *8*, 125-136.

Liu, W., Tanasa, B., Tyurina, O.V., Zhou, T.Y., Gassmann, R., Liu, W.T., Ohgi, K.A., Benner, C., Garcia-Bassets, I., Aggarwal, A.K.*, et al.* (2010). PHF8 mediates histone H4 lysine 20 demethylation events involved in cell cycle progression. Nature *466*, 508-512.

Liu, X., and Erikson, R.L. (2003). Polo-like kinase (Plk)1 depletion induces apoptosis in cancer cells. Proceedings of the National Academy of Sciences of the United States of America *100*, 5789-5794.

Liu, X., Lei, M., and Erikson, R.L. (2006). Normal Cells, but Not Cancer Cells, Survive Severe Plk1 Depletion. Molecular and Cellular Biology *26*, 2093-2108.

Lukas, C., Savic, V., Bekker-Jensen, S., Doil, C., Neumann, B., Pedersen, R.S., Grofte, M., Chan, K.L., Hickson, I.D., Bartek, J.*, et al.* (2011). 53BP1 nuclear bodies form around DNA lesions generated by mitotic transmission of chromosomes under replication stress. Nat Cell Biol *13*, 243-253.

Luzhna, L., Kathiria, P., and Kovalchuk, O. (2013). Micronuclei in genotoxicity assessment: from genetics to epigenetics and beyond. Front Genet *4*, 131.

Macheret, M., and Halazonetis, T.D. (2018). Intragenic origins due to short G1 phases underlie oncogene-induced DNA replication stress. Nature *555*, 112-116.

Machida, Y.J., Teer, J.K., and Dutta, A. (2005). Acute reduction of an origin recognition complex (ORC) subunit in human cells reveals a requirement of ORC for Cdk2 activation. J Biol Chem *280*, 27624-27630.

Magnaghi-Jaulin, L., Groisman, R., Naguibneva, I., Robin, P., Lorain, S., Le Villain, J.P., Troalen, F., Trouche, D., and Harel-Bellan, A. (1998). Retinoblastoma protein represses transcription by recruiting a histone deacetylase. Nature *391*, 601-605.

Majdzadeh, N., Wang, L., Morrison, B.E., Bassel-Duby, R., Olson, E.N., and D'Mello, S.R. (2008). HDAC4 inhibits cell-cycle progression and protects neurons from cell death. Dev Neurobiol *68*, 1076-1092.

Mao, X., Cai, T., Olyarchuk, J.G., and Wei, L. (2005). Automated genome annotation and pathway identification using the KEGG Orthology (KO) as a controlled vocabulary. Bioinformatics *21*, 3787-3793.

Matheson, C.J., Backos, D.S., and Reigan, P. (2016). Targeting WEE1 Kinase in Cancer. Trends Pharmacol Sci *37*, 872-881.

McIntosh, D., and Blow, J.J. (2012). Dormant origins, the licensing checkpoint, and the response to replicative stresses. Cold Spring Harb Perspect Biol *4*.

Meek, D.W. (2004). The p53 response to DNA damage. DNA Repair (Amst) *3*, 1049-1056.

Melcher, M., Schmid, M., Aagaard, L., Selenko, P., Laible, G., and Jenuwein, T. (2000). Structure-function analysis of SUV39H1 reveals a dominant role in heterochromatin organization, chromosome segregation, and mitotic progression. Mol Cell Biol *20*, 3728-3741.

Mendez, E., Rodriguez, C.P., Kao, M.C., Raju, S., Diab, A., Harbison, R.A., Konnick, E.Q., Mugundu, G.M., Santana-Davila, R., Martins, R.*, et al.* (2018). A Phase I Clinical Trial of AZD1775 in Combination with Neoadjuvant Weekly Docetaxel and Cisplatin before Definitive Therapy in Head and Neck Squamous Cell Carcinoma. Clin Cancer Res *24*, 2740-2748.

Meng, X., Bi, J., Li, Y., Yang, S., Zhang, Y., Li, M., Liu, H., Li, Y., McDonald, M.E., Thiel, K.W.*, et al.* (2018). AZD1775 Increases Sensitivity to Olaparib and Gemcitabine in Cancer Cells with p53 Mutations. Cancers (Basel) *10*.

Miller, J.J., Summers, M.K., Hansen, D.V., Nachury, M.V., Lehman, N.L., Loktev, A., and Jackson, P.K. (2006). Emi1 stably binds and inhibits the anaphase-promoting complex/cyclosome as a pseudosubstrate inhibitor. Genes Dev *20*, 2410-2420.

Min, J., Feng, Q., Li, Z., Zhang, Y., and Xu, R.M. (2003). Structure of the catalytic domain of human DOT1L, a non-SET domain nucleosomal histone methyltransferase. Cell *112*, 711-723.

Miotto, B., Ji, Z., and Struhl, K. (2016). Selectivity of ORC binding sites and the relation to replication timing, fragile sites, and deletions in cancers. Proc Natl Acad Sci U S A *113*, E4810-4819.

Mizuarai, S., Yamanaka, K., Itadani, H., Arai, T., Nishibata, T., Hirai, H., and Kotani, H. (2009). Discovery of gene expression-based pharmacodynamic biomarker for a p53 context-specific anti-tumor drug Wee1 inhibitor. Mol Cancer *8*, 34.

Moyer, S.E., Lewis, P.W., and Botchan, M.R. (2006). Isolation of the Cdc45/Mcm2-7/GINS (CMG) complex, a candidate for the eukaryotic DNA replication fork helicase. Proc Natl Acad Sci U S A *103*, 10236-10241.

Namdar, M., Perez, G., Ngo, L., and Marks, P.A. (2010). Selective inhibition of histone deacetylase 6 (HDAC6) induces DNA damage and sensitizes transformed cells to anticancer agents. Proc Natl Acad Sci U S A *107*, 20003-20008.

Naora, H., Takai, I., Adachi, M., and Naora, H. (1998). Altered cellular responses by varying expression of a ribosomal protein gene: sequential coordination of enhancement and suppression of ribosomal protein S3a gene expression induces apoptosis. The Journal of cell biology *141*, 741-753.

Neri, F., Rapelli, S., Krepelova, A., Incarnato, D., Parlato, C., Basile, G., Maldotti, M., Anselmi, F., and Oliviero, S. (2017). Intragenic DNA methylation prevents spurious transcription initiation. Nature *543*, 72.

Neumann, F., and Krawinkel, U. (1997). Constitutive expression of human ribosomal protein L7 arrests the cell cycle in G1 and induces apoptosis in Jurkat T-lymphoma cells. Exp Cell Res *230*, 252-261.

Nevis, K.R., Cordeiro-Stone, M., and Cook, J.G. (2009). Origin licensing and p53 status regulate Cdk2 activity during G(1). Cell Cycle *8*, 1952-1963.

Newbold, R.F., and Mokbel, K. (2010). Evidence for a tumour suppressor function of SETD2 in human breast cancer: a new hypothesis. Anticancer Res *30*, 3309-3311.

Nick McElhinny, S.A., Kumar, D., Clark, A.B., Watt, D.L., Watts, B.E., Lundström, E.-B., Johansson, E., Chabes, A., and Kunkel, T.A. (2010). Genome instability due to ribonucleotide incorporation into DNA. Nat Chem Biol *6*, 774-781.

Norbury, C., and Nurse, P. (1992). Animal cell cycles and their control. Annu Rev Biochem *61*, 441-470.

Olive, K.P., Tuveson, D.A., Ruhe, Z.C., Yin, B., Willis, N.A., Bronson, R.T., Crowley, D., and Jacks, T. (2004). Mutant p53 gain of function in two mouse models of Li-Fraumeni syndrome. Cell *119*, 847-860.

Olivier, M., Hollstein, M., and Hainaut, P. (2010). TP53 mutations in human cancers: origins, consequences, and clinical use. Cold Spring Harb Perspect Biol *2*, a001008.

Orphanides, G., LeRoy, G., Chang, C.H., Luse, D.S., and Reinberg, D. (1998). FACT, a factor that facilitates transcript elongation through nucleosomes. Cell *92*, 105-116.

Otto, T., and Sicinski, P. (2017). Cell cycle proteins as promising targets in cancer therapy. Nature Reviews Cancer *17*, 93.

Outchkourov, N.S., Muino, J.M., Kaufmann, K., van Ijcken, W.F., Groot Koerkamp, M.J., van Leenen, D., de Graaf, P., Holstege, F.C., Grosveld, F.G., and Timmers, H.T. (2013). Balancing of histone H3K4 methylation states by the Kdm5c/SMCX histone demethylase modulates promoter and enhancer function. Cell Rep *3*, 1071-1079.

Oza, A.M., Weberpals, J.I., Provencher, D.M., Grischke, E.-M., Hall, M., Uyar, D., Estevez-Diz, M.D.P., Marmé, F., Kuzmin, A., Rosenberg, P.*, et al.* (2015). An international, biomarker-directed, randomized, phase II trial of AZD1775 plus paclitaxel and carboplatin (P/C) for the treatment of women with platinum-sensitive, TP53-mutant ovarian cancer. Journal of Clinical Oncology *33*, 5506-5506.

Pai, C.C., Deegan, R.S., Subramanian, L., Gal, C., Sarkar, S., Blaikley, E.J., Walker, C., Hulme, L., Bernhard, E., Codlin, S.*, et al.* (2014). A histone H3K36 chromatin switch coordinates DNA double-strand break repair pathway choice. Nat Commun *5*, 4091.

Pai, C.C., Kishkevich, A., Deegan, R.S., Keszthelyi, A., Folkes, L., Kearsey, S.E., De Leon, N., Soriano, I., de Bruin, R.A.M., Carr, A.M.*, et al.* (2017). Set2 Methyltransferase Facilitates DNA Replication and Promotes Genotoxic Stress Responses through MBF-Dependent Transcription. Cell Rep *20*, 2693-2705.

Park, I.Y., Powell, R.T., Tripathi, D.N., Dere, R., Ho, T.H., Blasius, T.L., Chiang, Y.C., Davis, I.J., Fahey, C.C., Hacker, K.E.*, et al.* (2016). Dual Chromatin and Cytoskeletal Remodeling by SETD2. Cell *166*, 950-962.

Park, J.A., Kim, A.J., Kang, Y., Jung, Y.J., Kim, H.K., and Kim, K.C. (2011). Deacetylation and methylation at histone H3 lysine 9 (H3K9) coordinate chromosome condensation during cell cycle progression. Mol Cells *31*, 343-349.

Pavletich, N.P., Chambers, K.A., and Pabo, C.O. (1993). The DNA-binding domain of p53 contains the four conserved regions and the major mutation hot spots. Genes & Development *7*, 2556-2564.

Peixoto, P., Castronovo, V., Matheus, N., Polese, C., Peulen, O., Gonzalez, A., Boxus, M., Verdin, E., Thiry, M., Dequiedt, F.*, et al.* (2012). HDAC5 is required for maintenance of pericentric heterochromatin, and controls cell-cycle progression and survival of human cancer cells. Cell Death Differ *19*, 1239-1252.

Pfister, S.X., Ahrabi, S., Zalmas, L.P., Sarkar, S., Aymard, F., Bachrati, C.Z., Helleday, T., Legube, G., La Thangue, N.B., Porter, A.C.*, et al.* (2014). SETD2-dependent histone H3K36 trimethylation is required for homologous recombination repair and genome stability. Cell Rep *7*, 2006-2018.

Pfister, S.X., Markkanen, E., Jiang, Y., Sarkar, S., Woodcock, M., Orlando, G., Mavrommati, I., Pai, C.C., Zalmas, L.P., Drobnitzky, N.*, et al.* (2015). Inhibiting WEE1 Selectively Kills Histone H3K36me3-Deficient Cancers by dNTP Starvation. Cancer Cell *28*, 557-568.

Pomerantz, R.T., and O'Donnell, M. (2010). What happens when replication and transcription complexes collide? Cell Cycle *9*, 2537-2543.

Powers, N.R., Parvanov, E.D., Baker, C.L., Walker, M., Petkov, P.M., and Paigen, K. (2016). The Meiotic Recombination Activator PRDM9 Trimethylates Both H3K36 and H3K4 at Recombination Hotspots In Vivo. PLoS Genet *12*, e1006146.

Proudfoot, N.J. (2016). Transcriptional termination in mammals: Stopping the RNA polymerase II juggernaut. Science *352*, aad9926.

Pryde, F., Jain, D., Kerr, A., Curley, R., Mariotti, F.R., and Vogelauer, M. (2009). H3 k36 methylation helps determine the timing of cdc45 association with replication origins. PLoS One *4*, e5882.

Qin, S., and Min, J. (2014). Structure and function of the nucleosome-binding PWWP domain. Trends Biochem Sci *39*, 536-547.

Rajeshkumar, N.V., De Oliveira, E., Ottenhof, N., Watters, J., Brooks, D., Demuth, T., Shumway, S.D., Mizuarai, S., Hirai, H., Maitra, A*., et al.* (2011). MK-1775, a potent Wee1 inhibitor, synergizes with gemcitabine to achieve tumor regressions, selectively in p53-deficient pancreatic cancer xenografts. Clin Cancer Res *17*, 2799-2806.

Rasmussen, C.H., Petersen, D.R., Moeller, J.B., Hansson, M., and Dufva, M. (2015). Collagen Type I Improves the Differentiation of Human Embryonic Stem Cells towards Definitive Endoderm. PLoS One *10*, e0145389.

Ray Chaudhuri, A., Callen, E., Ding, X., Gogola, E., Duarte, A.A., Lee, J.E., Wong, N., Lafarga, V., Calvo, J.A., Panzarino, N.J*., et al.* (2016). Replication fork stability confers chemoresistance in BRCA-deficient cells. Nature *535*, 382-387.

Rayasam, G.V., Wendling, O., Angrand, P.O., Mark, M., Niederreither, K., Song, L., Lerouge, T., Hager, G.L., Chambon, P., and Losson, R. (2003). NSD1 is essential for early post-implantation development and has a catalytically active SET domain. EMBO J *22*, 3153-3163.

Rea, S., Eisenhaber, F., O'Carroll, D., Strahl, B.D., Sun, Z.W., Schmid, M., Opravil, S., Mechtler, K., Ponting, C.P., Allis, C.D*., et al.* (2000). Regulation of chromatin structure by site-specific histone H3 methyltransferases. Nature *406*, 593-599.

Reijns, M.A., Rabe, B., Rigby, R.E., Mill, P., Astell, K.R., Lettice, L.A., Boyle, S., Leitch, A., Keighren, M., Kilanowski, F*., et al.* (2012). Enzymatic removal of ribonucleotides from DNA is essential for mammalian genome integrity and development. Cell *149*, 1008-1022.

Remus, D., Beuron, F., Tolun, G., Griffith, J.D., Morris, E.P., and Diffley, J.F. (2009). Concerted loading of Mcm2-7 double hexamers around DNA during DNA replication origin licensing. Cell *139*, 719-730.

Rhind, N., and Russell, P. (2001). Roles of the mitotic inhibitors Wee1 and Mik1 in the G(2) DNA damage and replication checkpoints. Mol Cell Biol *21*, 1499-1508.

Rondinelli, B., Schwerer, H., Antonini, E., Gaviraghi, M., Lupi, A., Frenquelli, M., Cittaro, D., Segalla, S., Lemaitre, J.M., and Tonon, G. (2015). H3K4me3 demethylation by the histone demethylase KDM5C/JARID1C promotes DNA replication origin firing. Nucleic Acids Res *43*, 2560-2574.

Saldivar, J.C., Cortez, D., and Cimprich, K.A. (2017). The essential kinase ATR: ensuring faithful duplication of a challenging genome. Nat Rev Mol Cell Biol *18*, 622-636.

Sawan, C., and Herceg, Z. (2010). Histone modifications and cancer. Adv Genet *70*, 57-85.

Schaft, D., Roguev, A., Kotovic, K.M., Shevchenko, A., Sarov, M., Shevchenko, A., Neugebauer, K.M., and Stewart, A.F. (2003). The histone 3 lysine 36 methyltransferase, SET2, is involved in transcriptional elongation. Nucleic Acids Res *31*, 2475-2482.

Schulze, J.M., Jackson, J., Nakanishi, S., Gardner, J.M., Hentrich, T., Haug, J., Johnston, M., Jaspersen, S.L., Kobor, M.S., and Shilatifard, A. (2009). Linking cell cycle to histone modifications: SBF and H2B

monoubiquitination machinery and cell-cycle regulation of H3K79 dimethylation. Mol Cell *35*, 626-641.

Shahbazian, M.D., and Grunstein, M. (2007). Functions of site-specific histone acetylation and deacetylation. Annu Rev Biochem *76*, 75-100.

Sherr, C.J., and Roberts, J.M. (1999). CDK inhibitors: positive and negative regulators of G1-phase progression. Genes Dev *13*, 1501-1512.

Shin, S., and Janknecht, R. (2007). Diversity within the JMJD2 histone demethylase family. Biochem Biophys Res Commun *353*, 973-977.

Sogo, J.M., Lopes, M., and Foiani, M. (2002). Fork reversal and ssDNA accumulation at stalled replication forks owing to checkpoint defects. Science *297*, 599-602.

Song, H., Hollstein, M., and Xu, Y. (2007). p53 gain-of-function cancer mutants induce genetic instability by inactivating ATM. Nat Cell Biol *9*, 573-580.

Sorensen, C.S., Syljuasen, R.G., Falck, J., Schroeder, T., Ronnstrand, L., Khanna, K.K., Zhou, B.B., Bartek, J., and Lukas, J. (2003). Chk1 regulates the S phase checkpoint by coupling the physiological turnover and ionizing radiation-induced accelerated proteolysis of Cdc25A. Cancer Cell *3*, 247-258.

Spigel, D.R., Dakhil, S., Beck, J.T., Sadiq, A., Menon, S., Webb, C.D., Tsai, F.Y., Johnson, M., Jones, S.F., Greenlees, C.*, et al.* (2016). Phase II studies of AZD1775, a WEE1 kinase inhibitor, and chemotherapy in non-small-cell lung cancer (NSCLC): Lead-in cohort results. Annals of Oncology *27*.

Srinivasan, S.V., Dominguez-Sola, D., Wang, L.C., Hyrien, O., and Gautier, J. (2013). Cdc45 is a critical effector of myc-dependent DNA replication stress. Cell Rep *3*, 1629-1639.

Suda, M., Yamada, S., Toda, T., Miyakawa, T., and Hirata, D. (2000). Regulation of Wee1 kinase in response to protein synthesis inhibition. FEBS Lett *486*, 305-309.

Sun, X.J., Wei, J., Wu, X.Y., Hu, M., Wang, L., Wang, H.H., Zhang, Q.H., Chen, S.J., Huang, Q.H., and Chen, Z. (2005). Identification and characterization of a novel human histone H3 lysine 36-specific methyltransferase. J Biol Chem *280*, 35261-35271.

Takahashi, Y., Rayman, J.B., and Dynlacht, B.D. (2000). Analysis of promoter binding by the E2F and pRB families in vivo: distinct E2F proteins mediate activation and repression. Genes Dev *14*, 804-816.

Takebe, N., Coyne, G.H.O.S., Kummar, S., Do, K.T., Bruns, A., Juwara, L., Quinn, M.F., Harris, L., Piekarz, R., Prindiville, S.A.*, et al.* (2018). Safety, tolerability, and antitumor activity of once-daily Wee-1 inhibitor AZD1775. Journal of Clinical Oncology *36*, 2587-2587.

Tanaka, S., Nakato, R., Katou, Y., Shirahige, K., and Araki, H. (2011). Origin association of Sld3, Sld7, and Cdc45 proteins is a key step for determination of origin-firing timing. Curr Biol *21*, 2055-2063.

Tanaka, Y., Katagiri, Z., Kawahashi, K., Kioussis, D., and Kitajima, S. (2007). Trithorax-group protein ASH1 methylates histone H3 lysine 36. Gene *397*, 161-168.

Toledo, L.I., Altmeyer, M., Rask, M.B., Lukas, C., Larsen, D.H., Povlsen, L.K., Bekker-Jensen, S., Mailand, N., Bartek, J., and Lukas, J. (2013). ATR prohibits replication catastrophe by preventing global exhaustion of RPA. Cell *155*, 1088-1103.

Trapnell, C., Williams, B.A., Pertea, G., Mortazavi, A., Kwan, G., van Baren, M.J., Salzberg, S.L., Wold, B.J., and Pachter, L. (2010). Transcript assembly and quantification by RNA-Seq reveals unannotated transcripts and isoform switching during cell differentiation. Nat Biotechnol *28*, 511-515.

Tubbs, A., and Nussenzweig, A. (2017). Endogenous DNA Damage as a Source of Genomic Instability in Cancer. Cell *168*, 644-656.

Tvegard, T., Soltani, H., Skjolberg, H.C., Krohn, M., Nilssen, E.A., Kearsey, S.E., Grallert, B., and Boye, E. (2007). A novel checkpoint mechanism regulating the G1/S transition. Genes Dev *21*, 649-654.

Tyagi, S., Chabes, A.L., Wysocka, J., and Herr, W. (2007). E2F activation of S phase promoters via association with HCF-1 and the MLL family of histone H3K4 methyltransferases. Mol Cell *27*, 107-119.

Vandel, L., Nicolas, E., Vaute, O., Ferreira, R., Ait-Si-Ali, S., and Trouche, D. (2001). Transcriptional repression by the retinoblastoma protein through the recruitment of a histone methyltransferase. Mol Cell Biol *21*, 6484-6494.

Varier, R.A., and Timmers, H.T. (2011). Histone lysine methylation and demethylation pathways in cancer. Biochim Biophys Acta *1815*, 75-89.

Wahba, L., Amon, J.D., Koshland, D., and Vuica-Ross, M. (2011). RNase H and multiple RNA biogenesis factors cooperate to prevent RNA:DNA hybrids from generating genome instability. Mol Cell *44*, 978-988.

Wang, D., Han, S., Peng, R., Jiao, C., Wang, X., Yang, X., Yang, R., and Li, X. (2016). Depletion of histone demethylase KDM5B inhibits cell proliferation of hepatocellular carcinoma by regulation of cell cycle checkpoint proteins p15 and p27. J Exp Clin Cancer Res *35*, 37.

Westendorp, B., Mokry, M., Groot Koerkamp, M.J., Holstege, F.C., Cuppen, E., and de Bruin, A. (2012). E2F7 represses a network of oscillating cell cycle genes to control S-phase progression. Nucleic Acids Res *40*, 3511-3523.

Whetstine, J.R., Nottke, A., Lan, F., Huarte, M., Smolikov, S., Chen, Z., Spooner, E., Li, E., Zhang, G., Colaiacovo, M.*, et al.* (2006). Reversal of histone lysine trimethylation by the JMJD2 family of histone demethylases. Cell *125*, 467-481.

Williams, G.H., and Stoeber, K. (2012). The cell cycle and cancer. The Journal of Pathology *226*, 352-364.

Winston, F., and Allis, C.D. (1999). The bromodomain: a chromatin-targeting module? Nat Struct Biol *6*, 601-604.

Wu, G., Broniscer, A., McEachron, T.A., Lu, C., Paugh, B.S., Becksfort, J., Qu, C., Ding, L., Huether, R., Parker, M.*, et al.* (2012). Somatic histone H3 alterations in pediatric diffuse intrinsic pontine gliomas and non-brainstem glioblastomas. Nat Genet *44*, 251-253.

Xie, P., Tian, C., An, L., Nie, J., Lu, K., Xing, G., Zhang, L., and He, F. (2008). Histone methyltransferase protein SETD2 interacts with p53 and selectively regulates its downstream genes. Cell Signal *20*, 1671-1678.

Xie, Q., Bai, Y., Wu, J., Sun, Y., Wang, Y., Zhang, Y., Mei, P., and Yuan, Z. (2011). Methylation-mediated regulation of E2F1 in DNA damage-induced cell death. J Recept Signal Transduct Res *31*, 139-146.

Xu, B., Sun, Z., Liu, Z., Guo, H., Liu, Q., Jiang, H., Zou, Y., Gong, Y., Tischfield, J.A., and Shao, C. (2011). Replication stress induces micronuclei comprising of aggregated DNA double-strand breaks. PloS one *6*, e18618.

Xu, M., Sheppard, K.A., Peng, C.Y., Yee, A.S., and Piwnica-Worms, H. (1994). Cyclin A/CDK2 binds directly to E2F-1 and inhibits the DNA-binding activity of E2F-1/DP-1 by phosphorylation. Mol Cell Biol *14*, 8420-8431.

Yamaguchi, T., Cubizolles, F., Zhang, Y., Reichert, N., Kohler, H., Seiser, C., and Matthias, P. (2010). Histone deacetylases 1 and 2 act in concert to promote the G1-to-S progression. Genes Dev *24*, 455-469.

Yang, Y., Huang, Y., Wang, Z., Wang, H.T., Duan, B., Ye, D., Wang, C., Jing, R., Leng, Y., Xi, J.*, et al.* (2016). HDAC10 promotes lung cancer proliferation via AKT phosphorylation. Oncotarget *7*, 59388-59401.

Yao, N.Y., Schroeder, J.W., Yurieva, O., Simmons, L.A., and O'Donnell, M.E. (2013). Cost of rNTP/dNTP pool imbalance at the replication fork. Proc Natl Acad Sci U S A *110*, 12942-12947.

Yekezare, M., Gomez-Gonzalez, B., and Diffley, J.F. (2013). Controlling DNA replication origins in response to DNA damage - inhibit globally, activate locally. J Cell Sci *126*, 1297-1306.

Young, M.D., Wakefield, M.J., Smyth, G.K., and Oshlack, A. (2010). Gene ontology analysis for RNA-seq: accounting for selection bias. Genome Biology *11*, R14.

Zhang, J., Ding, L., Holmfeldt, L., Wu, G., Heatley, S.L., Payne-Turner, D., Easton, J., Chen, X., Wang, J., Rusch, M.*, et al.* (2012). The genetic basis of early T-cell precursor acute lymphoblastic leukaemia. Nature *481*, 157-163.

Zhang, Y., Wu, D., Xia, F., Xian, H., Zhu, X., Cui, H., and Huang, Z. (2016). Downregulation of HDAC9 inhibits cell proliferation and tumor formation by inducing cell cycle arrest in retinoblastoma. Biochem Biophys Res Commun *473*, 600-606.

Zhou, P., Wang, Z., Yuan, X., Zhou, C., Liu, L., Wan, X., Zhang, F., Ding, X., Wang, C., Xiong, S.*, et al.* (2013). Mixed lineage leukemia 5 (MLL5) protein regulates cell cycle progression and E2F1-responsive gene expression via association with host cell factor-1 (HCF-1). J Biol Chem *288*, 17532-17543.

Zhu, C., Chen, Q., Xie, Z., Ai, J., Tong, L., Ding, J., and Geng, M. (2011). The role of histone deacetylase 7 (HDAC7) in cancer cell proliferation: regulation on c-Myc. J Mol Med (Berl) *89*, 279-289.

Zou, L. (2007). Single- and double-stranded DNA: building a trigger of ATR-mediated DNA damage response. Genes Dev *21*, 879-885.

Appendix

Gene Symbol	Sequence
ON-TARGETplus Non-targeting Control	UGGUUUACAUGUCGACUAA
ON-TARGETplus Non-targeting Control	UGGUUUACAUGUUGUGUGA
ON-TARGETplus Non-targeting Control	UGGUUUACAUGUUUUCUGA
ON-TARGETplus Non-targeting Control	UGGUUUACAUGUUUUCCUA
MGA	CGUCAGGAAUGAAGAUAAU
MGA	GAUGAGAGUUGUACGAAGA
MGA	UGAGAGGGAUUCAGUAUAA
MGA	AGGUUAAUGGUAAGAGUUA
ZMYM3	UAUCACAUGUGGAUCGUAA
ZMYM3	GCCCAAUGGUGAACGAUAU
ZMYM3	GGACAUUAAUCCCAGUGUA
ZMYM3	GAGAGGAUCUACUGGAAUC
CDK12	GUUCAAAGCGUUCGAAUGA
CDK12	CUACAGAGCGACUUCCUUA
CDK12	CCGAGAAGCAUCUUGUUAA
CDK12	UGAAUUGGCAGUGUUAUUA
MSH6	CGAAGUAGCCGCCAAAUAA

MSH6	CCACAUGGAUGCUCUUAUU
MSH6	GCAGAAGGGCUAUAAAGUA
MSH6	GGGCCAAGAUGGAGGGUUA
PDS5B	GAAAUAUGCUUUACAGUCA
PDS5B	UGAUAAAGAUGUUCGCUUA
PDS5B	GCAUAGUGAUGGAGACUUG
PDS5B	GGUCAAUGAUCACUUACUU
ZFHX3	GAACAAGGUUUACGGACUA
ZFHX3	CCAAAGAGCACCCUAGUUU
ZFHX3	GACAAGCGUUUGAGAACAA
ZFHX3	GUACAGAGACCACUACGAU
ATF7IP	GAUAUAGCCUCUAGUGAAA
ATF7IP	GCUACCAUCUCUAUGCUUA
ATF7IP	AAAGAUGAGUCUGAAGUUA
ATF7IP	GUACAAGGUCAAAGAAGAA
ATR	GAGAAAGGAUUGUAGACUA
ATR	GCAACUCGCCUAACAGAUA
ATR	CCACGAAUGUUAACUCUAU
ATR	CCGCUAAUCUUCUAACAUU
SCAF4	GAAAGACGGGAUCGAGAAA
SCAF4	AGAGAGAGAACGUCGACAA
SCAF4	GAUAAUAGUAACCGUGACA
SCAF4	CAAGAGGUUAAGCGACAUA
SIN3A	GAGGAUAUAUGCUGAUAAA

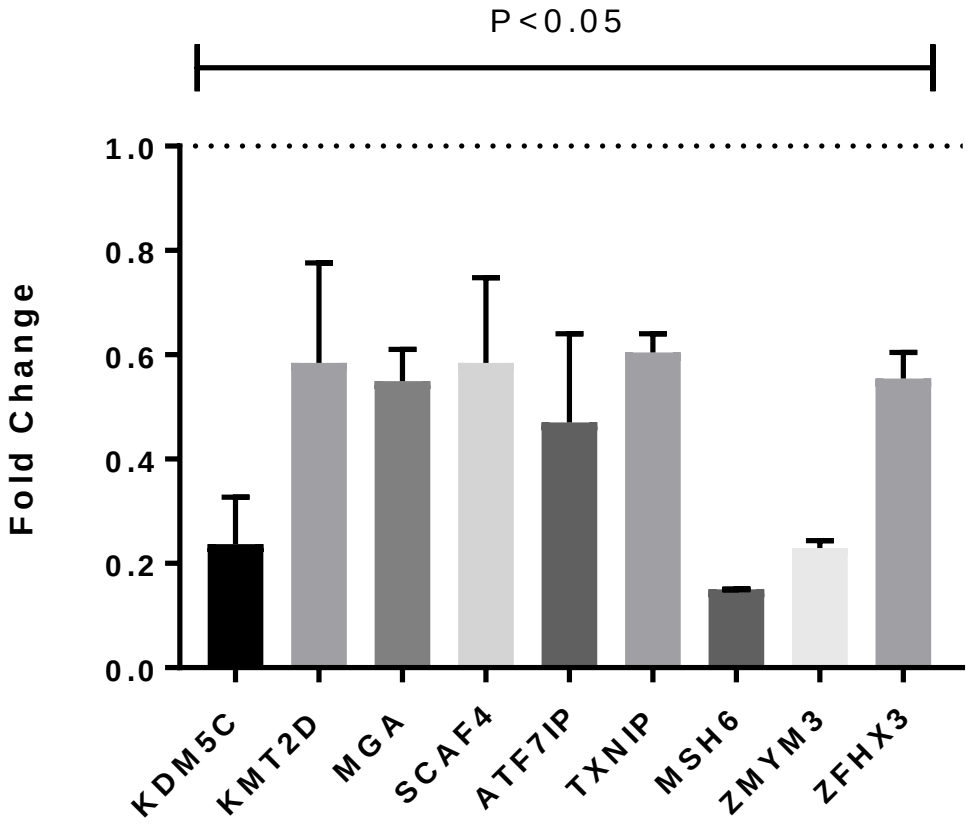
SIN3A	UAACAAGUAUCGUGUCAAA
SIN3A	UCAGAGAGGCUUUAACAAA
SIN3A	CAGACUACGUGGAGCGAUA
KMT2B	GCUAUGAAGACAACGACUA
KMT2B	GAAUCAAAGUGCCCAACUA
KMT2B	GGGCGAGGCCUGUUCUGUA
KMT2B	AGACAUCUCUCCUUUAGUG
CHD3	GAAUAUCCCUGAAUACGAA
CHD3	CCAGAAUGAUGCUCAAUUU
CHD3	CAUAAGAGGCGGAGUAAGA
CHD3	CGUAUGAGCUGAUCACCAU
LATS1	GGUGAAGUCUGUCUAGCAA
LATS1	UAGCAUGGAUUUCAGUAAU
LATS1	GGUAGUUCGUCUAUAUUAU
LATS1	GAAUGGUACUGGACAAACU
LATS2	GCACGCAUUUUACGAAUUC
LATS2	ACACUCACCUCGCCCAAUA
LATS2	AAUCAGAUAUUCCUUGUUG
LATS2	GAAGUGAACCGGCAAAUGC
GPS2	CAAGUGACCAUCAGAUUAU
GPS2	AUAAGAUGAUGGAACAGAA
GPS2	GAACUCAUCUCCUCAGCAU
GPS2	GAUGGAACAUGCUAACCAG
CDKN1B	CAAACGUGCGAGUGUCUAA

CDKN1B	GCAGCUUGCCCGAGUUCUA
CDKN1B	ACGUAAACAGCUCGAAUUA
CDKN1B	GCAAUGCGCAGGAAUAAGG
FOXQ1	UGGCGGAGAUCAACGAGUA
FOXQ1	UCGACAGCAUCCUGCGCAA
FOXQ1	CGUGUACGUAUGUGGCAUU
FOXQ1	CCUUAAAGCUAAAGCAUUU
TXNIP	GAAUACAUGUUCCCGAAUU
TXNIP	GCAAACAGACUUCGGAGUA
TXNIP	CGAACCAGCUCUGAGAUGA
TXNIP	GUCAGAGGCAAUCAUAUUA
TCEB1	GGCCAUGAAUUUAUUGUAA
TCEB1	GCUGCGAACUUCUUAGAUU
TCEB1	GUACAAGGUUCGCUACACU
TCEB1	CAUGUGCUAUCGAAAGUAU
KDM5C	GAGCAGGCUACCCGGGAAU
KDM5C	UCGCAGAGAAAUCGGGCAU
KDM5C	GACAAGACUCUGCGGAAGA
KDM5C	CUACGAACGCAUUGUUUAU
NIPBL	GAUAUAAACCGCCCACUAA
NIPBL	CAACAGAUCACAUAGAGUU
NIPBL	ACACUUCACUUCUAACAAA
NIPBL	GGGCUUGUUUCAAUAGAUA
AJUBA	UGAAUAGGCAUGAGGCAUA

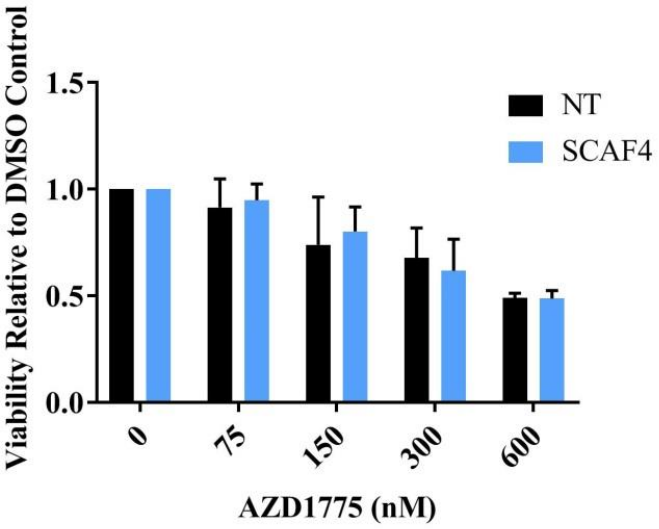
AJUBA	CUGAGAGGUAGCAAGUCUA
AJUBA	GUAAUAACUAAAAGGGUGA
AJUBA	GAUAGCUUCUUCUGAACUA
HUWE1	GCUUUGGGCUGGCCUAAUA
HUWE1	GCAGUUGGCGGCUUUCUUA
HUWE1	GAGCCCAGAUGACUAAGUA
HUWE1	UAACAUCAAUUGUCCACUU
RFC1	GUAAAUAGCUCCCGUAAAG
RFC1	GGAAUUAAUUGGCCUGAUA
RFC1	GUCCAAAGAUCUAAUAAGA
RFC1	CAUAUGCGAUGGUGACCUA
BTG2	GAACCGACAUGCUCCCGGA
BTG2	GCAUUCGCAUCAACCACAA
BTG2	GGUCAUAGAGCUACCGUAU
BTG2	AGACAAAGGUUACUAAUUG
BRCA1	CAACAUGCCCACAGAUCAA
BRCA1	CCAAAGCGAGCAAGAGAAU
BRCA1	UGAUAAAGCUCCAGCAGGA
BRCA1	GAAGGAGCUUUCAUCAUUC
KMT2D	GCAAAUCGCUAGCAUCAUU
KMT2D	GAUAUUAGCUACCACACAU
KMT2D	GAAAGGGCACUGAGGGAUA
KMT2D	GCAUGAAGCCGCAGCAAUU
CDKN2D	CAAUCCAUCUGGCAGUUCA

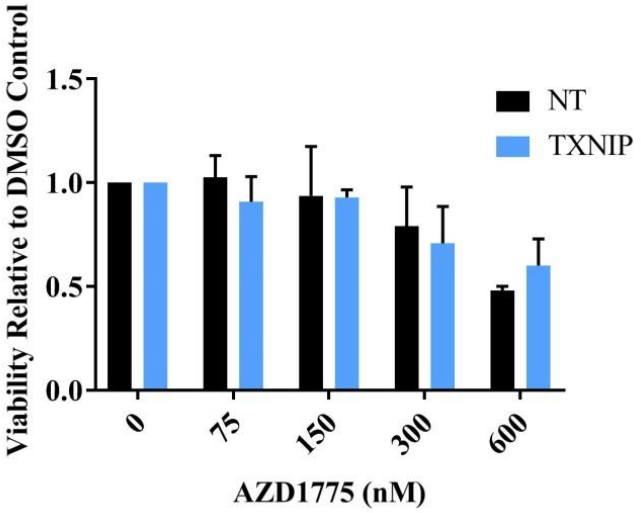
CDKN2D	AAUCUGAUCUCCAUCGCAG
CDKN2D	GUACCAGUCCAGUCCAUGA
CDKN2D	CUGCAGGUCAUGAUGUUUG
HDAC3	AAAGCGAUGUGGAGAUUUA
HDAC3	GCACCCGCAUCGAGAAUCA
HDAC3	GGAAUGCGUUGAAUAUGUC
HDAC3	AACAAGAUCUGUGAUAUUG

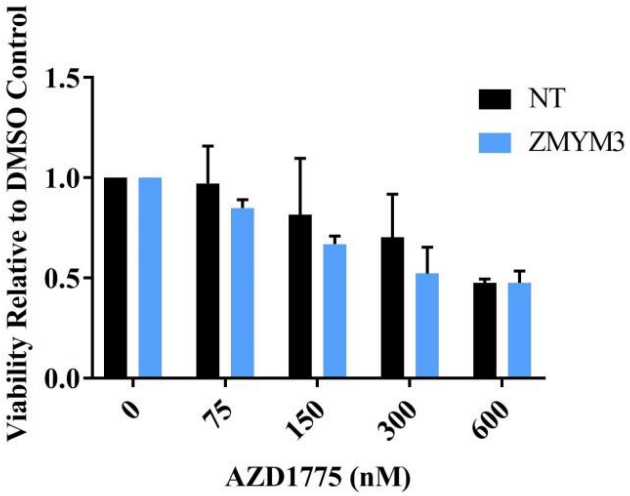
Appendix Table 1: siRNA library sequences targeting tumour suppressor genes

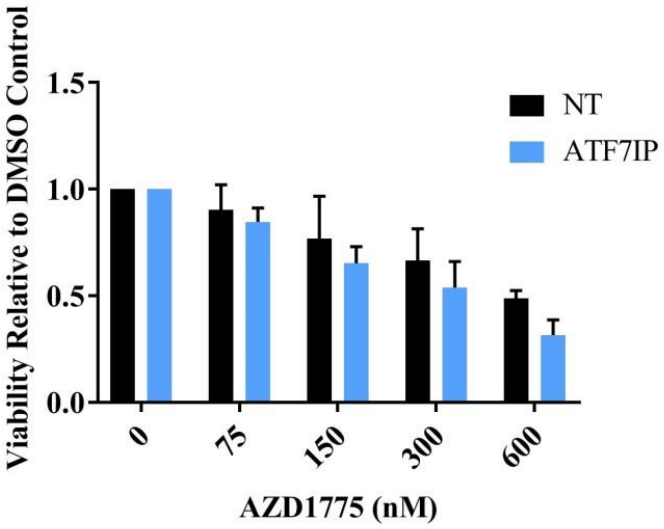


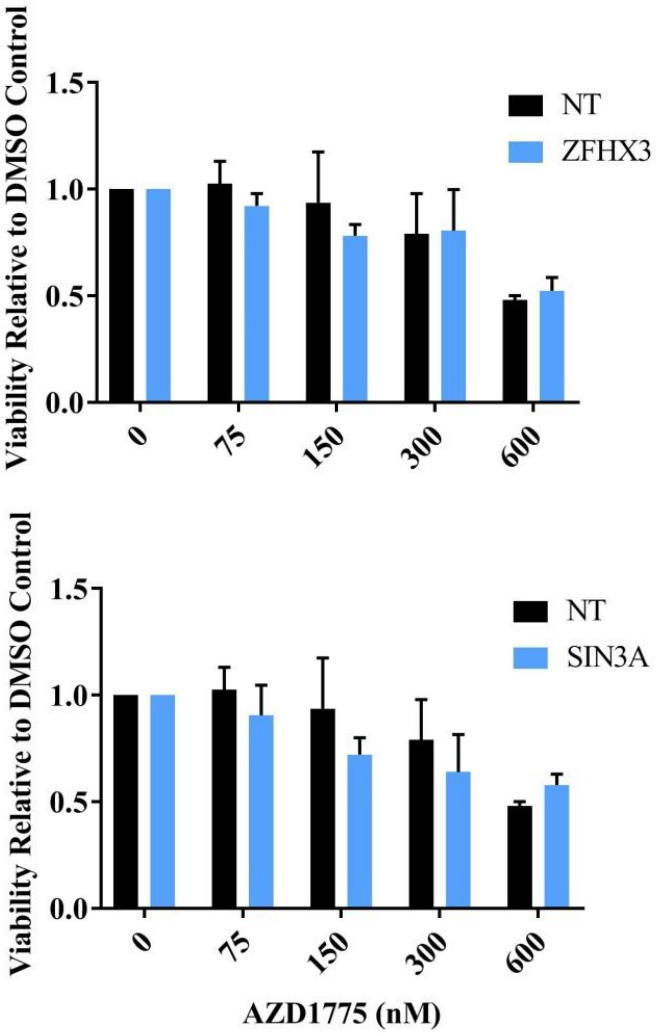
Appendix Figure 1: Change in expression of the selected tumour suppressor genes after transfection with siRNA targeting indicated genes. mRNA levels measured by qRT-PCR.

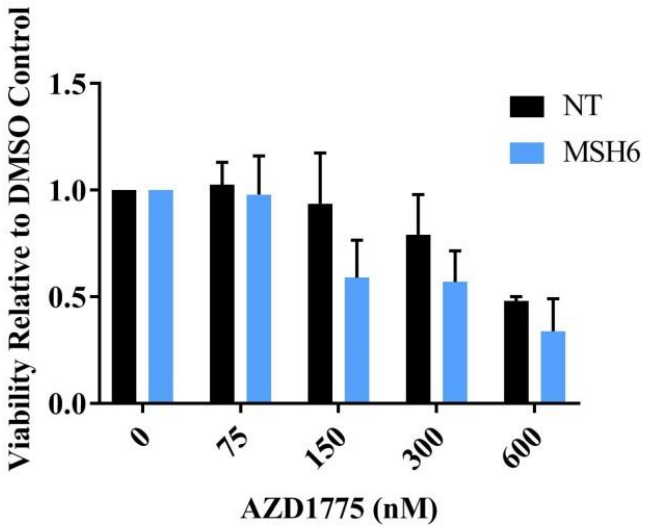

Viability Relative to DMSO Control
1.5
1.0
0.5
0.0
NT
SCAF4
0
75
150
300
600
AZD1775 (nM)


Viability Relative to DMSO Control
1.5
1.0
0.5
0.0
NT
TXNIP
0
75
150
300
600
AZD1775 (nM)


Viability Relative to DMSO Control
1.5
1.0
0.5
0.0
NT
ZMYM3
0
75
150
300
600
AZD1775 (nM)


Viability Relative to DMSO Control
1.5
1.0
0.5
0.0
NT
ATF7IP
0
75
150
300
600
AZD1775 (nM)


Viability Relative to DMSO Control
1.5
1.0
0.5
0.0
NT
ZFHX3
0
75
150
300
600
Viability Relative to DMSO Control
1.5
1.0
0.5
0.0
NT
SIN3A
0
75
150
300
600
AZD1775 (nM)



Appendix Figure 2: Viability assay of U2OS cells after treatment with indicated concentrations of AZD1775 for 48 hours relative to DMSO control. Experiment performed by Thomas Foord under supervision from Lee Armfield.